University of Florence

School of engineering - Department of industrial engineering of Florence "DIEF"

Thesis submitted in fulfilment of the requirements for the award of degree of:

Doctor of Philosophy in

Energy Engineering and Innovative Industrial Technologies

PhD School in Industrial Engineering – XXVI Cycle (2011-2013)

Advanced methodology for the characterization of reciprocating compressors

Tutor

Prof. *Ennio Carnevale*

Co-Tutor

Prof. *Giovanni Ferrara*

Candidate

Dr. *Luca Romani*

PhD Course Coordinator

Prof. *Maurizio De Lucia*

Florence, Italy, December 2013

Declaration

I hereby declare that this submission is my own work and, to the best of my knowledge and belief, it contains no material previously published or written by another person, nor material which to a substantial extent has been accepted for the award of any other degree or diploma at University of Florence or any other educational institution, except where due references are provided in the thesis itself.

Any contribution made to the research by others I have been working with is explicitly acknowledged in the thesis.

_____

Luca Romani

December 2013

Acknowledgments

This research is the result of a fulfilling synergic work: more than one person has been important - in his own way - to make it real, reachable and captivating day by day.

Special thanks to:

Ennio Carnevale, the work team leader;

Giovanni Ferrara, careful supervisor and precious -and not only technical- advice giver;

Lorenzo Ferrari, a valiant supporter and a stimulating professional.

All the Linea Laboratory guys:

Alfonso (the technician), Andrea (the new entry), Francesco (the electronic problem solver), Giulio (the Lab veteran).

All the PhD group colleagues, one by one:

Alessandro, Davide, Francesco, Giovanni, Fabio, Isacco (tireless collaborator on this research project).

Thanks also to Alberto Babbini, GE Nuovo Pignone referent.

Contents

Declaration.....I

Acknowledgments II

Contents III

List of figure V

List of tables X

List of symbols and acronyms XI

Introduction.....1

1 The reciprocating compressor.....6

1.1 The reciprocating compressor: structure and functioning.....9

1.2 Ideal cycle 10

1.3 Theoretical cycle 12

1.3.1 Effects due to valves.....13

1.3.2 The other sources of loss 17

1.3.3 Cylinder performances.....22

1.4 Piping system and auxiliaries.....24

1.4.1 Pulsating flow issue, acoustic filter design.....28

2 Acoustic theory.....32

2.1 Propagation of waves in ducts.....32

2.1.1 Theory of acoustic filter 34
2.1.2 Electro acoustic analogies 36
2.2 Transfer matrix method 39
2.2.1 Characterization of an acoustic problem, reciprocating compressor discharge chamber example 40
3 Numerical model 47
3.1 Reciprocating compressor numerical model 47
3.1.1 Valve dynamic 55
3.2 Calibration of the numerical model 59
3.2.1 Experimental setup 59
3.2.2 Numerical model calibration 69
3.2.3 Results 73
3.3 Acoustic hybrid approach 79
3.3.1 Pipeline elements (frequency domain) 80
3.3.2 Interaction between source and pipeline 83
3.3.3 FFT analysis 84
3.3.4 Base example: Wave propagation in a duct 88
4 Hybrid model 90
4.1 Configuration 1 90
4.2 Configuration 2 96
4.3 Configuration 3 103
5 Conclusion 109
5.1 Numerical models 110
5.2 Analyses 112
6 Bibliography 114

List of figure

Figure 1.1 - Engraving taken from 'Experimental Nova' (1672) by Otto von Guericke showing his experiment, carried out at Magdeburg, with an evacuated sphere . In this demonstration 16 horses could not pull apart the two halves of an evacuated sphere, known from then on as Magdeburg hemispheres. On 8 May 1654, he performed the experiment. 6

Figure 1.2 - An example of reciprocating compressor acted by a steam engine 7

Figure 1.3 – Field of application of the compressors in function of pressure and volumetric flow 8

Figure 1.4 – Typical reciprocating compressor 9

Figure 1.5 – Double acting arrangement 9

Figure 1.6 – Reciprocating compressor automatic valve 10

Figure 1.7 – p-v diagram for the ideal cycle 11

Figure 1.8 – Theoretical cycle vs Ideal cycle 12

Figure 1.9 – Schematic of a valve 14

Figure 1.10 – Effect of springs preloads on the theoretical cycle 14

Figure 1.11 - Ideal compression cycle, modified by the springs and by the valves pressure drop 15

Figure 1.12 - Ideal cycle with “real” compression 18

Figure 1.13 - Theoretical compression cycle with clearance effect 19

Figure 1.14 - Effects of higher clearance volume on the capacity 21

Figure 1.15 - Effects of an increase of pressure ratio on the capacity 21

Figure 1.16 - Propagation of the pulsating flow along the intake duct 25

Figure 1.17 - Propagation of the pulsating flow along the outlet duct 25

Figure 1.18 - Example of pulsating flow at the inlet of a double effect-compressor 25
Figure 1.19 - Example of pulsating flow at the discharge of a double effect-compressor 25
Figure 1.20 - Typical compressed gas plant 27
Figure 1.21 - Scheme of the interaction between the pulsation design and the entire compressor design. 28
Figure 1.22 - Acoustic filter scheme 29
Figure 1.23 - Filter Impedance function 29
Figure 1.24 - Two bottle acoustic filter for low speed compressors 30
Figure 1.25 - Single bottle acoustic filter for high speed compressors 31
Figure 2.1 - a) open duct, b) duct with rigidly closed end, c) duct with anechoic end 35
Figure 2.2 Lumped impedance 36
Figure 2.3 Lumped compliance 37
Figure 2.4 - Electrical circuit representation 37
Figure 2.5 - Three basic elements in an equivalent circuit, distributed element, lumped element, shunt lumped element. 39
Figure 2.6 - Scheme of an n-elements acoustic filter 40
Figure 2.7 - Reciprocating compressor inlet and discharge chamber 41
Figure 2.8 - Discharge chamber 2 input 1 output 42
Figure 2.9 - Reciprocating compressor discharge chamber, internal volume mesh (and additional volume mesh) 44
Figure 2.10 - Acoustic fem modelling of discharge chambers 44
Figure 3.1 Flow chart of the 0D numerical model 49
Figure 3.2 - Crank mechanism 50
Figure 3.3 - Decisional logic 50
Figure 3.4 - Internal energy balance, suction phase 52
Figure 3.5 - Internal energy balance, compression (expansion) phase 54
Figure 3.6 - Internal energy balance, discharge phase 55
Figure 3.7 Valve dynamics flow chart 57
Figure 3.8 - H503CS Dorin Compressor 59

Figure 3.9 - Reciprocating compressor test bed 60
Figure 3.10 - Experimental apparatus for indicating cycle measurement 63
Figure 3.11 - Hall sensor signal (yellow), CAC revolution signal (blue)..... 63
Figure 3.12 - Experimental pressure measurement, red curve indicating cycle, blue curve suction pressure, green curve discharge pressure 64
Figure 3.13 - Experimental setup for the measurement of the reed valve stiffness 66
Figure 3.14 - Detail of the mechanical comparator positioning, fit out in order to the measure the reed valve displacement 66
Figure 3.15 - Discharge reed valves stiffness diagram..... 67
Figure 3.16 - Suction reed valves stiffness diagram..... 67
Figure 3.17- On the left, the suction reed valves; on the right, the discharge reed valves..... 68
Figure 3.18 - Detail of the valve fixing: on the left, the discharge valve on the right, the suction valve 68
Figure 3.19 - Experimental PV Diagram of the H503CS compressor 70
Figure 3.20 - Comparison between the experimental and the numerical cylinder pressures..... 72
Figure 3.21 - Mass flow rate [kg/s], in blue the suction phase, in red the discharge phase..... 72
Figure 3.22 - Valve lift [m]..... 73
Figure 3.23 - Analysis of the influence of the clearance-volume variation on the PV diagram 74
Figure 3.24 - Analysis of the influence of the compressor speed on the PV diagram 75
Figure 3.25 - Analysis of the influence of the reed valve mass on the PV diagram 76
Figure 3.26 - Detail of the discharge section (valve mass)..... 76
Figure 3.27 - Analysis of the influence of the reed valve stiffness on the PV diagram 77
Figure 3.28 - Detail of the discharge section (valve stiffness) 78

Figure 3.29 - Analysis of the functioning of the compressor provided with different gasses; in blue the indicating cycle with R404A and in red the indicating cycle with Air 78
Figure 3.30 - Hybrid system scheme 80
Figure 3.31 - Duct discontinuity 81
Figure 3.32 - Lateral discontinuity 82
Figure 3.33 - Scheme of plenum with one inlet and one exit 82
Figure 3.34 - Mass flow rate at the discharge valve 83
Figure 3.35 - Source / line interaction 84
Figure 3.36 - FFT analysis of a composed signal 85
Figure 3.37 - Comparison between the original signal and the processed signal .. 86
Figure 3.38 - Analysis of a null - sinusoidal - null signal 86
Figure 3.39 - Analysis of a null - sinusoidal - null signal with mean value different from 0 87
Figure 3.40 - Real mass flow rate original signal vs reconstructed signal 87
Figure 3.42 - Open end duct simulation 89
Figure 4.1 - Scheme of the compressor provided with the plenum on the suction and the discharge line 90
Figure 4.2 - Plenum scheme 91
Figure 4.3 - PV diagram, blue in-cylinder pressure, red discharge pressure, green suction pressure. Plenum cylindrical body diameter D2=0.55m 92
Figure 4.4 - PV diagram, blue in-cylinder pressure, red discharge pressure, green suction pressure. Plenum cylindrical body diameter D2=0.2m 93
Figure 4.5 - Suction: transmitted pressure downstream the plenum. Plenum cylindrical body dimension: blue D2=0.55 m, green D2= 0.2 m 94
Figure 4.6 - Discharge: transmitted pressure downstream the plenum. Plenum cylindrical body dimension: blue D2=0.55 m, red D2= 0.2 m 94
Figure 4.7 - Comparison between the PV diagrams, in blue plenum with the greater volume, in red the plenum with the smaller volume 95
Figure 4.8 - Bi-cylindrical compressor scheme 96
Figure 4.9 - Plenum scheme, 2 inlet - 1 outlet 96
Figure 4.10 - Flow diagram of the bi-cylindrical configuration 97

Figure 4.11 - P-theta diagram of the bi-cylindrical compressor, the phase shift between the cylinders is 180°; cylinder 1 continuous lines, cylinder 2 dashed lines 98
Figure 4.12 - P-Theta diagram of the bi-cylindrical compressor, the phase shift between the cylinders is 90°; cylinder 1 continuous lines, cylinder 2 dashed lines 99
Figure 4.13 - Comparison between the pressure fluctuations upstream the suction plenum; the blue line is relative to the compressor with a phase shift between the cranks of the two cylinders of 90°, the red is relative to a phase shift between the cranks of the two cylinders of 180°. 100
Figure 4.14 - Comparison between the pressure fluctuations downstream the discharge plenum; the blue line is relative to the compressor with a phase shift between the cranks of the two cylinders of 90°, the red is relative to a phase shift between the cranks of the two cylinders of 180°. 100
Figure 4.15 - Comparison of the in-cylinder pressure trends varying the plenum Din dimension 101
Figure 4.16 - Pressure fluctuation at the suction side, comparison between plenum of different Din dimension 102
Figure 4.17 - Pressure fluctuation at the discharge side, comparison between plenum of different Din dimension 102
Figure 4.18 - Suction and discharge chambers of a compressor for refrigeration applications 103
Figure 4.19 - Scheme of the hybrid approach with the introduction of the modelling of a 3D element 104
Figure 4.20 - Bi-cylindrical compressor scheme 105
Figure 4.21 - Cylinder 1, blue line in cylinder pressure, red line discharge pressure, green line suction pressure 106
Figure 4.22 - Cylinder 2, blue line in cylinder pressure, violet line discharge pressure, green line suction pressure 107

List of tables

Table - 3.1 H503CS Compressor features 60
Table - 3.2 Experimental conditions for the compressor testing 69
Table - 4.1 Plenum geometry values 91
Table - 4.2 Plenum geometry values -Two inlets and one outlet configuration.... 98

List of symbols and acronyms

a: sound velocity [m/s]

Av: passage section [m^2]

b: dumper coefficient

BDP: bottom dead point

cD: drag coefficient

Cp: specific heat at constant pressure [kJ/kgK]

Cv: specific heat at constant volume [kJ/kgK]

D: discretization parameter;

HT: Heat transfer [kJ]

k: spring stiffness

Ks: flow coefficient

l: connecting rod [m]

P01: upstream total pressure [Pa]

P2: downstream static pressure [Pa]

r: crank [m]

R: gas constant [xx]

RE.CO.A: reciprocating compressor analysis

reb: rebound coefficient

RPM: revolution per minute

S: duct section [m^2]

s: piston translation [m]

TDP: top dead point

u: particle velocity [m/s]

vf: flux velocity [m/s]

α: angular rotation [°]

γ: Cp/Cv;

γ_c: calibration coefficient for the polytropic compression

γ_e: calibration coefficient for the polytropic expansion

ρ: density [kg/m^3]

ρ_1: upstream fluid density [kg/m^3]

Introduction

The reciprocating compressor is a mechanical apparatus designed for the compression of the gasses and is extensively adopted in everyday life both for industrial and for civil application; since its wide diffusion, nowadays, the manufacturers pay particular attention to its efficiency and reliability. In order to face the above-mentioned issues, the design process of the new reciprocating compressors passes inevitably through the preliminary numerical modelling and through the necessary experimental tests. Several works dealing with the numerical modelling can be found in literature, for example: works about the compressor performances prediction, about the fluid-dynamic analysis of the gas flow across the suction and the discharge sections, about the heat transfer between the compressor parts and the refrigeration system, about the mechanical analysis for the structural optimization. A far wide range of simulation tools can be adopted, this variety depends on the different issue to analyse, for example: the 0D models, quick and relatively simple, allows a global prediction of the compressor performances; the 3D Computational Fluid-Dynamics (CFD) analysis is good to calculate the fluid-dynamic losses associated to the suction and discharge process. By the way, focusing on the performance prediction, the work by R. Aigner et al. [1] deals with the study of the internal flow in the reciprocating compressor and the analysis of the automatic valves motion: the authors performs a one-dimensional and two-dimensional numerical model for the prediction of the valve motion and compares them with the experimental measurements. Moreover, the work by E.Winandy et al. [2] is an example of a simplified numerical tool for the estimation of the compressor performances, here the results of the numerical model are compared with the experimental measurement too. M. Elhaj et al. [3] makes, in his work, the same kind of comparison between the 0D numerical model and the experimental measurement of the in-cylinder pressure on a two

stage reciprocating compressor. It is so proved the great interest in the prediction capability of such a numerical modelling. The reference literature proves the interest in the prediction capability of the compressor global performances using simplified numerical model.

The coupling of the reciprocating machine with the line is a recurrent topic in industrial applications; in fact this interaction is at the origins of noise, vibrations and mechanical failures. An exemplifying works examining in depth these phenomena is the report by Marybeth G. Nored et al. [4], in which the object of the investigation is the analysis of the acoustic noise on the pipeline. The Southwest Research Institute [5] exposes in detail the issue of the pressure wave propagation in the pipeline and the relative consequences on the mechanical structure: it brings not only theoretical but also technical solutions.

A way to investigate numerically the interaction between the source of the noise and the source-connected system is to realise an hybrid model in which both the source and the system are contemporary modelled and interact with each other. In the field of the internal combustion engine some literary example is the work by P. Davies et al. about the control of the acoustic noise [6]; or the work by Y. Sathyanarayana et al. about the acoustic analysis of the exhaust system [7]. In the field of the reciprocating compressors interesting is the work by K. H. An about the analysis of the compressor-line coupling [8], considering the interaction between the machine and the line.

In this scenario, the Department of Industrial Engineering of Florence University (D.I.E.F) has devised and defined a numerical model for the analysis of the interaction between the reciprocating compressor and the piping system. This research of an advanced methodology aims to estimate the pressure wave propagation along the suction and the discharge line of a reciprocating compressor and to predict the compressor performance in terms of in-cylinder pressure. The input to investigate this phenomenon has come from oil & gas industry and from the branch of industry involved in refrigeration systems and collaborating with the D.I.E.F department. These are some reasons why it has been resorted to a numerical model able to support the design phase of the reciprocating compressor; a numerical model predictive, flexible and fast enough which allows to easily estimate various compressor configurations. According to the

predetermined aim and through Matlab environment a 0D code has been realised for both for the simulation of the reciprocating compressor performance and the simulation of the wave propagation.

The numerical model can be divided into two main parts: the first is thermodynamic model of the compressor and the second is the model of the elements composing the compressor piping system. The compressor simulation is based on a quasi-stationary modelling; the thermodynamic parameters (like pressure, temperature, density etc., of the processed gas) are analytically computed step by step. During the simulation the gas flow across the compressor is managed by the automatic valves which dynamics is computed in parallel to the thermodynamic cycle. To model the compressor line elements (such as ducts, plenums, orifices, etc.,) it has been followed the mono-dimensional acoustic approach; this approach allows to calculate the pressure wave propagation across elements of simple geometry with a mono-dimensional development. In order to achieve a good simulation tool for the preliminary estimation of the interaction between the compressor and the piping system, the two models above-mentioned are matched together. To be more precise the signal produced by the reciprocating compressor model, in terms of pressure fluctuations (or of mass flow rate) at the discharge section and at the suction section, represents the input for the acoustic model of the pipeline elements; as a consequence the response of the pipeline represents the boundary conditions for the reciprocating compressor mode. The hybrid model has the task to predict the machine line interaction and the wave propagation along the line.

The 0D model of the compressor produces the input signal for the acoustic model of the line, the mass flow rate calculated at the suction and discharge of the compressor represents the driving forces of the line. The acoustic model elaborates the input data and as a consequence generates an acoustic response for the compressor. The compressor is, then, the source of the hybrid model while the pipeline elements are the boundary conditions for the compressor. The interaction between the two subsystems is reciprocal.

The present work consists of 4 chapters:

Chapter 1 contains the basic informations about the reciprocating compressor, its mechanical structure, the treating about its thermodynamic cycle and the causes that influence its normal behavior. Special mention is dedicated to the issue of the interaction between the compressor and the piping system.

Chapter 2 illustrates the basis of the theory of the acoustic wave propagation and, precisely, remarks the theory of the acoustic plane waves and their applicability domain: the solution of simple acoustic configurations, using the theory of the transfer matrix method, is shown. The characterization of an acoustic problem is described and the analysis of a volume whit a 3D complex geometry (discharge chamber of a reciprocating compressor) has been carried out.

Chapter 3 is dedicated to the description of the numerical models: the model of the compressor analysis, named RE.CO.A (reciprocating compressor analysis) and the hybrid model. The RE.CO.A code is a quasi-stationary model defined in the time domain; step by step all the thermodynamics parameter of the cycle are computed. For the simulation of the valve dynamics a proper sub model is defined in order to compute with accuracy the valve motion. Then it is described the calibration process of the numerical model, based on the indicating cycle measured on a real reciprocating compressor; the experimental setup for the measurement of the indicating cycle is reported too. According to the experimental data, it is then performed the procedure adopted for the calibration of the numerical model. The second part of the third chapter refers to the hybrid approach, focusing on the interaction between the time domain model of the compressor and the frequency domain model of the piping system elements. The reliability of this passage is proved by studying simple cases in which the signal passes from the time domain to the frequency domain, and vice versa, using the FFT and IFFT tools.

Chapter 4 includes the results of this activity demonstrating the potentiality of this kind of approach and the reliability of the methodology adopted. Some configurations of the compressor-pipeline system are tested: the first configuration is the simulation of the compressor provided with the plenum on the suction and on the discharge; the reciprocal influence of the compressor on the pipeline and vice versa is investigated. Even the sensibility to the variation of the pipeline geometry is tested in order to evaluate the coherence of the hybrid model. The same analysis has been carried out for a twin cylinder

compressor provided with a plenum on the discharge and on the suction side. The configuration of the suction plenum is: two inlets and one outlet, the suction ducts of both the cylinders converge to the inlets, while the outlet is connected to the pipeline. The same description is valid for the discharge plenum; even in this case the coherence of the hybrid model has been tested. Finally it is shown the possibility to perform the simulations with the hybrid model in case of pipeline elements with a complex 3D geometry. A test case, in which the reciprocating compressor model is coupled with the model of its real suction and discharge chambers (located in the compressor head), has been performed. The test has the aim to examine the feasibility of this kind of modelling, making the hybrid model attractive even for the analysis of configurations characterized by elements with a marked 3D shape. The modelling of 3D elements with hybrid approach is very innovative and can overcome the limitation of a mono-dimensional modelling which cannot simulate geometrical complex elements.

1 The reciprocating compressor

The reciprocating compressor is a machine able to increase the pressure of a gas. Pressure increase of air by applying mechanical work had already been realised in early times. In the Middle Ages hand operated bellows were used in metal foundries. Otto von Guericke developed in 1641 an air pump to create vacuum: that was the basis of the spectacular test, with the Magdeburg semi-spheres (illustrated in Figure 1.1). This engraving, so elementary but at the same time so innovative, can be considered and taken as the forerunner of today's piston compressors.

Figure 1.1 - Engraving taken from 'Experimental Nova' (1672) by Otto von Guericke showing his experiment, carried out at Magdeburg, with an evacuated sphere. In this demonstration 16 horses could not pull apart the two halves of an evacuated sphere, known from then on as Magdeburg hemispheres. On 8 May 1654, he performed the experiment.

The development of reciprocating compressors has been supported by the born of the steam engine, in fact the machines are both conceptually analogous even though the

compressor transfers the work to the fluid and the steam engine, otherwise, receives the work from the fluid. Figure 1.2 shows an example of a reciprocating compressor acted by a steam engine.

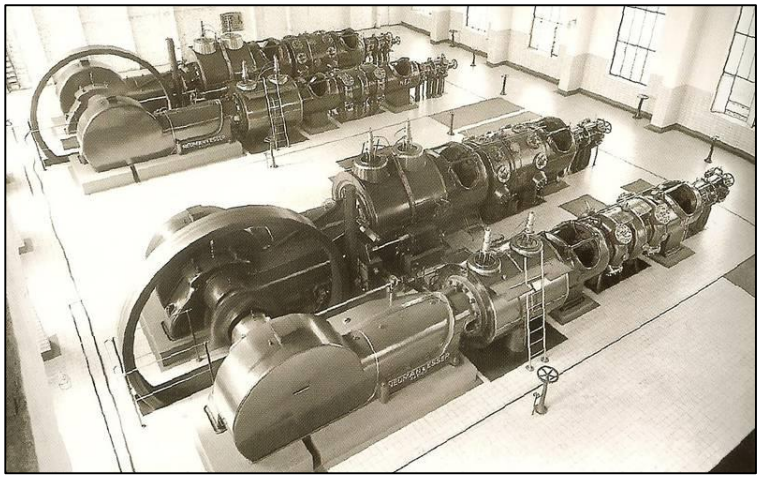

Figure 1.2 - An example of reciprocating compressor acted by a steam engine

Nowadays reciprocating compressors are employed in many various daily applications: from the little compressors for refrigeration systems (like refrigerators or heat pumps) to the big multistage compressors for industrial applications. A far wide range of applications of reciprocating compressors can be found in oil & gas industry: oil refineries use them in processes requiring high pressure delivery of essential gases. Natural gas industry utilizes reciprocating compressors to transport gas via cross country pipelines; these compressors can also be found in chemical plants, refrigeration plants, air compressors for tooling and so on. The following picture, Figure 1.3, depicts the application chart of the industrial compressors in which is specified the field of application of the main typologies of compressors: reciprocating, centrifugal and screw compressors. The main advantages taken by the use of the reciprocating compressor are:

- High compression efficiency respect to centrifugal compressor for the same flow; rate and pressure ratio, especially for pressure ratios over 2;

- Capability to achieve high compressor ratio with few stages;

- Low sensitive to changes in gas properties, especially molecular weight;
- Effective even for low molecular weight gases;
- Good adaptability to varying the flow rate.

The main disadvantages of reciprocating compressors are:

- High plot area for installation for a given flow rate respect to centrifugal compressors;
- Machine is big and heavy with respect to its flow rate capacity;
- Installation costs are higher respect to centrifugal compressor;
- Presence of many pressure pulsation above surge point;
- Necessity of auxiliary plenum systems above the surge point in order to minimize the pulsation phenomena;
- Presence of lube oil contamination in the process gas because of the necessity to lubricate the crank thrust.

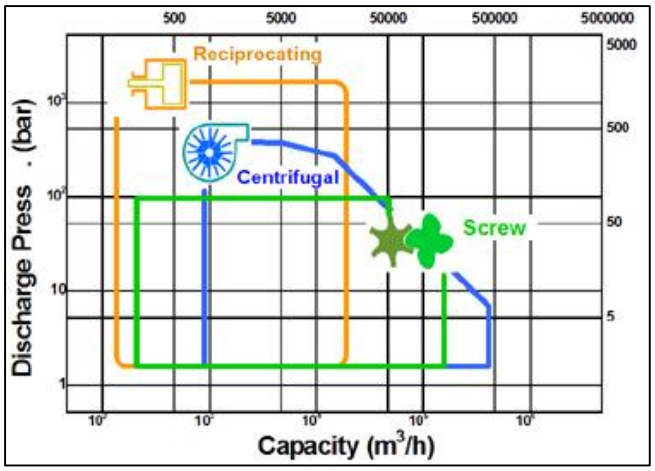

Figure 1.3 – Field of application of the compressors in function of pressure and volumetric flow

1.1 The reciprocating compressor: structure and functioning

The *reciprocating compressor*, Figure 1.4, is an operative machine acted by a driver unit, dedicated to the compression of gas. The main compressor shaft receives a rotating movement that, through a system composed by connecting-rod and crank, is converted in reciprocating motion to be then transferred to crosshead, rod and piston. This last component slides into a cylinder and produces the compression of the gas inside the two cylinder ends, that's to say, forward (cylinder head side) and backward (crank-mechanism side): this is the -so called- *double acting* arrangement (Figure 1.5). Sometimes the piston compresses the gas into one of the cylinder ends only: a cylinder having such an arrangement is named *single end*.

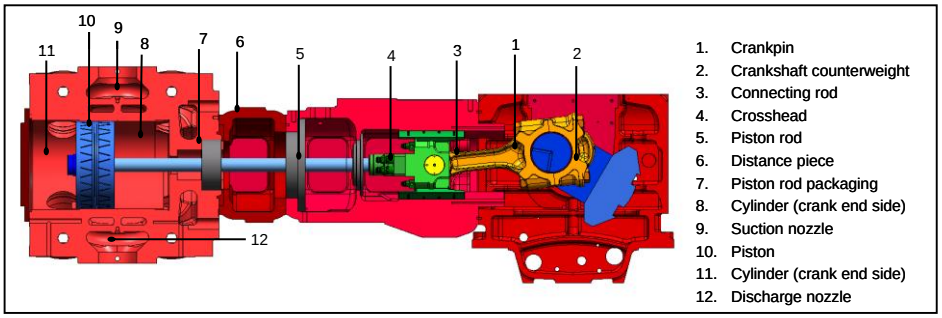

Figure 1.4 – Typical reciprocating compressor

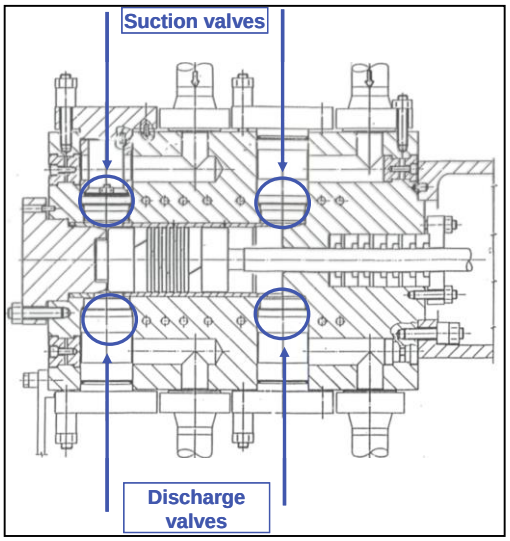

Figure 1.5 – Double acting arrangement

The inlet and the outlet of the gas from the cylinder, usually, takes place through automatic valves: the valves get opened by the action of a differential pressure (upstream and downstream of themselves) and closed by the work of dedicated springs, whose loads are opposed to the direct gas flow housed just into the valves (Figure 1.6).

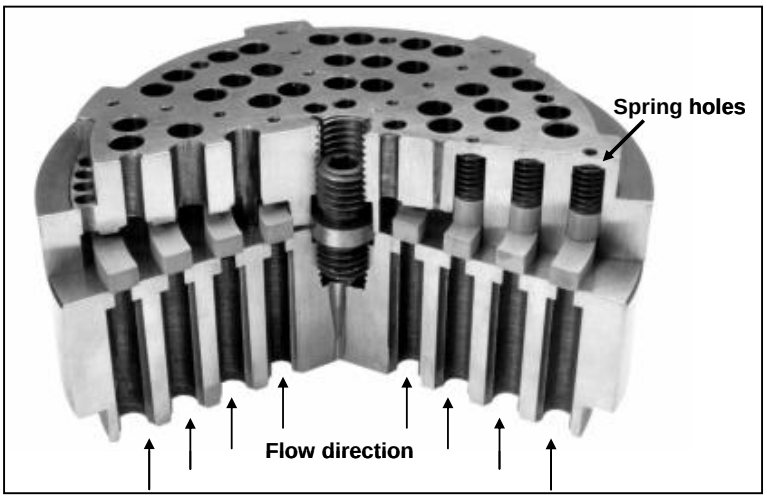

Figure 1.6 – Reciprocating compressor automatic valve

1.2 Ideal cycle

The reciprocating compressor is a machine that transfers the power received at the shaft to the handled gas by increasing its pressure from the suction value to the discharge one; the necessity to predict its performance in terms of adsorbed power, volumetric efficiency, maximum discharge temperature, real mass flow rate etc., imposes a rigorous analysis of the thermodynamics cycle characterizing such a kind of machine. The analysis of the ideal cycle is the first and easiest way to approach the problem: Figure 1.7 shows, through the Clapeyron diagram, the trend of the in-cylinder pressure vs the displacement; the graph is obtained considering only ideal transformation of the gas.

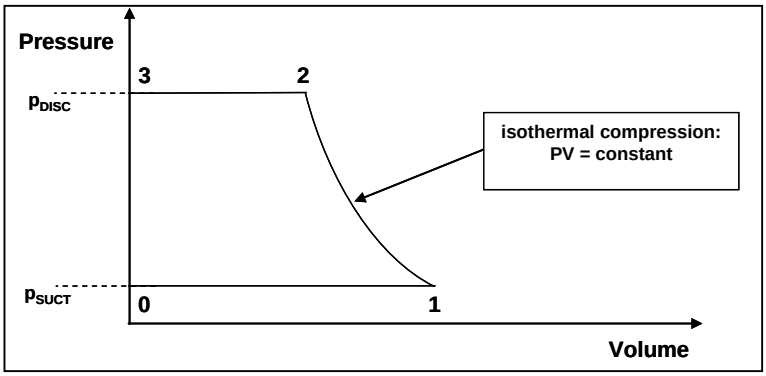

Figure 1.7 – p-v diagram for the ideal cycle

A such represented ideal cycle consists of the following *phases*:

- *0–1→suction*, or gas inlet into the cylinder: at constant pressure p_s (the suction ambient pressure), the piston moves from the top death point (TDP) to the bottom death point (BDP) and the entire displacement get fill up with the gas at suction pressure and temperature;

- *1–2→ compression* at constant temperature (isothermal): for an ideal cycle it is associated to the minimum expenditure of power;

- *2–3→ discharge*, or compressed gas outlet from the cylinder: at constant pressure p_d which is the pressure of the discharge ambient;

- *3–0→pressure drop*: due to the complete delivery of the gas at the end of the discharge phase and to the reversal piston motion. It is important to highlight that in case of presence of a clearance between the piston at the TDP and the cylinder head the residual gas undergoes to an isothermal expansion process.

Therefore, reading the graph, the cycle is made of four phases: two isobaric curves occurring at the gas inlet/outlet phases, one isothermal corresponding to the gas compression (its pressure increase from the suction value up to the discharge one), one phase at constant volume (isochoric transformation) corresponding to the instantaneous pressure reduction into the cylinder and due to the complete delivery of all compressed gas. The *power spent* because of gas compression is represented by the closed area of the cycle.

1.3 Theoretical cycle

The real gas compression cycle does not correspond to the aforementioned processes: the behaviour is indeed different because of the influence of particular phenomena occurring in the real machine.

The *theoretical cycle* can be often considered a good approximation of the real one, whereby it takes into account the main aspects of the real physical processes. However some secondary effects are, in general, neglected, such as (for example): the presence of the lubricant oil, the increase of certain losses due to the wear of the components and many others. Figure 1.8 shows a typical theoretical cycle. The blue dashed lines indicate an ideal cycle which operates in the same discharge and suction pressure conditions, handling the same gas capacity per cycle; one can immediately notice that the work (equal to the internal area of the corresponding cycle), spent for the ideal cycle, is sensibly lower than the theoretical one.

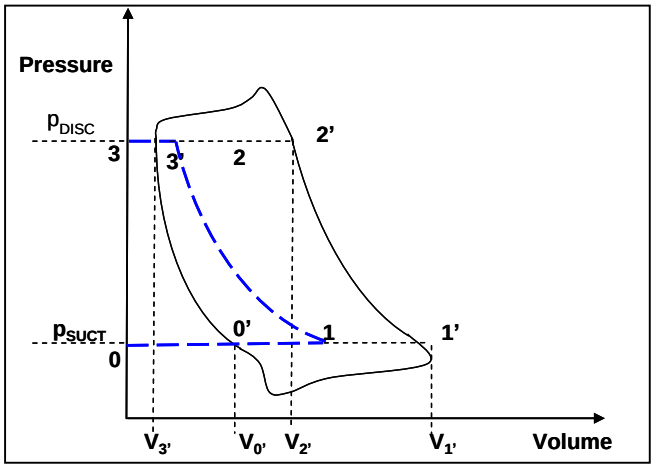

Figure 1.8 – Theoretical cycle vs Ideal cycle

The non-idealities considered and modelled in a theoretical cycle are subsequently listed:

- Gas heating at the suction side modelling;
- Deviation from isothermal compression;

- Cylinder pockets;
- Gas leakages;
- Pressure drops due to valves.
- The phases of the ideal cycle are consequently modified:
- *0'–1'*: the intake phase actually takes place from point *0'* to *1'* (see the last bulleted point of this paragraph). Furthermore the suction pressure is lower than the ideal cycle: this is due to the opposition of the valves to their opening and to the pressure losses occurring along the suction components;
- *1'–2'*: the compression does not follow an isothermal process but it can be described by a polytrophic law, which is steeper than the isothermal one;
- *2'–3'*: similarly to suction phase, the discharge pressure inside the cylinder is different from the ideal constant discharge pressure, in particular it is higher, thus causing the increase of the compression work;
- *3'–0'*: the pressure drop is not instantaneous but it occupies a share of the piston stroke, from point *3'* to point *0',* which in the ideal cycle belonged to the gas intake. This change is due to the re-expansion of the gas, trapped into the cylinder clearances, from discharge to suction pressure. The net part of the suction stroke dedicated, to the intake, is then reduced and the working fluid capacity of the real machine decreased.

1.3.1 Effects due to valves

The ideal compression cycle is modified by two main effects deriving from the presence of valves. The first one is provoked by the preload of the springs and the other one is due to the gas pressure drop during its passage through the valves. The two influences of springs preload and valve pressure drop on the theoretical cycle are examined separately for a better clarification even if, actually, they occur simultaneously. A scheme of a valve in Figure 1.9.

First of all it must be taken into account that an automatic valve is equipped with antagonist springs, required to assure its closure: because of the preload, the valve offers a certain opposition to its opening.

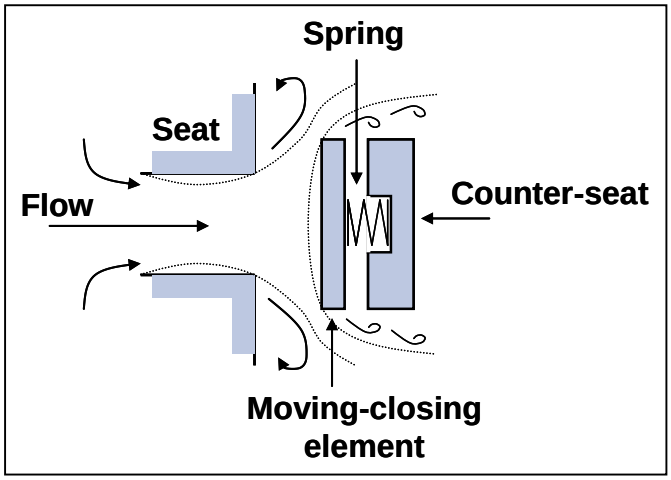

Figure 1.9 – Schematic of a valve

This opposition delays the opening of the valve: a lower initial suction pressure, inside the cylinder, and a higher initial pressure, during the discharge event, are established with reference to the pressures considered in the ideal cycle. Therefore this effect results in a higher compression ratio (with the same nominal suction and discharge pressures) developed only to overcome the already described springs opposition.

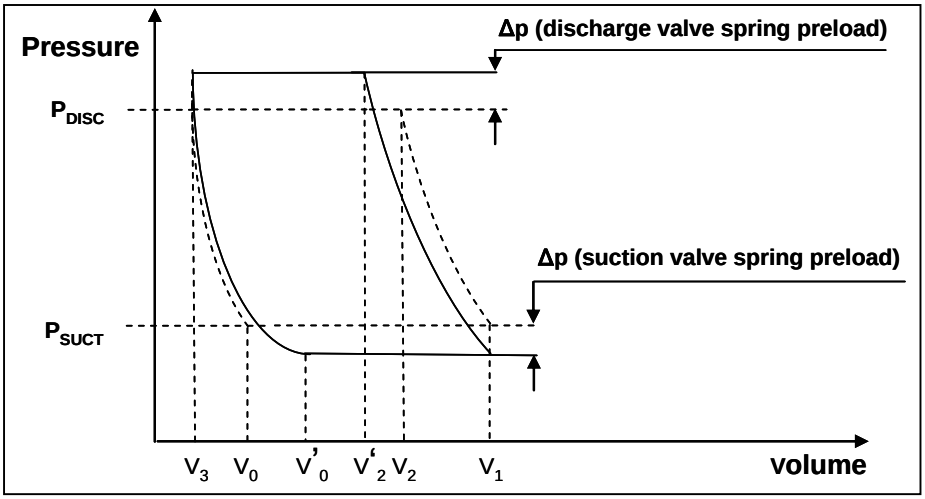

Figure 1.10 – Effect of springs preloads on the theoretical cycle

Due to the higher compression ratio, the capacity decreases because of two main causes (refer to Figure 1.10):

- The overpressure -at the end of the discharge phase- establishes a sucked capacity reduction for the re-expansion, starting at a higher pressure, gets completed at a bigger volume;

- The decrease in intake pressure determines a proportional decrease in gas density, thus reducing the mass flow rate.

The power spent for the gas compression is increased by the contributes of the valves opposition at their opening (almost rectangular areas between the isobars, related to the nominal pressures, and the new cylinder inner and discharge pressures), and partially reduced by the smaller handled gas capacity. At this point it must be taken into account the second effect, due to the fact that the opening valves allow a certain gas passage area, and which consequently establishes no negligible pressure drops during the gas passage. The compression cycle is consequently modified as shown down by Figure 1.11.

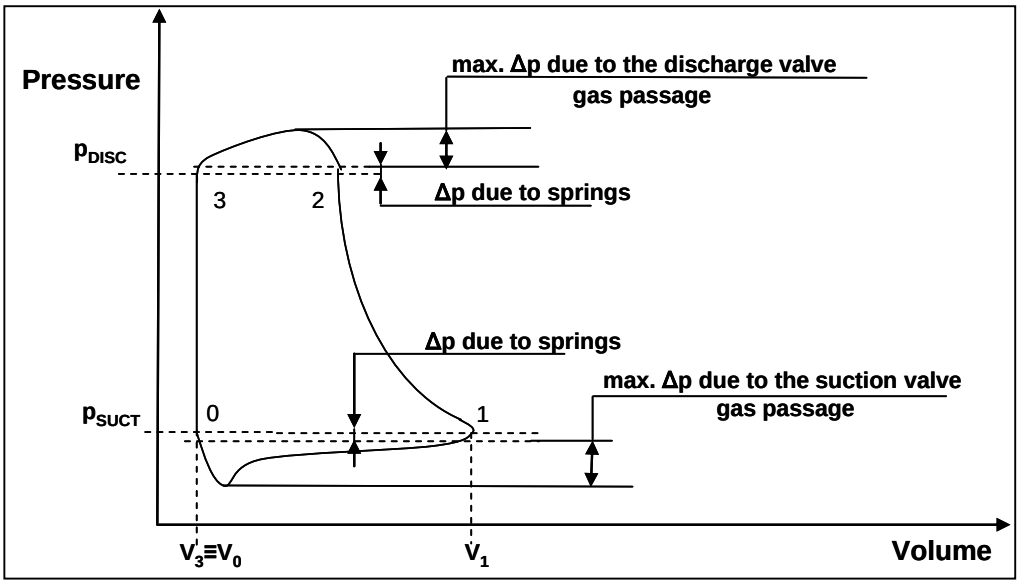

Figure 1.11 - Ideal compression cycle, modified by the springs and by the valves pressure drop

These pressure drops are proportional to the square of gas passage instantaneous velocities, which are variable during one revolution of the compressor shaft, being

directly proportional to the piston instantaneous velocity. The opposition of the valves to the gas passage establishes further pressure drops acting to reduce the cylinder inner pressure at the suction phase and to increase the cylinder inner pressure during the discharge phase. It results in a greater compression ratio (at the same nominal suction and discharge pressures) developed only to overcome the further pressure drops due to the flow motion. Consequence of the greater compression ratio is that gas discharge temperature and power spent for the compression are both increased. The effect of the valves losses can be taken into account by introducing a corrective factor [9] (ψ_v) smaller than one, to reduce the nominal sucked gas capacity.

Finally, we have to consider how to evaluate two of the most important parameters of the valve that can give indication about their performances: valve pressure drop and valve absorbed power. The valve pressure drops Δp_v, due to the gas passages can be evaluated, in a simplified way, with the well-known formula:

$$\Delta p = \rho \xi \frac{V^2}{2} \qquad \textbf{1.I}$$

Where:

- ξ is the loss coefficient of the valve, depending on its fluid dynamics features and its geometrical size;
- ρ is the gas density at the thermodynamic conditions of its passage through the valve;
- V is the gas velocity through the valve.

On the base of this formula it is possible to calculate, in first approximation, both the maximum valve pressure drop and the average pressure drop depending only on the values of the valve gas velocities: maximum or average. The valve absorbed power (or the energy dissipated during the passages of the gas through the valves during suction, P_{suct}, and discharge, P_{disc}, phases) can be evaluated by the following formulas [9]:

$$P_{suct} = {V_{suct}}^2 C \xi_{suct} \lambda (3 - 2\lambda) \qquad \textbf{1.II}$$

$$P_{disch} = {V_{disch}}^2 C \xi_{disch} \frac{\lambda}{r^{\frac{1}{\gamma}}} \left(3 - 2 \frac{\lambda}{r^{\frac{1}{\gamma}}} \right) \qquad \textbf{1.III}$$

Where:

- P_{suct} and P_{disch} are the powers absorbed by, respectively, the suction and discharge valves;
- V_{suct} and V_{disch} are, respectively, the suction and discharge valve gas average velocities;
- C is the volumetric capacity of gas passing through the valve;
- r is the compression ratio (discharge pressure divided suction pressure);
- γ is the ratio between the specific heat capacities;
- λ is a parameter that will be defined in the next paragraph, called filling coefficient.

1.3.2 The other sources of loss

Hereafter there are depicted the other sources of loss affecting the reciprocating compressor thermodynamic cycle. First there is the problem of the gas heating at the suction side. Since the work spent for the compression establishes an increase in temperature of the compressed gas, consequently the latter transfers part of the received heat to the cylinder, both to its mechanical components and to its cooling medium (if provided). Therefore the gas sucked at the intake side at cycle by cycle increases its temperature while is approaching the cylinder. The latter keeps an intermediate temperature between suction and discharge ones: it follows that at the end of the suction phase, the cylinder is effectively filled with a gas warmer than that arriving at the compressor from the suction line; consequently its density is lower and the capacity reduced. This effect can be taken into account by introducing a corrective factor (ψ_H) smaller than one, in order to reduce the nominal sucked gas capacity.

Another significant problem is represented by the deviation from isothermal compression during the compression stage. The phenomenon of gas heating during the phase of its pressure increasing, due to friction both between gas molecules and

mechanical parts, proves that the isothermal curve is replaced by a polytrophic compression curve. Generally the compression polytrophic curve can be considered adiabatic (without heat exchange) with sufficient approximation, according to the following law:

$$pv^{\gamma} = constant \qquad \textbf{1.IV}$$

Where:

- p is the gas pressure inside the cylinder,
- v is the volume of the gas inside the cylinder.

We should notice that the assumption of adiabatic compression is in contrast with what explained before. In other words, the phenomenon of gas heating at the suction side implies the presence of heat release during the compression process. This is obviously in conflict with the just made approximation of adiabatic compression. Therefore it is not possible to calculate the amount of gas heating at the suction side if this kind of transformation is supposed. This contrast is common in the reference literature and it is going to be neglected in the next exposure: to put it better, the compression work is calculated assuming an adiabatic transformation and the heat transfer is calculated apart, making the two phenomena disconnected, at least in first approximation. The new cycle is shown in Figure 1.12.

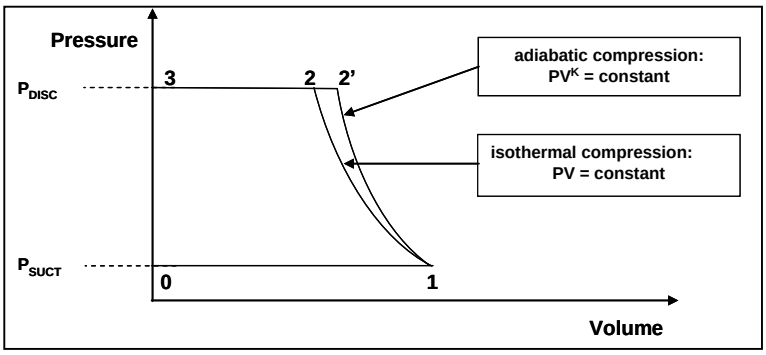

Figure 1.12 - Ideal cycle with "real" compression

Then the presence of the cylinder clearance affects the amount of total volume where the gas is compressed. When the piston arrives at the dead centre at the end of the

discharge phase, the cylinder inner volume left at the gas disposal cannot be zero due to the following physical residual volumes:

- Volumes between piston circular base surfaces and front surfaces of the head (forward end) and of the cylinder (backward end), necessary to avoid mechanical impacts;
- Inner volumes own of the valves;
- Volumes between valves and cylinder bore;
- Volumes between the outer profile of the piston and the cylinder bore.

Therefore a certain amount of residual gas still remains to fill all the volume at its disposal at the discharge pressure. During the next phase (expansion) the piston reverts the motion direction resulting in both a re-expansion of residual gas entrapped into the cylinder and a temperature reduction (phenomenon opposed to what instead happens during the polytrophic compression).

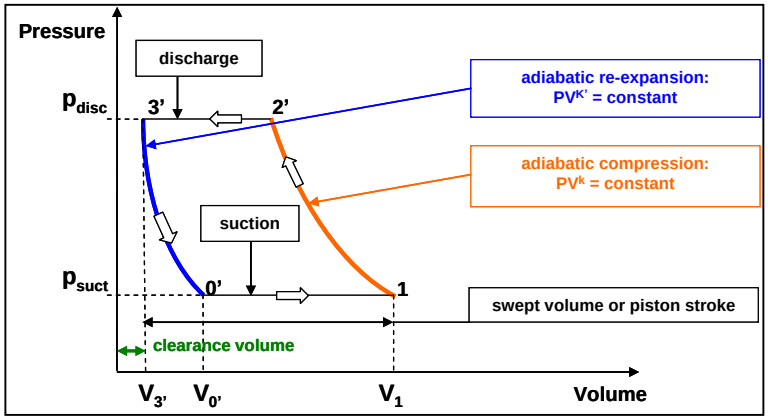

Figure 1.13 - Theoretical compression cycle with clearance effect

Also this re-expansion curve can be considered adiabatic in first approximation (Figure 1.13) and that does not happen with the same γ-exponent of the compression, but according to a new factor, γ', lower than the one relative to the adiabatic compression:

$$\gamma' = \gamma - 1 \qquad \textbf{1.V}$$

The re-expansion is completed when the cylinder inner pressure is reduced to the value of the suction pressure, allowing the opening of the suction valve. It derives that the piston stroke dedicated to the gas suction is reduced. In the *p-v* cycle, the volume

difference v_1-v_3' corresponds to the cylinder displacement (v_c), i.e. the volume swept by the piston. The effect of the clearance volume v_3' on the reduction of the handled capacity is higher as higher are both the clearance itself and the compression ratio, as Figure 1.14 and Figure 1.15 highlight. The main parameters that fix the effect of the clearance volume on the capacity, from an analytical standpoint, are the following two [9]:

- *filling coefficient*, that gives indication about how much of the cylinder volume is effectively used in order to get the cylinder capacity:

$$\lambda = \frac{v_1 - v_{0'}}{v_1 - v_{3'}} \qquad \textbf{1.III}$$

- *clearance volume ratio*, that gives indication about how much of the cylinder volume is corresponding to the gas residual volume inside the cylinder at the end of the discharge phase:

$$\sigma = \frac{v_{3'}}{v_1 - v_{3'}} \qquad \textbf{1.IIII}$$

These two parameters are connected together by the following law that just establishes the filling coefficient as function of the clearance volume:

$$\lambda = 1 - \sigma\left[\left(\frac{p_d}{p_s}\right)^{\frac{1}{\gamma'}} - 1\right] \qquad \textbf{1.IVII}$$

The parameter λ gives indication about the capacity that can be got from the particular selected cylinder, once the clearance volume σ is known as a function of the compression ratio and, similarly it can be used to compare cylinders involved in the same application, assuming that all the other sources of losses are not taken into account in the comparison.

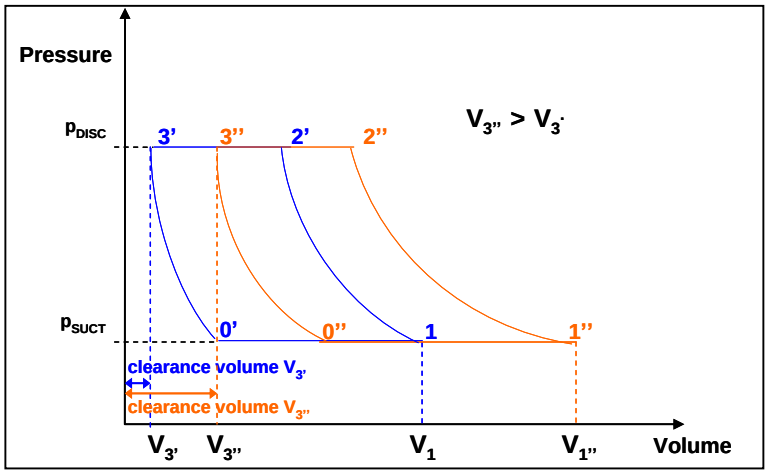

Figure 1.14 - Effects of higher clearance volume on the capacity

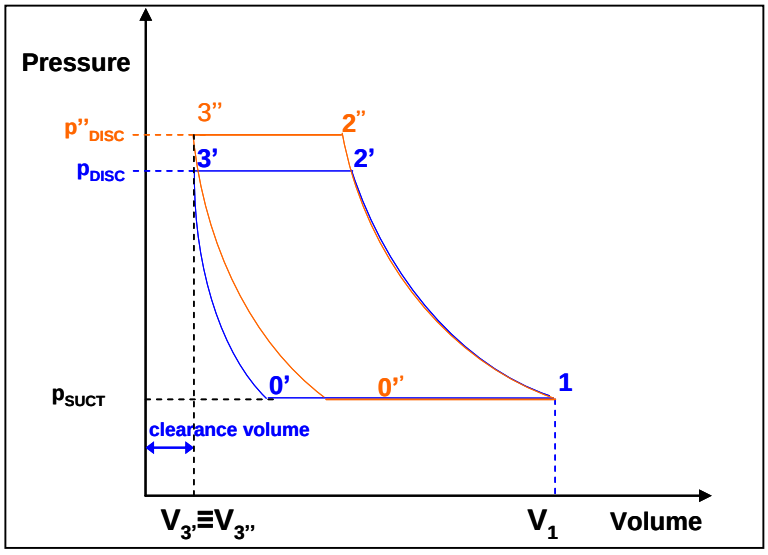

Figure 1.15 - Effects of an increase of pressure ratio on the capacity

The enclosed area of the cycle, between the two isobars related to the suction and discharge pressures and between the two transformations of compression and re-expansion, represents the work spent for the gas compression. Therefore from such area, taking into account the compressor rotational speed, it can be obtained the indication of the spent power for the gas compression.

Another effect affecting the ideality of the thermodynamic cycle is represented by the gas leakages: this phenomenon inside the compressor cylinders can always occur for the seals (mechanical, with or without dedicated gaskets) cannot assure perfect gas tight.

These leakages, even if minimum, involve the following aspects, with reference to the gas path into the cylinder:

- Gas leakages through the suction and discharge valves, due to an imperfect sealing between the moving closing elements and the valve seats and to an imperfect sealing between valve seats and cylinder seats both;

- Gas leakages between the two cylinder ends through the piston rings. In fact, when on one side the pressure reaches its maximum value, on the other side it approaches its minimum, so the pressure difference equals the design pressure ratio.

The amount of the gas leakages depends on some parameters such as:

- molecular weight of the gas (greater leakages occur with lower molecular weight);

- compression ratio (greater leakages occur with greater *r*);

- rotational speed (greater leakages occur with lower speed);

- cylinders arrangement (greater leakages occur for dry lube cylinders and lower for the lubricated ones);

- operating hours after the last maintenance (greater leakages occur when the wear rate of the employed components is at the maximum level, close to the next scheduled routine maintenance of the cylinders).

This effect can be taken into account by introducing a corrective factor (ψ_L) smaller than 1, to reduce the nominal sucked gas capacity.

1.3.3 Cylinder performances

Generally it can be stated that each compression stage should have compression ratios within a certain defined and restricted range, in order to optimize the general performances of the compression system. In general it is recommended:

- to avoid very low compression ratios (indicatively not lower than 1,5), otherwise it will result a rather low compression efficiency due to the very high power dissipated

at the cylinder valves, compared to the adiabatic power necessary for the gas compression;

- to avoid very high compression ratios (indicatively not higher than 4), otherwise it will result both a rather low volumetric efficiency (low efficiency of the cylinder in terms of capacity) and an excessive discharge gas temperature.

Here are reported the expressions allowing to determine the fundamental mentioned parameter, that's to say the *volumetric efficiency*:

$$\eta = \frac{v_{suct}}{v_c} = \frac{C_{suct}}{C_c} \qquad \textbf{1.IX}$$

Where:

- − v_{suct} is the volume of the sucked gas by the compressor;
- − C_{suct} is the medium volumetric capacity, during intake phase, of sucked gas (not known parameter in general);
- − C_{cyl} is the volumetric capacity corresponding to the volume of the cylinder, calculated as a function of geometrical and operational parameters (like bore diameter, rod diameter, stroke, rotational speed):

$$C_{cyl=}\Omega_{cyl}V_p \qquad \textbf{1.X}$$

Where

- − Ω_{cyl} is the useful area of the cylinder;
- − V_p is the average piston velocity.

Since the volumetric efficiency can be expressed as a product of the filling coefficient λ and of the capacity total loss coefficient ψ, taking into account the phenomena previously described (gas heating, effects of the valves, gas leakages), it results:

$$\eta = \psi\lambda$$
$$\psi = \psi_v\psi_H\psi_L \qquad \text{1.V}$$

From the previous formula it can be calculated the sucked gas capacity:

$$C_{suct} = \eta C_{cyl} = (\psi\lambda)(\Omega_{cyl}V_p) \qquad \text{1.VI}$$

If the compressor handled gas capacity is one of the fundamental parameter for its sizing, necessary is to consider the value of the gas discharge adiabatic temperature too:

$$T_{disch} = T_{suct} r^{\frac{\gamma-1}{\gamma}} \qquad \text{1.VII}$$

Where:

- T_{disc} is the discharge adiabatic temperature;
- T_{suct} is the suction temperature.

This temperature must be restricted within a certain limit in order not to negatively affect the efficiency and the life of all cylinder components, especially of the non-metallic ones, particularly those of the piston seals, valves and packing.

The design of compressor with a too high compressor ratio leads to a low volumetric efficiency or to an excessive discharge gas temperature; it should be taken into account the possibility to divide the compression ratio in several compression stages, having all the same compression ratio, in primis to minimize the total power spent for the gas compression, consequently distributing and balancing it between all the stages. Nevertheless the multistage arrangement will involve a more complex and more expensive compressor

1.4 Piping system and auxiliaries

The reciprocating compressor in industrial application is necessarily composed of a lot of extra components that assure its properly functioning for a specific aim. A reciprocating compressor generates a pulsating flow through the inlet and outlet ducts,

so, a simple way to look at the problem is to consider the flux flow along the ducts as a consecution of some periodic pulses of flow that can be assimilated to portions of sinusoid (marked area in the graph of Figure 1.16). Figure 1.16 offers a scheme of the pulsating flow along the inlet duct, similarly Figure 1.17 shows a scheme of the pulsating flow along the outlet duct.

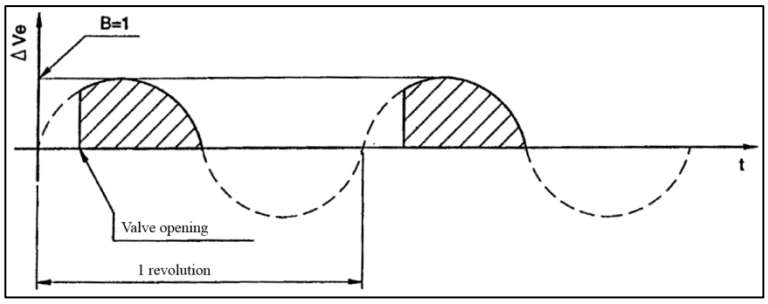

Figure 1.16 - Propagation of the pulsating flow along the intake duct

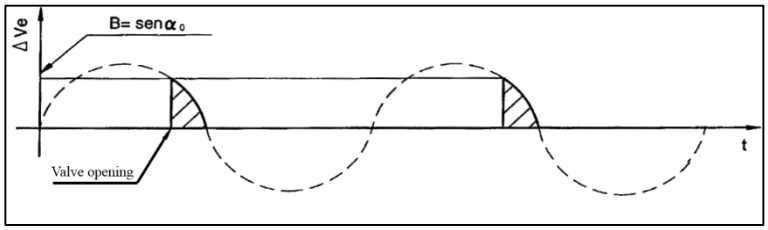

Figure 1.17 - Propagation of the pulsating flow along the outlet duct

For a double effect-reciprocating compressor the pulsating flow has a double frequency as Figure 1.18 and Figure 1.19 reveal.

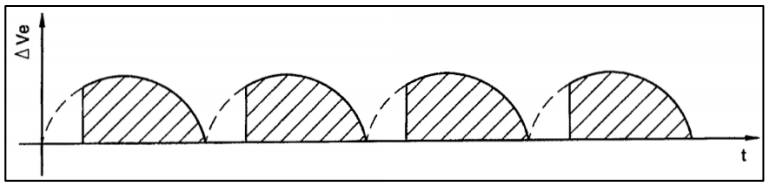

Figure 1.18 - Example of pulsating flow at the inlet of a double effect-compressor

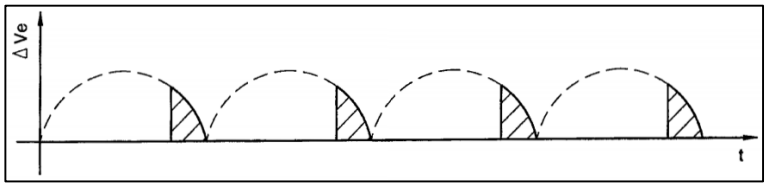

Figure 1.19 - Example of pulsating flow at the discharge of a double effect-compressor

This pulsating flow causes the propagation of pressure waves along the ducts. These pressure waves have a complex shape: they are composed by a fundamental wave, having the same frequency the reciprocating compressor cycle has, and by a sum of other harmonic waves with a frequency equal to a multiple of the base frequency and a decreasing amplitude. The fundamental wave is produced by the piston motion, while, the harmonic waves are originated by the flow passage through the valves. Along the ducts the pressure waves spread at the sound velocity interacting with the line singularities like curves, cross section variations, valves, etc.: this interaction causes the arise of reflected waves. The interaction between incident and reflected waves generates therefore the presence of acoustic resonances responsible of a series of phenomena affecting the pipe lines and the compressor itself [10].

Common problematic points affecting the reciprocating compressor system are:

- *Natural dynamic overeating (or underfeeding) of the cylinder*, it occurs when the suction stroke is near to an over pressure peak, so the gas goes inside the cylinder at a density higher than that at normal conditions (and vice versa);

- *Malfunctioning of the automatic valves*, it happens when the acoustic frequency of the pressure waves is the same frequency the natural resonance of the mechanical system of the valves has;

- *Sacking forces on the pipe line components*, the phase shift of the pressure wave at the ends of a component like a plenum causes an unbalancing of the forces acting on it, this phenomenon is the responsible of strong vibrations and sackings;

- *Mechanical vibration*s, they are the consequence of the pulsating forces inside a component of the system;

- *Noise*, it arises from the pulsating flux and from the pressure waves in the system;

- *Structural damages to the line and to the supports*, they are the undesired consequences of the mentioned phenomena.

A typical simplified scheme of a compressed gas plant is represented Figure 1.20; it is composed of the following components:

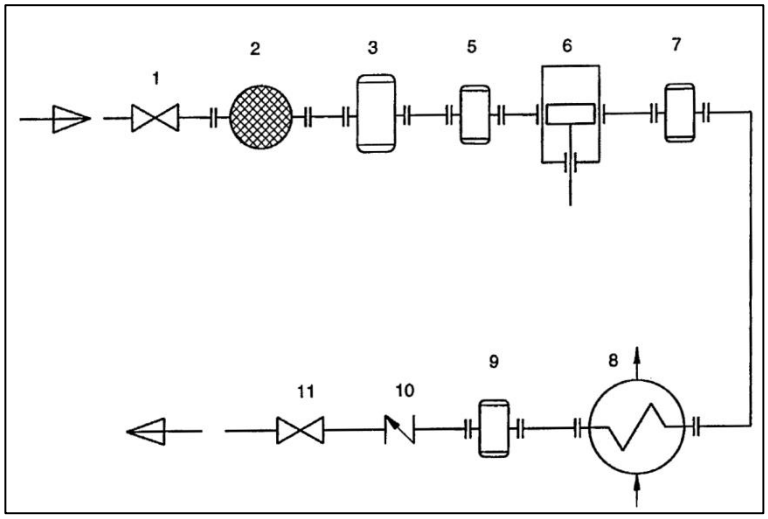

Figure 1.20 - Typical compressed gas plant

- 1 Interception Valve;

- 2 Gas filter to avoid the entrance of dust or abrasive particulate;

- 3 Separator, to eliminate the presence of vapor or oil particles in the gas flow;

- 4 Cooler, (eventually) to reduce the gas inlet temperature. As a consequence there is the increase of the gas density and then a reduction of the energy absorbed by the compressor;

- 5 Plenum, to reduce the pulsating pressure waves upstream the compressor;

- 6 Reciprocating compressor;
- 7 Plenum, to reduce the pulsating pressure waves downstream the compressor;
- 8 Cooler, (eventually) to reduce the gas outlet temperature;
- 9 Separator, to eliminate the presence of condense caused by the cooling system or oil due to the lubrication in case of lubricated compressor;
- 10 Non return valve, to avoid a return of the compressed gas to the compressor in case of machine stop;
- 11 Interception valve,

The pulsation generated by a reciprocating compressor can be particularly high causing an increase of downtime and maintenance costs.

1.4.1 Pulsating flow issue, acoustic filter design

In order to face the issue of the transient pulsating flow, generated by a reciprocating compressor, it is important to provide the pipe line with the right acoustic filters. The design of the acoustic filters is strongly related whit the entire reciprocating compressor design [11] as depicted into the scheme of Figure 1.21

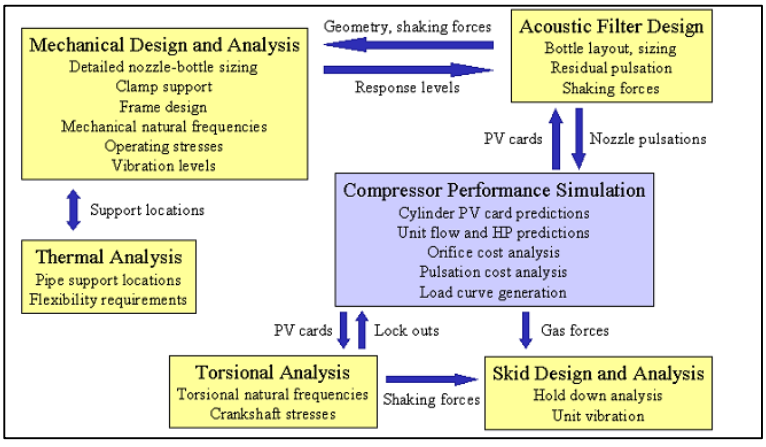

Figure 1.21 - Scheme of the interaction between the pulsation design and the entire compressor design.

The elements commonly used in order to alter the flow pulsation are: surge volumes, pressure drop elements like orifice and restrictions, and acoustic filters. To

reduce pulsation in high flow environment, using only surge volume, it would require an unrealistic large sure volume, for this reason acoustic filter represents a better solution. An acoustic filter is typically characterized by a volume-choke-volume configuration and it is associated to a specific Helmholtz resonance, this resonance depends directly on the choke tube length and diameter and on each volume elements. Commonly acoustic filters are designed to have a Helmholtz response a 20 - 30% below the lower frequency, so they attenuate pulsating frequencies above the Helmholtz frequency, they let them pass on (below Helmholtz frequency) and amplify pulsation near Helmholtz frequency, Figure 1.22.

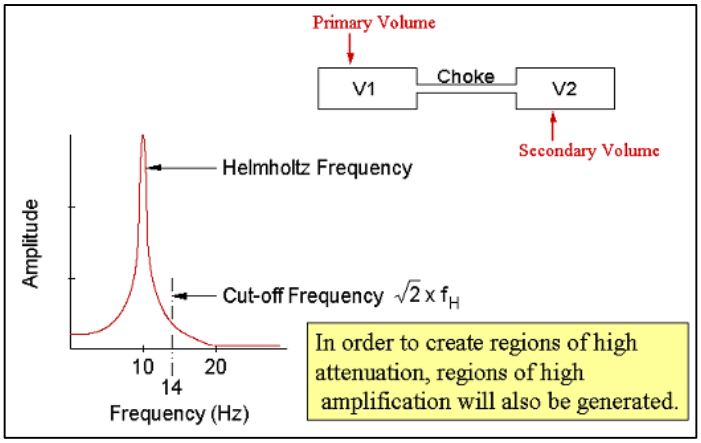

Figure 1.22 - Acoustic filter scheme

The impedance function of an acoustic filter is characterized by three zone of attenuation and three zone of resonance; for the sake of simplicity in Figure 1.23 is depicted the major response left to the system once the pulsation filter is installed [11].

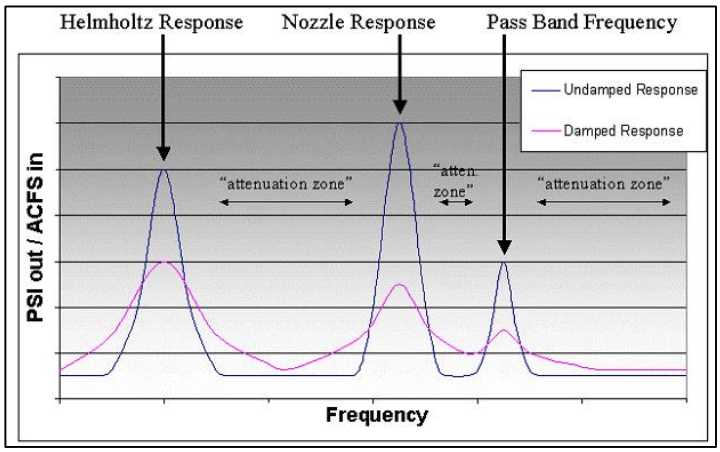

Figure 1.23 - Filter Impedance function

The nozzle response depends on the cylinder nozzle length, on the internal dimension of the cylinder and the first surge volume dimension; the Helmholtz and Pass Band response depends on filter dimensioning. The challenge for the designers is to avoid the resonance zones; modern variable high speed unit get this aim very difficult to achieve.

The acoustic filters are divided into two typologies, two bottle acoustic filters and one bottle acoustic filters; the first typology is used in case of low speed (~300rpm) double acting reciprocating compressors, the second typology is applied to high speed (~1000rpm) single acting reciprocating compressor. In Figure 1.24 is depicted an example of a two bottle acoustic filter, it is designed to allow the positioning of the Helmholtz response between the first and the second order frequency of the system. Its main features are:

- Symmetry minimizing pass band responses. For example, the external choke tube and secondary bottle may be identical in length, thereby generating a single pass band frequency;

- Baffles and internal choke tubes establishing separate cylinder chambers and minimizing bottle acoustic shaking forces.

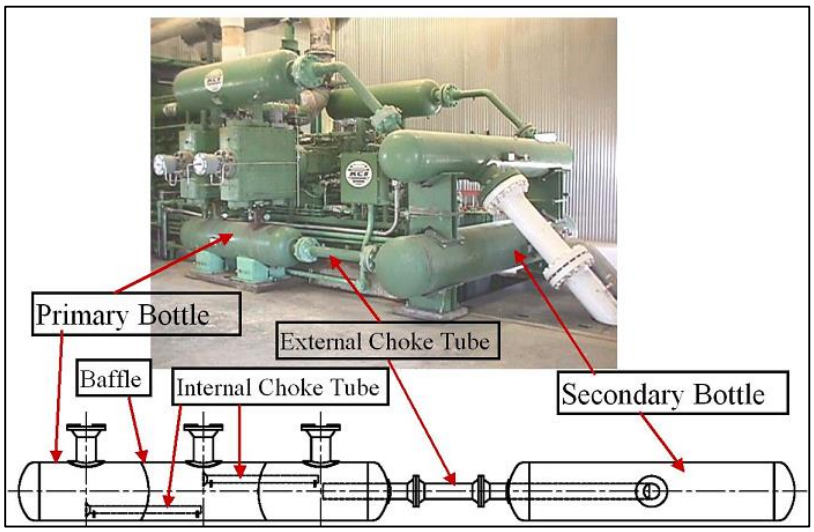

Figure 1.24 - Two bottle acoustic filter for low speed compressors

An example of single bottle acoustic filter designed for high speed compressor is shown in Figure 1.25.

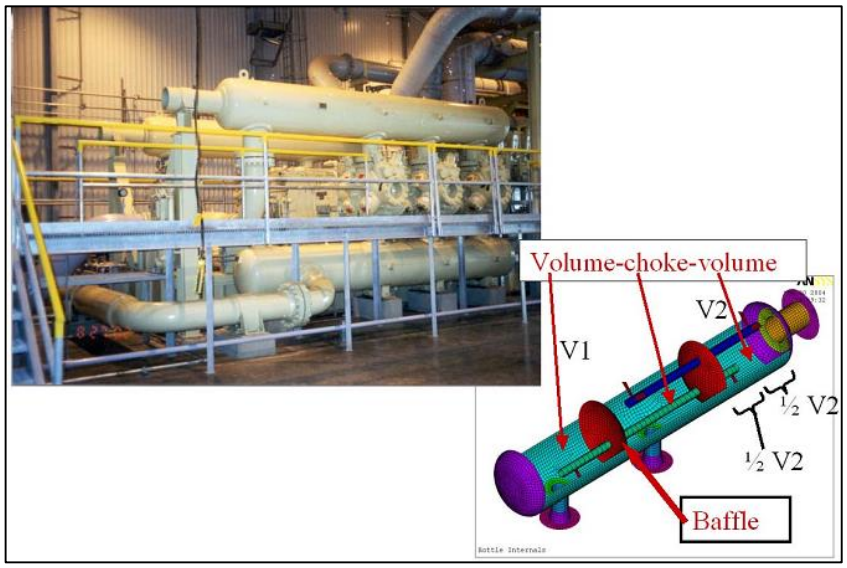

Figure 1.25 - Single bottle acoustic filter for high speed compressors

Its main features are:

- Baffles and internal choke tubes to establish separate cylinder chambers, which minimize bottle acoustic shaking forces and create a secondary volume (V2) for filtering;

- Center feeding pulsations from the compressor into the cylinder chambers to minimize excitation of a chamber length response. Inlets and outlets of internal choke tubes are located at the midpoints of cylinder chambers and line chamber whenever possible to again incorporate center feeding of pulsations;

- A separate choke tube for each cylinder, which typically reduces pressure drop; in fact a limiting factor associated with placement of the Helmholtz response is maintaining a reasonable pressure drop in the choke tubes.

2 Acoustic theory

2.1 Propagation of waves in ducts

In acoustic theory the perturbations of a fluid in a duct can be considered as acoustic plane waves if the following conditions are verified [12]:

- Not viscous fluid;
- Infinitely rigid duct walls;
- Limited perturbation amplitude.

In this case the perturbation of the fluid in the duct is the same on a defined section and it is normal to the flux direction. At the basis of acoustic theory there are the following equations:

Mass continuity

$$\rho_0 \frac{\delta u}{\delta z} + \frac{\delta \rho}{\delta t} = 0 \qquad \textbf{2.I}$$

Dynamic equilibrium

$$\rho_0 \frac{\delta u}{\delta t} + \frac{\delta p}{\delta z} = 0 \qquad \textbf{2.II}$$

Energy equation (isoentropicity)

$$\left(\frac{\delta p}{\delta \rho}\right)_s = \frac{y(P_0 + P)}{\rho_0 + \rho} \cong \frac{yP_0}{\rho_0} = a_0^2 \qquad \textbf{2.III}$$

Considering that, $\rho = \frac{P}{a_0}$, $\frac{\delta \rho}{\delta t} = \frac{1}{a_0}\frac{\delta P}{\delta t}$, $\frac{\delta \rho}{\delta z} = \frac{1}{{a_0}^2}\frac{\delta P}{\delta z}$, where a_0 is the sound velocity, equation 2.III can be defined:

$$\left[\frac{\delta^2}{\delta t^2} - a_0^2 \frac{\delta^2}{\delta z^2}\right]\rho = 0 \qquad \textbf{2.IV}$$

Equation 2.IV is the basic description of the wave propagation and its solution is the composition of 2 waves having velocity a_0, opposite direction and amplitude (C_1 and C_2 respectively); the equation 2.V (2.VI) describes the solution we had referred to:

$$p(z,t) = C_1 f(z - a_0 t) + C_2 g(z + a_0 t) \qquad \textbf{2.V}$$

$$p(z,t) = [C_1 e^{-jk_0 z} + C_2 e^{jk_0 z}]e^{jwt} \qquad \textbf{2.VI}$$

In the same way it is possible to obtain the mass flow ($v=\rho u S$) relation:

$$v(z,t) = \frac{1}{y_0}[C_1 e^{-jk_0 z} - C_2 e^{jk_0 z}]e^{jwt} \qquad \textbf{2.VII}$$

Where:

- $z_0 = \rho_0 a_0$ is the characteristic impedance of the medium;
- $y_0 = \frac{a0}{S}$ is the characteristic impedance of the duct;
- $k_0 = \frac{w}{a0}$ is the wave number or propagation number, for plane wave.

The subscript "0" indicates the inviscid stationary medium condition. In case of viscous medium the acoustic wave propagation undergoes a progressive reduction in amplitude. So the standing wave solution becomes:

$$p(z,t) = [C_1 e^{-\alpha z - jkz} + C_2 e^{\alpha z - jkz}] e^{jwt} \quad \textbf{2.VIII}$$

$$v(z,t) = \frac{1}{y}[C_1 e^{-\alpha z - jkz} + C_2 e^{\alpha z + jkz}] e^{jwt} \quad \textbf{2.IX}$$

Where:

- $y = y_0 \left[1 - \frac{\alpha}{k_0} + j\frac{\alpha}{k_0}\right]$, is the acoustic impedance in the vicous medium;
- $k = k_0 + \alpha$, is the wave numeber in the viscous medium;
- $\alpha = \frac{1}{r_0 a_0}\left(\frac{u\mu}{2\rho_0}\right)^{\frac{1}{2}}$ is the attenuation constant; r_0 duct radius, μ fluid viscosity.

2.1.1 Theory of acoustic filter

An acoustic filter consists in an element or in a series of elements inserted between a source of acoustic signals and a receiver. In the theory of acoustic filter the medium is considered as stationary and the wave propagation as one-dimensional, the reference equation is 2.IV (equation for plane wave propagation). The variables characterizing an acoustic wave are: the acoustic pressure *p(t)* and the particle velocity *u(t)* [12]. A very important and proper parameter is the characteristic impedance:

$$Y = \frac{acoustic\ pressure\ associated\ with\ a\ progessive\ wave}{acoustc\ mass\ velocity\ associated\ with\ a\ progessive\ wavewave}$$

Y is the impedance relative to the medium and the flow section related to the progressive wave. Defining the state variables *p as*:

$$p_z = Ae^{-jk_0 z} + Be^{+jk_0 z} \quad \textbf{2.X}$$

and *v* as:

$$v_z = \frac{Ae^{-jk_0 z} - Be^{+jk_0 z}}{Y_0} \qquad \textbf{2.XI}$$

you get the specific acoustic impedance $\zeta(z)$ which represents the equivalent impedance of the whole subsystem downstream of the axial coordinate z point:

$$\zeta(z) = \frac{p(z)}{v(z)} = Y_0 \frac{Ae^{-jk_0 z} + Be^{+jk_0 z}}{Ae^{-jk_0 z} - Be^{+jk_0 z}} \qquad \textbf{2.XII}$$

A and B are the constants containing, respectively, the parameters C_1 and C_2 and the exponential factor. e^{jwt}.

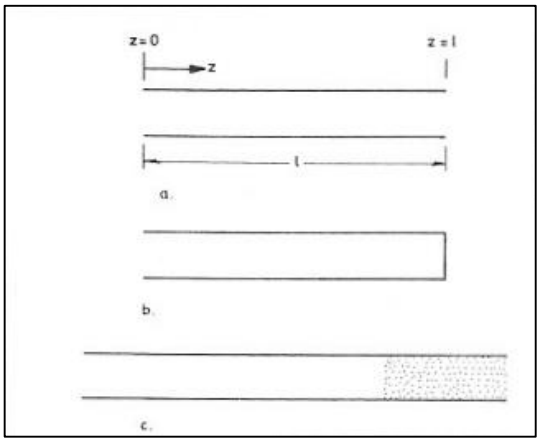

Figure 2.1 - a) open duct, b) duct with rigidly closed end, c) duct with anechoic end

For a duct of length *l*, with open ends (Figure 2.1a), can be defined:

$$\zeta(0) = Y_0 \frac{A + B}{A - B} \qquad \textbf{2.XIII}$$

$$\zeta(l) = \frac{\zeta 0) cosk_0 l - j sink_0 l}{-j\zeta(0)/Y_0 sink_0 l} \qquad \textbf{2.XIV}$$

For a duct with an infinite rigid end *v(l)=0* Figure 2.1b, the following equations can be wrote:

$$\zeta(l)_{rigid} = \infty$$

2.XV

$$\zeta(0)_{rigid} = -jY_0 cosk_0 l$$

2.XVI

Another fundamental parameter in acoustic theory is the reflection coefficient *R:*

$$R = |R|e^{j\omega\theta}$$

2.XVII

It is the ratio between the reflected wave pressure and the incident wave pressure. In case of rigid termination *R=1* and in case of an anechoic termination *R=0;* from these considerations it follows that $\zeta_{anech}=Y$. Generally it is possible to define the acoustic impedance ζ in function of the reflection coefficient *R* and of the characteristic impedance *Y*, as shown in the equation below:

$$\zeta = Y_0 \frac{1+R}{1-R}$$

2.XVIII

2.1.2 Electro acoustic analogies

There are strong analogies between acoustic impedance characterization and the frequency domain analysis of electrical transmission theory; there are listed the principal analogies [12].

A tube of very small length (Figure 2.2) represents a lumped impedance for the waves propagation, on the basis of Newton's second law its equation can be defined:

$$z_{li} = j\omega \frac{l}{s}$$

2.XIX

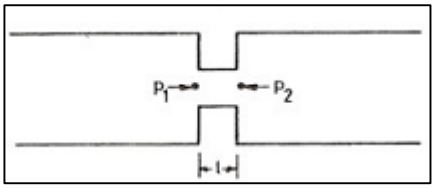

Figure 2.2 Lumped impedance

It is immediate the correspondence between z_{li} and the electrical inductance. A cavity of volume *V* that can allow acoustic motion at its neck, it represents a lumped compliance, Figure 2.3. Considering an acoustic pressure applied at the neck of our cavity and the consequent adiabatic volume reduction ΔV, it is possible to obtain this formulation:

$$z_{lc} = \frac{1}{j\omega\left(\frac{V}{{a_0}^2}\right)} \qquad \textbf{2.XX}$$

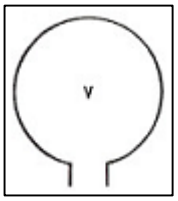

Figure 2.3 Lumped compliance

Where $C = \frac{V}{{a_0}^2}$ is the acoustic compliance equivalent to the electric capacitance. The analogies between acoustic theory and electrical transmission theory allows to model acoustic issues with the well-established electrical circuit representation. In Figure 2.4 is depicted an electrical circuit representing an acoustic system composed by a source, an acoustic filter and an acoustic load. The acoustic pressure p_n is represented by the voltage V_n and the acoustic velocity u_n by the current; ζn is the specific acoustical impedance of the passive subsystem.

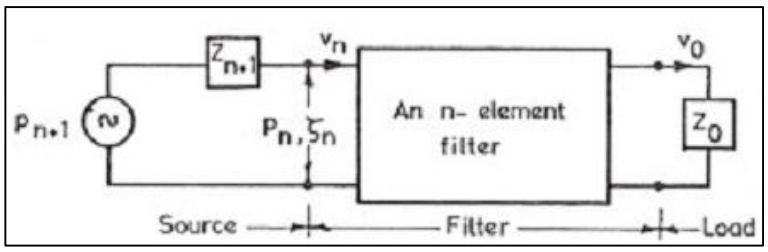

Figure 2.4 - Electrical circuit representation

The performance of an acoustic filter is commonly measured in terms of one of the following parameters:

- Insert loss, IL

- Trasnsmission loss, TL

The insertion loss, *IL*, is defined as the difference between the acoustic power radiated without any filter and the one radiated in presence of a filter [12]:

$$IL = L_{W1} - L_{W2} = \log\left(\frac{W_1}{W_2}\right) \qquad \textbf{2.XXI}$$

Where subscripts "*1*" and "*2*" represent, respectively, system without and whit a filter. In case of zero temperature gradient and constant pressure source, the IL becomes:

$$IL = 20\log\left(\frac{p_n}{p_0}\right) \qquad \textbf{2.XXII}$$

The transmission loss, *TL*, is defined as the difference between the power incident on the acoustic filter and that transmitted downstream the acoustic filter. This quantity is independent from the source but presumes the presence of an anechoic termination.

$$TL = L_{W1} - L_{W1}{}' = 10\log\left(\frac{S_n A_n^2}{2}\frac{2}{S_1 A_1^2}\right) \qquad \textbf{2.XXIII}$$

Where subscripts "*n"* and "*1"* refer respectively to the sections upstream and downstream the filter, S refers to the flow section, and $A_1 = p_1$ and $A_n = \frac{p_n + Y_n v_n}{2}$ are the incident and the transmitted pressure.

In acoustic field it is clear that the performance of an acoustic filter is represented by the insertion loss parameter but it needs a prior knowledge of the acoustic impedance of the source. If one needs to define the acoustic transmission behavior of an element it is preferable to use the transmission loss parameter because it is independent both from the ambient impedance (anechoic end) and from the source.

2.2 Transfer matrix method

To correlate in a simple way upstream and downstream state variables, acoustic pressure *p* and mass velocity *v*, of an acoustic filter it can be used the transfer matrix method [13] [14]. Equation 2.XXIV represents the relation between the different state variables for a *rth* element of an acoustic filter [12]:

$$\begin{bmatrix} p_r \\ v_r \end{bmatrix} = [A\ [2x2]\ rth\ element] \begin{bmatrix} p_{r-1} \\ v_{r-1} \end{bmatrix} \quad \textbf{2.XXIV}$$

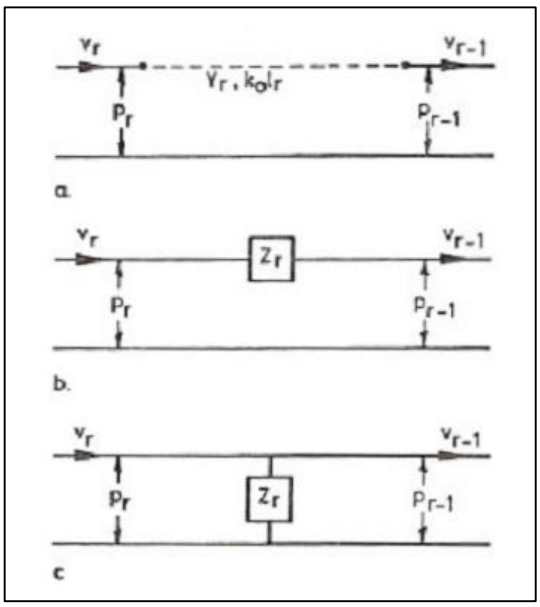

Figure 2.5 - Three basic elements in an equivalent circuit, distributed element, lumped element, shunt lumped element.

From equations 2.X, 2.XI it is possible to infer and define the transfer matrix of three basic elements used for the description of an acoustic filter: distributed element, lumped element and shunt lumped element. The transfer matrix for a distributed element, Figure 2.5 a, is described below:

$$\begin{bmatrix} p_r \\ v_r \end{bmatrix} = \begin{bmatrix} cosk_0 l_r & jY_r sink_0 l_r \\ -\frac{j}{Y_r} cosk_0 l_r & cosk_0 l_r \end{bmatrix} \begin{bmatrix} p_{r-1} \\ v_{r-1} \end{bmatrix} \quad \textbf{2.XXV}$$

For an in line lumped element, Figure 2.5 b, it can be written by electro-acoustic theory the following transfer matrix relation:

$$\begin{bmatrix} p_r \\ v_r \end{bmatrix} = \begin{bmatrix} 1 & z_r \\ 0 & 1 \end{bmatrix} \begin{bmatrix} p_{r-1} \\ v_{r-1} \end{bmatrix} \quad \textbf{2.XXVI}$$

For a branch lumped element, Figure 2.5 c, it is possible to obtain the following transfer matrix:

$$\begin{bmatrix} p_r \\ v_r \end{bmatrix} = \begin{bmatrix} 1 & 0 \\ \frac{1}{z_r} & 1 \end{bmatrix} \begin{bmatrix} p_{r-1} \\ v_{r-1} \end{bmatrix} \quad \textbf{2.XXVII}$$

In general, for a dynamic acoustic filter consisting of n-elements, Figure 2.6 it is possible to apply the transfer matrix method, as successive products of the transfer matrices of each element.

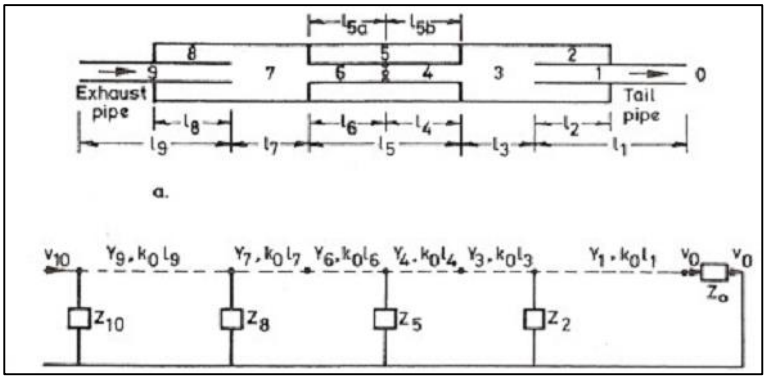

Figure 2.6 - Scheme of an n-elements acoustic filter

$$\{S_{n+1}\} = [T_{n+1}][T_n] \dots [T_r] \dots [T_1]\{S_0\} \quad \textbf{2.XXVIII}$$

Where S is the vector of the state variables *p* and *v*, and T is the transfer matrix of the *nth* element.

2.2.1 Characterization of an acoustic problem, reciprocating compressor discharge chamber example

The acoustic characterization of a simple component, in terms of transfer matrix, can be obtained in analytic way as shown in the preceding paragraph. Validations of the acoustic model for simple geometry can be found in literature for example in the works by A. Selamet et al, dealing with the wave attenuation in a catalytic converter [15]. In case of complex 3D geometry the characterization of an acoustic configuration passes

necessary through the FEM modelling in order to take into account the real behaviour of the component.

In the reciprocating compressors field, the acoustic analyses are performed in order to study the behaviour of the pipe lines in terms of fluid pulsations which are the responsible of the mechanical failures and acoustic noise [16] [17]. The elements that constitute the suction or the discharge line usually have a simple geometry, like a plenum with one or multiple inlets and one or multiple outlets, ducts, orifices etc. This typology of elements can be modelled using the acoustic 1D theory as described in the foregoing paragraph. The source of the pulsating flow is the reciprocating machine, so it is very important to know how it interacts with the line in order to study the pressure waves propagation. The interface between the compressor and the line is represented by the suction and the discharge chambers which have the aim to dampen the pressure wave pulsations. An example of suction and discharge chambers is shown in Figure 2.7; it is clear the complexity of this geometry and the impossibility to analyse its acoustic behaviour using a 1D acoustic modelling. In this case the full 3D fem analysis is the only way to face the issue.

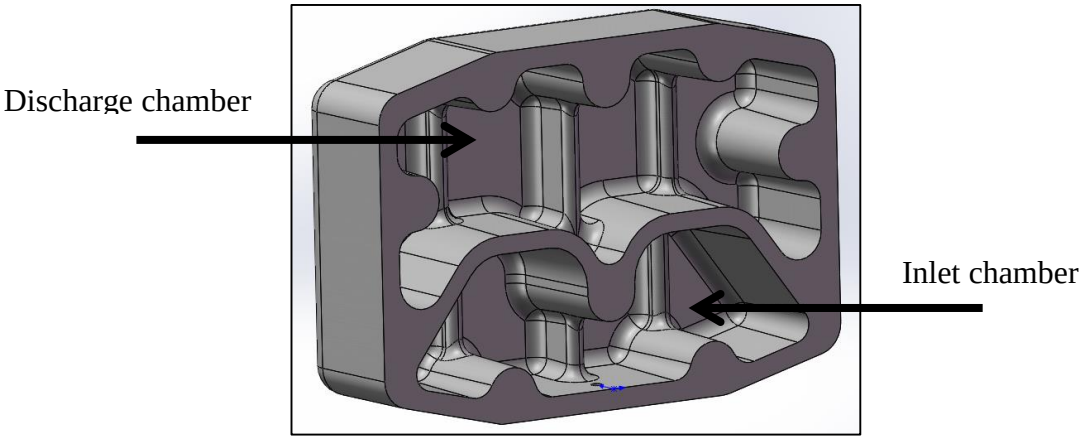

Figure 2.7 - Reciprocating compressor inlet and discharge chamber

Taking into account the discharge chamber of a reciprocating compressor (Figure 2.9) the procedure adopted to determine its transfer matrix is described below. First of all the component is analysed in a schematic way as shown in Figure 2.8.

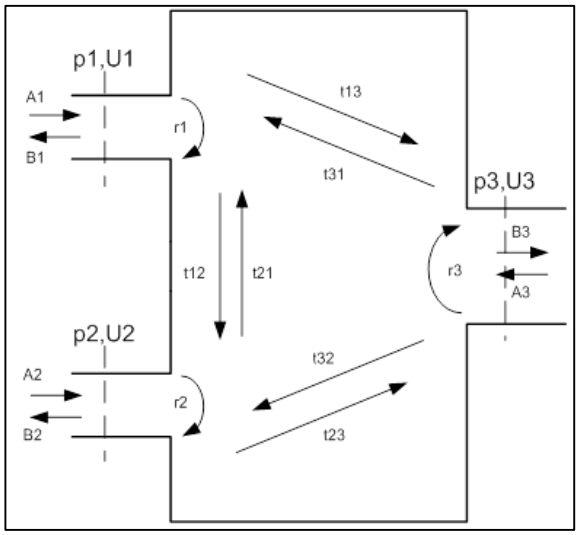

Figure 2.8 - Discharge chamber 2 input 1 output

A and *B* are respectively the incident and the reflected wave, *r* is the reflection coefficient and *t* the transmission coefficient characteristic of the considered geometry; the subscripts *1*, *2* and *3* refers respectively to inlet *(1)*, inlet *(2)*, and outlet *(3)*. Observing the scheme of Figure 2.8 it can be written the system of equation that follows:

$$\begin{cases} B_1 = A_1 r_1 + A_2 t_{21} + A_3 t_{31} \\ B_2 = A_1 t_{12} + A_2 r_2 + A_3 t_{32} \\ B_3 = A_1 t_{13} + A_2 t_{23} + A_3 r_3 \end{cases} \quad \textbf{2.XXIX}$$

The equation 2.X and 2.XI, can describe the incident and reflected waves in function of the particle pressure *p* and the particle velocity *v*, shown in equation 2.XXX and 2.XXXI:

$$A = \frac{p + Yv}{2} \quad \textbf{2.XXX}$$

$$B = \frac{p - Yv}{2} \quad \textbf{2.XXXI}$$

System 2.XXXII is obtained rearranging system 2.XXIX with the equation of the incident and the reflected wave:

$$\begin{aligned}(p_1 - v_1Y_1) &= (p_1 + v_1Y_1)r_1 + (p_2 + v_2Y_2)t_{21} + (p_3 + v_3Y_3)t_{31}\\ (p_2 - v_2Y_2) &= (p_1 + v_1Y_1)t_{12} + (p_2 + v_2Y_2)r_2 + (p_3 + v_3Y_3)t_{32}\\ (p_3 - v_3Y_3) &= (p_1 + v_1Y_1)t_{13} + (p_2 + v_2Y_2)t_{23} + (p_3 + v_3Y_3)r_3\end{aligned} \quad \textbf{2.XXXII}$$

Proceeding with algebraic passages, equation 2.XXXII can be written in matrix way:

$$\begin{bmatrix}1 - r_1 & -Y_1(1 + r_1) & -t_{21} & -Y_2t_{21}\\ -t_{12} & -Y_1t_{12} & 1 - r_2 & -Y_2(1 + r_2)\\ -t_{13} & -Y_1t_{13} & -t_{23} & -Y_2t_{23}\end{bmatrix}\begin{Bmatrix}p_1\\ v_1\\ p_2\\ v_2\end{Bmatrix} = \\ = \begin{bmatrix}t_{31} & Y_3t_{31}\\ t_{32} & Y_3t_{32}\\ -1 + r_3 & Y_3(1 + r_3)\end{bmatrix}\begin{Bmatrix}p_3\\ v_3\end{Bmatrix} \quad \textbf{2.XXXIII}$$

So, in synthetic form:

$$[M_{12}]\begin{Bmatrix}p_1\\ v_1\\ p_2\\ v_2\end{Bmatrix} = [M_3]\begin{Bmatrix}p_3\\ v_3\end{Bmatrix} \quad \textbf{2.XXXIV}$$

$$\begin{Bmatrix}p_1\\ v_1\\ p_2\\ v_2\end{Bmatrix} = pinv[M_{12}][M_3]\begin{Bmatrix}p_3\\ v_3\end{Bmatrix} \quad \textbf{2.XXXV}$$

Where the matrixes M_{12} and M_3 contain the reflection and the transmission coefficients of the considered geometry. In this way, known the inlet (1-2) pressure and velocity values, it is possible to get obtain the acoustic response of the chamber at outlet 3.

The just described procedure illustrates the possibility to create the transfer matrix of an element with a complex 3D geometry but, as it is clear, the characteristic coefficients of the matrix must be defined performing an acoustic *fem* analysis of the component.

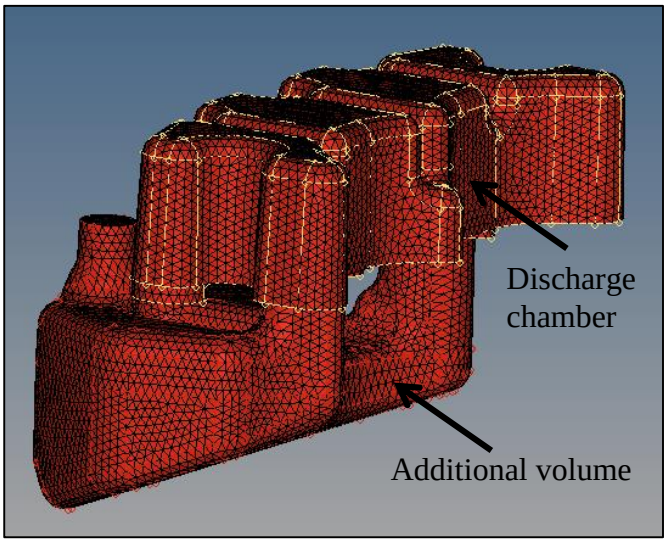

Figure 2.9 - Reciprocating compressor discharge chamber, internal volume mesh (and additional volume mesh)

In order to characterize a 3D acoustic problem, the first step is to extract the amount of volume, taken by the fluid during the real functioning of the machine, and to realize the associated CAD. So it is possible to realize the 3D mesh of the model which is at the basis of the acoustic modelling. The objective of the 3D acoustic analysis is to obtain the transmission coefficients between the inlet and outlet accesses and the reflection coefficients of each access.

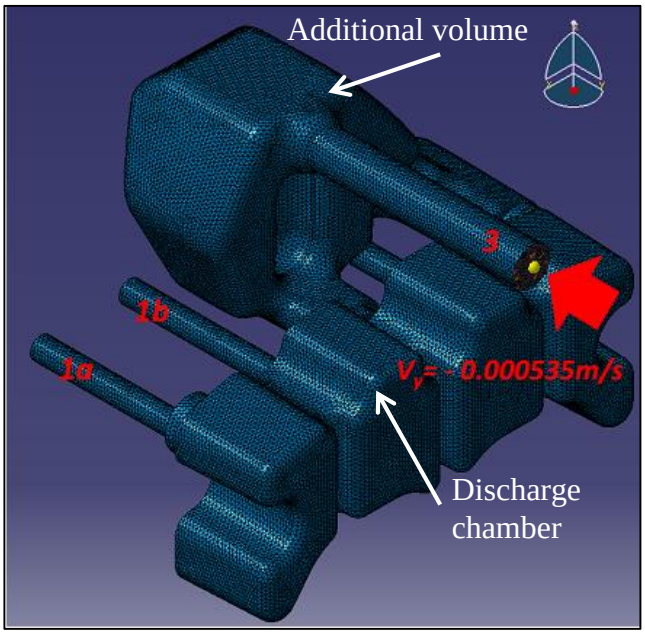

Figure 2.10 - Acoustic fem modelling of discharge chambers

Looking at Figure 2.10 you can identify the flow inlet accesses 1a and 1b, the outlet 3; the inlet 2a and 2b are covered by the additional volume. In detail, the coefficients that characterize this geometry are:

- the transmission coefficients t_{13} between inlets 1a, 1b and the single outlet 3, and viceversa, t_{31};
- the transmission coefficients t_{23} between inlets 2a, 2b (not visible in the picture) and the single outlet 3 and viceversa, t_{32};
- the reflection coefficents at each acess, r_1, r_2 and r_3.

For clarity the determination of the t_{13} coefficient is obtained imposing the anechoic termination at the accesses 2 and 3, while at access 1 it is imposed the driving force condition. The driving force causes a perturbation on the fluid imposing an oscillating velocity at a defined frequency. The anechoic termination guarantees the total absence of reflected waves at accesses 2 and 3. The simulation is performed for the rage of frequencies of interest at specific intervals; in this way it is possible to evaluate the behaviour of the component in all operating conditions. The same procedure is replied to obtain the others parameters.

In order to perform a 3D simulation, the other parameters that need to be set are:

- the fluid properties, temperature, pressure, density;
- the structure material properties, typology of material, stifness.

The fluid properties are necessary in order to define the characteristic impedance of the fluid: $z = \rho c$; the structure parameters influence the internal response of the chamber in terms of reflection and transmission coefficient. In this specific case the structure is considered infinitely rigid because of the thickness of the chamber walls.

Once obtained the reflection and transmission coefficients of the component, the relative transfer matrix can be assembled. The described procedure allows to analyse elements with complex geometry in addition to other simple or complex elements using

the transfer matrix methodology. Using this approach, it is possible to combine the desired elements of the inlet and discharge line and to study the pressure wave propagations.

3 Numerical model

This chapter deals with the numerical modelling of a reciprocating compressor and with the coupling of this reciprocating compressor and a pipeline; precisely the object of the elaboration is the 0D numerical model of the thermodynamic cycle of the above-mentioned reciprocating compressor, paying particular attention to the motion of the automatic valves, following and extending the ideas of Costigliola [18]. Our research wants to study the coupling of the reciprocating machine and the pipeline and, because of the complexity of this aim, the approach chosen to face such a hard subject matter is represented by the 0D thermodynamic model. In literature for example the work by Aigner shows a different approach to the reciprocating compressor modelling [1]; (1D - 2D modelling).

3.1 Reciprocating compressor numerical model

The code for the compressor analysis is named RE.CO.A (which stands for reciprocating compressor analysis). The numerical model allows to calculate the physic quantities characterizing the thermodynamic cycle of the reciprocating compressor; a 0D modelling is defined in the time domain.

In first analysis, the thermodynamic cycle can be divided into 4 main phases:

- suction phase;
- compression phase;

- discharge phase;

- expansion phase.

Each of the above mentioned phases is controlled by the motion of the piston that causes the variation of volume and pressure inside the cylinder and, as a consequence, the opening or the closing of the automatic valves. Therefore the numerical model follows the real behaviour of the compressor and calculates, in a quasi-stationary way, the physic parameters. In practice step by step the thermodynamic parameters of the compressor are calculated and the phenomena estimated in stationary mode. The entire cycle is discretized in the following mode:

- i=(0:1/D:360°), the calculation step: in order to obtain a detailed analysis the step is divided for the D parameter,where D>0;

- dt = 1/(rpm·60), the time necessary to execute one step;

So the numerical model follows the flow chart described in ***Figure 3.1***, stepwise, up to complete the entire cycle. The complete iteration from 0° to 360° is executed K times, K=0 : N, where N is the iteration in which the convergence criterion is verified. First of all, the model presents a section where are listed all the parameters that allow to define the geometry of the machine, the gas properties and the thermodynamic properties of suction and discharge environments. At starting condition: the piston is supposed to be at the top dead point (TDP), the surge and discharge valves are closed; all the thermo fluid-dynamic conditions (pressure, temperature, cp, cv, R, etc.) of the fluid at discharge and surge points are defined.

The piston executes a first translation toward the bottom dead point (BDP), the amount of translation is given by the equation of the kinematics of slider-crank mechanism once imposed a defined angular rotation (Δα).

$$\Delta s = \sqrt{l^2 - (r \cdot \sin\alpha)^2} + r \cdot \cos\alpha \qquad \textbf{3.I}$$

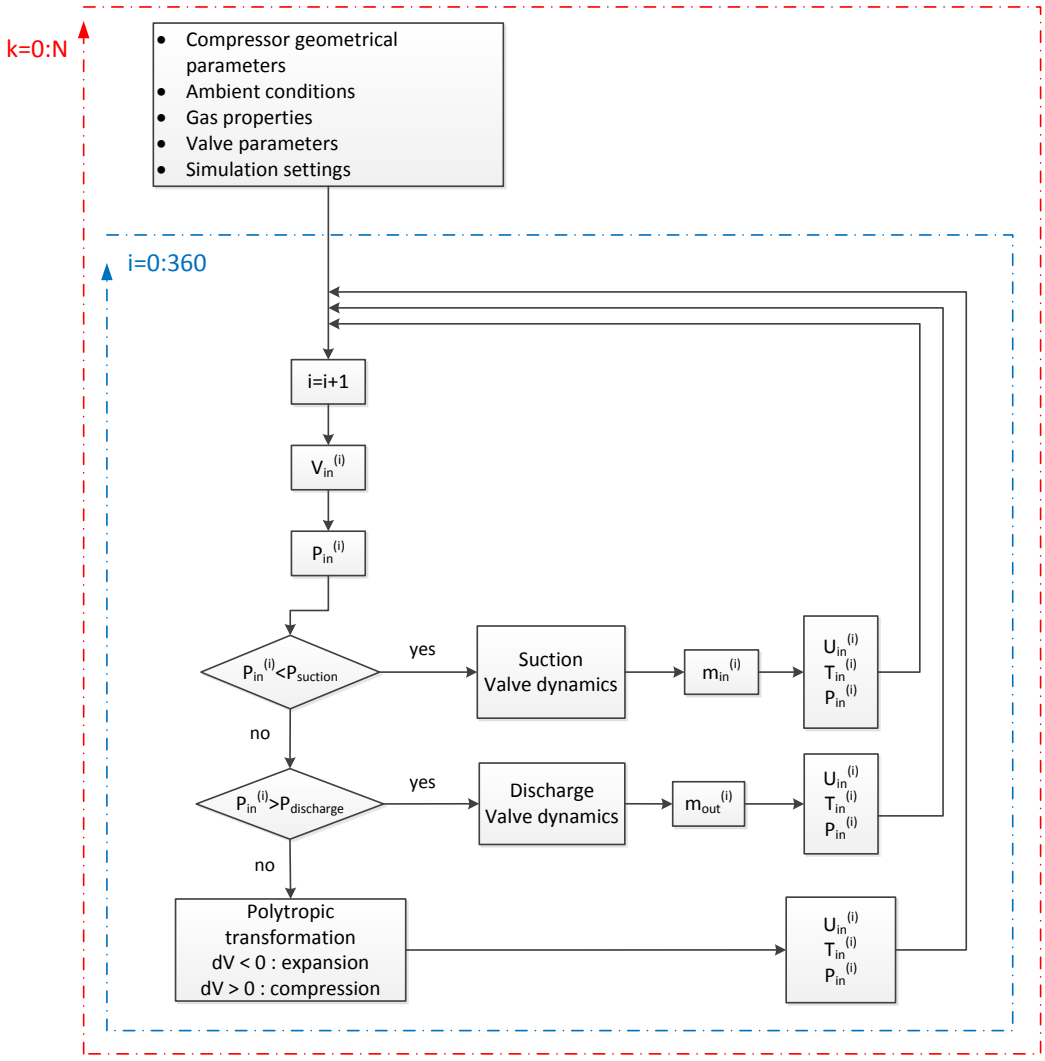

Figure 3.1 - Flow chart of the 0D numerical model

So to a crank shaft angular rotation (Δα) is associated a variation in terms of volume (Δv). Since the automatics valve are closed, inside the cylinder the pressure decreases (in fact in this first phase there is no gas flow inside the cylinder); this is a value of pressure of first attempt: now it is evaluated the difference between the pressure inside the cylinder and the pressure present at the inlet and discharge nozzle.

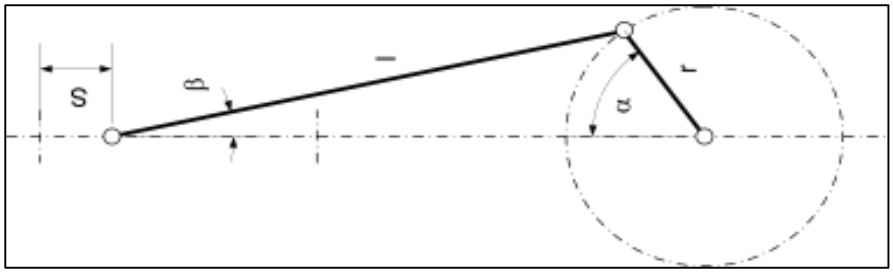

Figure 3.2 - Crank mechanism

The model, basing on the logic depicted in Figure 3.3, identifies the phase: suction or discharge phase, compression or expansion phase.

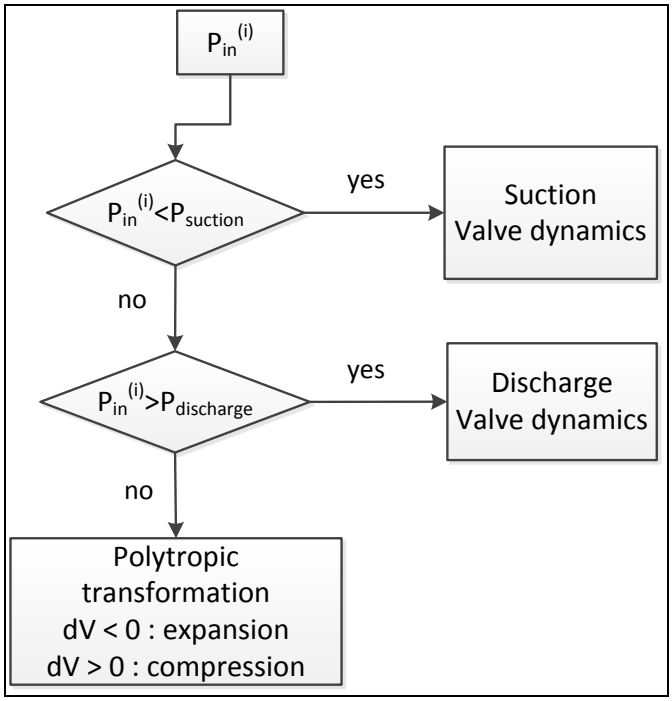

Figure 3.3 - Decisional logic

When the pressure becomes lower than the suction nozzle pressure, the gas stars to flow inside the cylinder. The flow of the gas is conditioned by the way the suction valve opens, (the valve dynamic is descripted in detail later on). The way adopted to model the gas flow across the valve is that to consider the gas flow through an isentropic nozzle, [19], in fact the gas rate flow is mainly influenced by the pressure drop across the valve and the flow coefficient characterizing the passage section [20], [21]. The following equation represents the gas flow [kg/s] across an isentropic nozzle:

$$\dot{m} = K_s \cdot A_v \cdot \sqrt{\left[\frac{2\gamma}{\gamma-1}\right]\left\{\rho_1 \cdot P_{01} \cdot \left[\left(\frac{P_2}{P_{01}}\right)^{\frac{2}{\gamma}} - \left(\frac{P_2}{P_{01}}\right)^{1+\frac{1}{\gamma}}\right]\right\}} \qquad \textbf{3.II}$$

Where:

- K_s is the flow coefficient;
- A_v is the flow section;
- γ is the cp/cv ratio;
- ρ_1 is the upstream fluid density;
- P_{01} is the upstream total pressure;
- P_2 is the downstream static pressure;

Once imposed the flow section A_v, which is defined by the valve dynamic modelling, the flow of the gas is conditioned by K_s, P_{01} and P_2, (where P_{01} and P_2 are, respectively, the total pressure at the inlet ambient and the static pressure of first attempt inside the cylinder). So at each time step the gas inlet phase is supposed to occur in two times: in the first time the piston translates without the opening of the valve, then the valve opens and the fluid passes into the cylinder; this approximation is at the basis of this kind of approach. As a consequence it is possible to calculate the amount of gas that is trapped at each time step inside the cylinder, in fact it is known the mass flow [kg/s] and the time necessary to complete a piston translation Δs (since the rotational speed of the compressor [rpm] is defined:

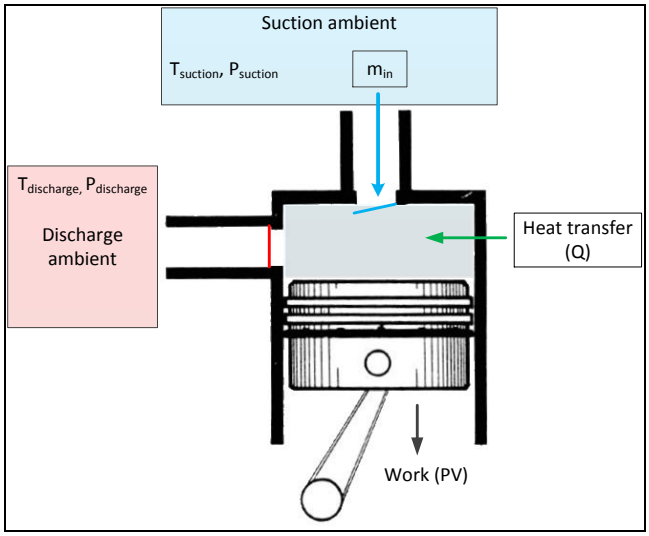

Figure 3.4 - Internal energy balance, suction phase

At this point it is possible to calculate the internal energy U contained inside the control volume highlighted in Figure 3.4; the internal energy balance (applying the first law of thermodynamics) done at the time step-i takes into account:

- The internal energy inside the cylinder at the step-(i-1);
- The mass flow rate at the time step-i;
- The work done by the fluid on the piston surface;
- The heat exchange.

The equation 3.III shows the energy balance at time step-i:

$$U_{in}(i) = \frac{\dot{m_{in}}(i) \cdot dt \cdot C_p \cdot T_{in} + M_{in}(i-1) \cdot C_v \cdot T_{in}(i-1) - dV(i,1) \cdot P_{in(i-1)} + HT(i)}{M_{in}(i)}; \quad \textbf{3.III}$$

The model can take into account the heat transfer (HT), but in first approximation it is considered equal to 0 (more properly it is taken into account with specific corrective coefficients applied during the compression and expansion phases); the estimation of the heat exchange of a reciprocating compressor is a wide argument that needs a detailed and specific activity [22]. Once calculated the internal energy U, it is

possible to define the characteristics parameters of the gas inside the cylinder at the time step-i:

- the temperature inside the cylinder T_{in};

$$T_{in}(i) = \frac{U_{in}(i)}{C_v(i)}$$

3.IV

- the pressure inside the cylinder $P_{in,}$ on the basis of the perfect gas law;

$$P_{in}(i) = M_{in}(i) \cdot \frac{R \cdot T_{in}(i)}{V(i)}$$

3.V

- the density of the gas ρ_{in}.

$$\rho_{in}(i) = \frac{M_{in}(i)}{V(i)}$$

3.VI

The code allows the accurate calculation of the real gas properties, just at each step; once the gas pressure and temperature are calculated, the code deals with a commercial software for the real gas properties calculation: RefProp® (or EES®); in this way the real behavior of the gas is considered. During the compression (and the expansion) stage the automatics valves are closed: there is no mass flow but only a variation of the internal pressure as a consequence of the volume variation and of the heat transfer(Figure 3.5).

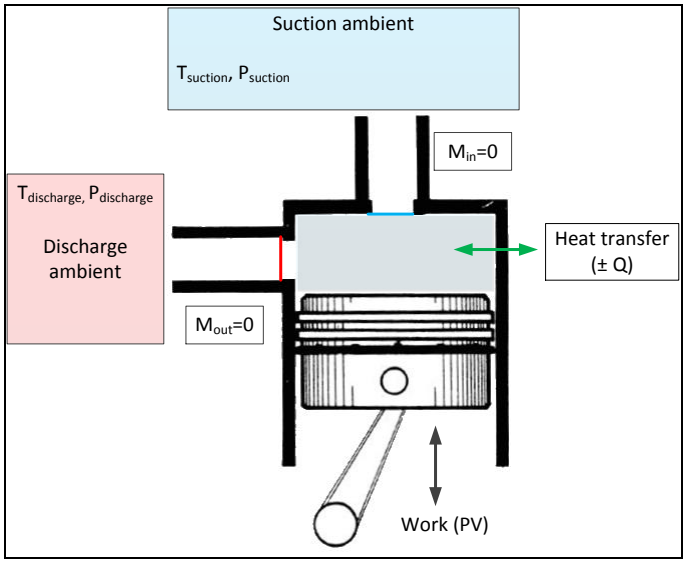

Figure 3.5 - Internal energy balance, compression (expansion) phase

The pressure at the time step-i is estimated considering a polytrophic compression (expansion), precisely in first approximation it is considered an adiabatic transformation:

$$P_{in}(i) = P_{in}(i-1) \cdot \left(\frac{V(i-1)}{V(i)}\right)^{\gamma} \qquad \textbf{3.VII}$$

The internal energy and the other parameters are calculated using the same technique used for the suction stage. When the internal pressure overcomes the discharge ambient pressure, the discharge valves get opened and the gas starts going out, Figure 3.6.

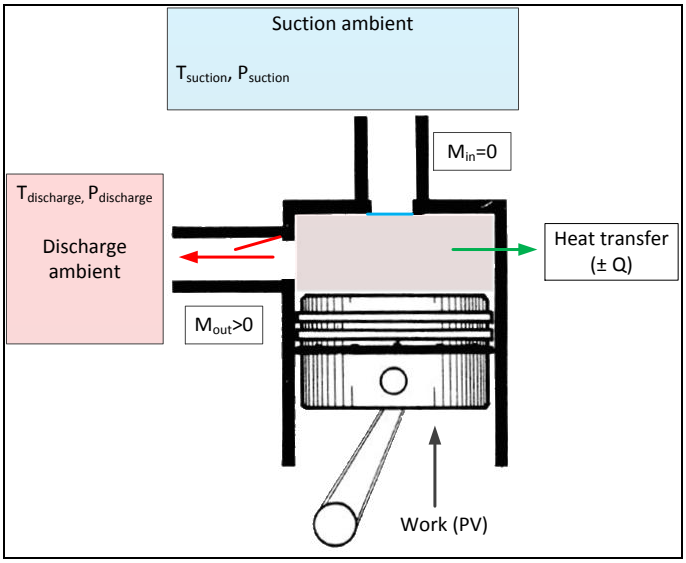

Figure 3.6 - Internal energy balance, discharge phase

The same considerations we did about suction phase can be done for discharge phase: mostly important is to notice that the mass flow rate -in this case- is outgoing the cylinder and it depends on the pressure difference between the cylinder and the discharge ambient. When the pressure inside the cylinder decreases under the discharge ambient pressure, the expansion phase starts, the piston is in proximity of the TDP and moves through the BDP; the considerations done for the compression stage are valid for this phase too.

The RE.CO.A model iterates up to reach the convergence between the last thermodynamic cycle and the previous cycle; the convergence criterion implies that the difference between the in-cylinder pressure value -calculated at the step i of the cycle k-1- and the in-cylinder pressure -calculated at the step i of the cycle k- is less than a tolerance value; the control is done for i=1:360.

3.1.1 Valve dynamic

The in-cylinder pressure prediction is strongly influenced by the automatic valves opening, so it is fundamental to realize a detailed model of the valve dynamic [23] , [24]. The valves are characterized by the following parameters:

- Typology: multiple rings valve, reed valve;
- Valve flow section, overall section through which the gas flows;
- Rings numbers;
- Rings surface, surface on which acts the fluid pressure;
- Rings mass;
- Springs stifness;
- Springs number;
- Springs preload;
- Valve surface drag coefficent.

The valve dynamic is implemented inside the reciprocating compressor model and is calculated at each time step. In Figure 3.7 is depicted through the flow chart the logic at the basis of the valve dynamic model.

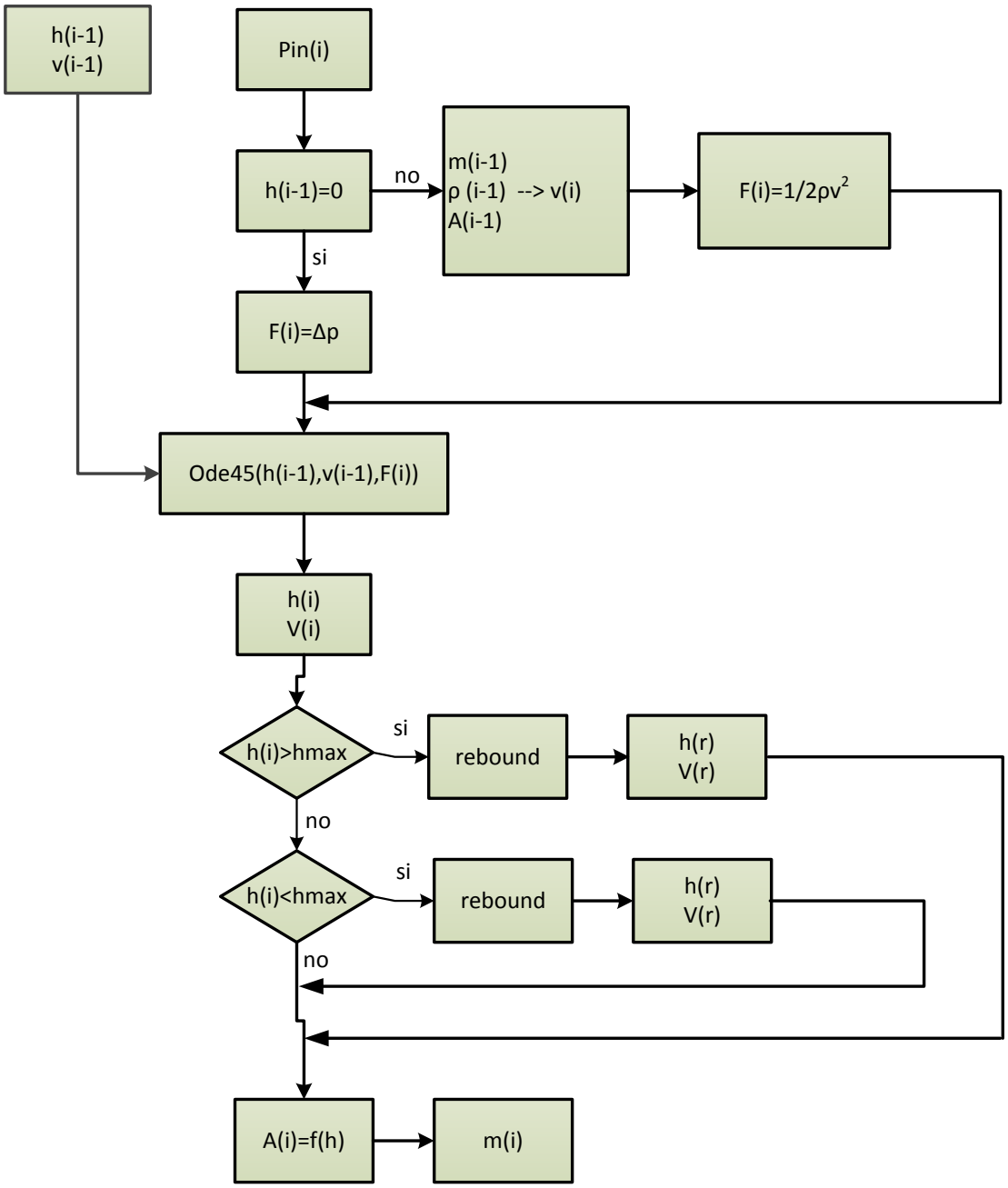

Figure 3.7 Valve dynamics flow chart

The valve dynamic calculation starts when the pressure inside the cylinder is higher (lower) than the pressure of the discharge ambient (suction ambient). The valve dynamic is comparable to the dynamic of a mass-spring-dumper model, where the movable mass is represented by the rings mass, the spring stiffness is represented by the springs of the valve and the dumper is represented by the overall dumping of the system. The dynamic is mathematically described by a second order differential equation as shown below:

$$m\ddot{x} + b\dot{x} + kx = f(t)$$

3.VIII

Where *m* is the mass of the system, *b* the overall damping, *k* the global stiffness, *x* the rings movement and *f* is the driving force acting on the system. Observing the scheme of Figure 3.7, the driving force, $F^{(i)}$, is represented by the pressure that acts on the rings surface; if the valve is closed, $h^{(i-1)}=0$, the pressure is equal to the difference between the inlet (outlet) ambient pressure and the in-cylinder pressure, when the valve opens, $h^{(i-1)}>0$, the pressure is represented by the stagnation pressure of the flux on the rings surface. In the first case it is simple to evaluate the driving force, once the pressure drop across the valve is known. In the second case the driving force is described by the equation below (drag force):

$$f(t) = \frac{1}{2} \cdot cD \cdot \rho \cdot Vf^2 \cdot Sr$$

3.IX

Where *cD* is the drag coefficient of the rings and *Vf* is the gas velocity at the valve section. At each time step the flow velocity *Vf*, considered in the valve dynamic model, is the one calculated at the previous time step, this approximation is at the basis of this kind of numerical model and is minimized increasing the number of steps for thermodynamic cycle (reducing $\Delta\alpha$). The solution of the differential equation 3.IX is obtained applying the ODE45 Matlab solver for ordinary differential equation [25], [26]; the valve lift $h^{(i)}$ and the valve velocity $v^{(i)}$ are computed. During their motion the valve rings move up to the maximum allowable height, h_{max}; when this condition is reached, the rings rebound on the valve seat. In order to model this condition the rebound coefficient is defined, so when the condition of max lift is verified the sign of the second term of equation 3.VIII is changed and its module is multiplied for the rebound coefficient, $b<1$. Once known the valve lift, the geometrical flow section can be calculated. The spring stiffness is introduced as a function of the valve displacement in order to model even in case of not linear springs. The model also takes into account the presence of a spring preload, which is computed in the right term of equation 3.VIII; the spring preload is a force that acts against the valve natural motion causing a delay to its opening.

3.2 Calibration of the numerical model

The predictability of the 0D numerical model of the reciprocating compressor can be considered reliable only after a proper calibration. The trend of the pressure values inside the cylinder is the most representative term of comparison so, the calibration is done in order to predict the real indicating cycle of the machine [27]. To perform the calibration, reference has been made to the indicating cycle of a compressor for cooling application; the experimental measurements have been performed at the laboratory of the industrial department of Florence University.

3.2.1 Experimental setup

The experimental measurements of the in-cylinder pressure are done on a reciprocating compressor provided with automatic valves for cooling system for industrial applications; the specific model is the H503CS produced by Dorin factory, Figure 3.8.

Figure 3.8 - H503CS Dorin Compressor

The features of the compressor are shown in the following table:

Bore	0.061 [m]
Stroke	0.052 [m]
Connecting rod	0.098 [m]
Dead volume	0.95% of the displacement
RPM	1440[rev/min]
Gas	R404A
Compressor ratio	9.4
Suction ambient pressure	2.2 [barA]
Suction ambient temperature	20 [°C]
Discharge ambient pressure	19 [barA]
Discharge ambient temperature	119 [°C]

Table - 3.1 H503CS Compressor features

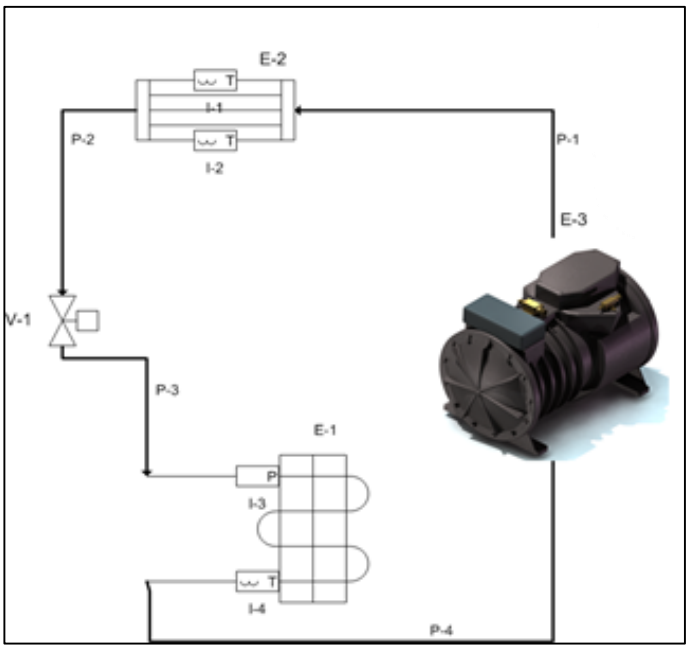

Figure 3.9 - Reciprocating compressor test bed

In Figure 3.9 is schematized the test bed used for the in cylinder pressure measurements. The test bed consists in a simple refrigeration circuit composed of:

- reciprocating compressor (E3);
- evaporator (E2);
- lamination valve (V1);
- condenser (E1);
- accumulation tank.

The circuit is realized for testing the compressor during its real functioning; the scheme does not show the presence of an accumulation tank containing water; the accumulator is implemented into the circuit in order to guarantee a thermal transfer point for the cold, produced by the evaporator, and for the heat, produced by the condenser. For the measurement of the indicating cycle a proper measurement apparatus has been designed; the experimental chain must allow the correct timing of the in-cylinder pressure with the crank shaft rotation. In details the experimental apparatus is composed by:

- High frequency pressure sensor, mod. Kulite XTL-123C-190;
- National Instrument high frequency acquisition electronic board, mod. PCI 6208;
- ELEN hall sensor;
- AVL carnck angle calculator;

The high frequency pressure sensors are placed inside the compressor head; precisely the sensor is placed on the plate containing the compressor valves, and faces on the upper limit of the compressor chamber. The sensor is of piezoelectric typology and it is internally provided with the amplification system. The hall sensor for the measurement of the crank shaft angular position is placed on the compressor external case; particular attention is paid to the sensor positioning since the compressor case contains high pressure gas and oil (for lubrication reasons). So a hall sensor for high pressure environment has been chosen. At the side end of the crank shaft it is positioned (coaxially to the shaft) a steel disc with 24 less 2 holes (markers) on the external circumference. The hall sensor is perpendicular to the disc and is placed at 0.65 mm of distance in correspondence of the

markers. In this way the hall sensor can read the passage of the markers. The two missing holes allow to identify the revolution start (and finish).

Figure 3.10 shows the experimental setup for the dynamics pressures measurement. The dynamic pressure analog signals (voltage) and the digital signal of the crank angle calculator are the input signals for the electronic board. The AVL crank angle calculator (CAC) is used in order to reconstruct a virtual encoder signal using the information of the hall sensor. Precisely the signals of the hall sensor go to CAC in form of voltage peak, in fact at each marker corresponds a voltage peak; for the identification of the single revolution passage no peak voltage is transmitted to CAC (because of the missing markers). So the CAC, starting from the signal information of the hall sensor, reconstructs a detailed virtual encoder signal with the desired resolution and provides as outputs an angle digital signal and a revolution digital signal. In Figure 3.11 is depicted the trends of the hall sensor voltage output (yellow signal) and CAC revolution digital signal (blue); the red line underlines the TDC angular position. Because the angular resolution is set to 0.5 degrees (and that means 720 outputs per revolution), the angular digital signal is not shown for reason of graphical clarity. For the reconstruction of the indicating cycles a proper software has been developed in Labview environment, the SW allows the visualization of the pressure-volume diagram of the compressor and the data storage. In detail the acquisition of the pressure voltage signals starts at the passage of the revolution digital signal (hardware trigger); each pressure signal is sampled every 0.5 degrees. The system allows a rigorous monitoring of the pressure trends, in fact possible rotational speed variations of the crank shaft, during the compression-expansion phases, don't cause any mistakes on the PV diagram reconstruction.

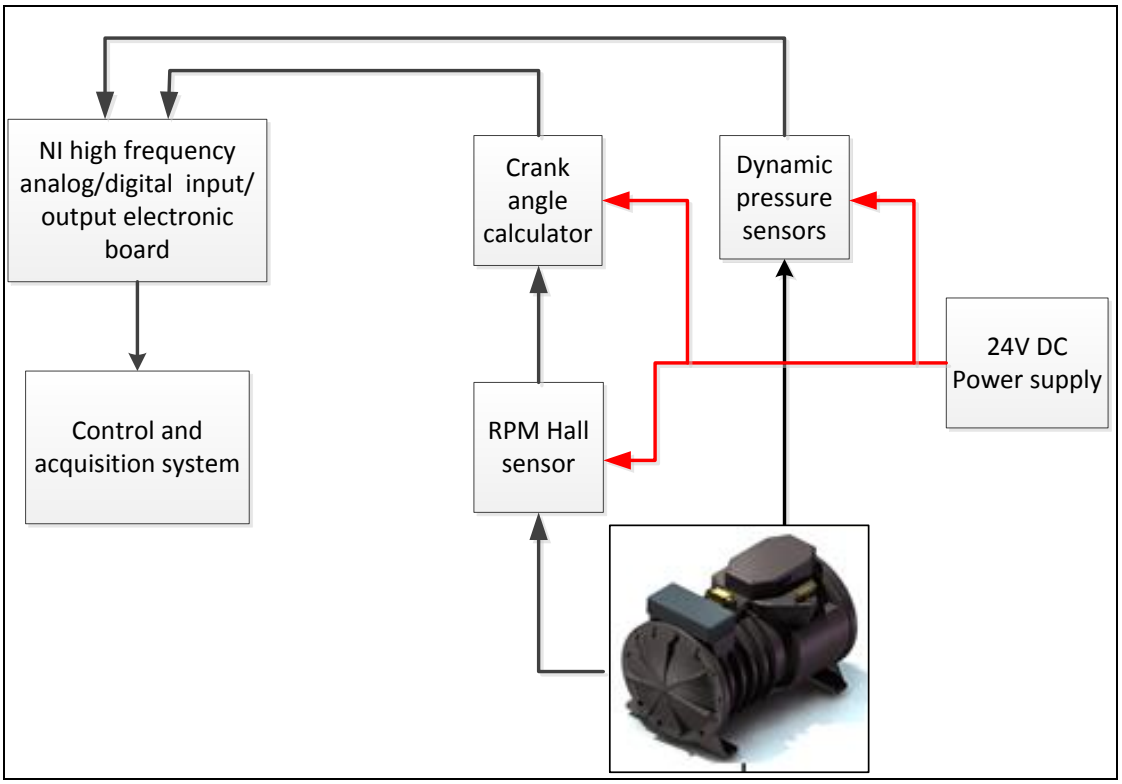

Figure 3.10 - Experimental apparatus for indicating cycle measurement

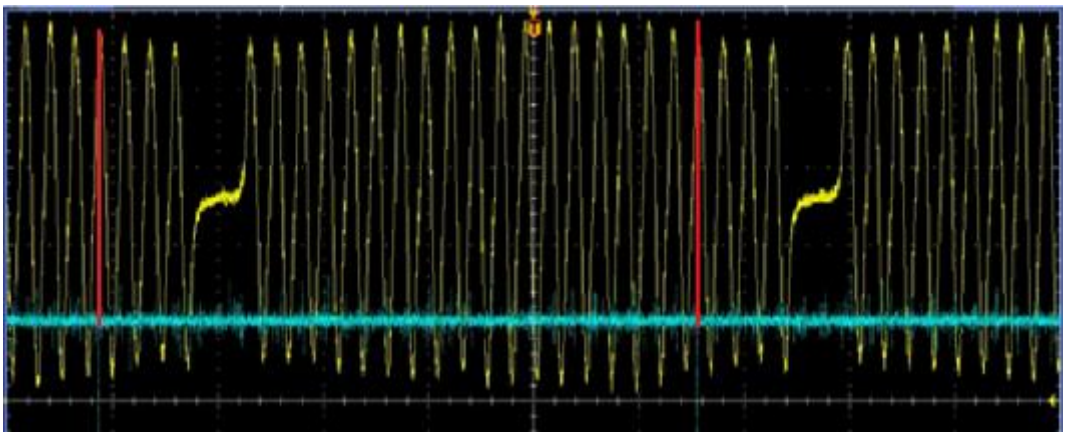

Figure 3.11 - Hall sensor signal (yellow), CAC revolution signal (blue)

Figure 3.12 depicts the pressures measured with the experimental apparatus, in red the in-cylinder pressure, in blue the suction pressure and in green the discharge pressure. The graph demonstrates the well-functioning and the capability of the measurement chain; the graphs obtained represent the base for the tuning of the reciprocating compressor numerical model.

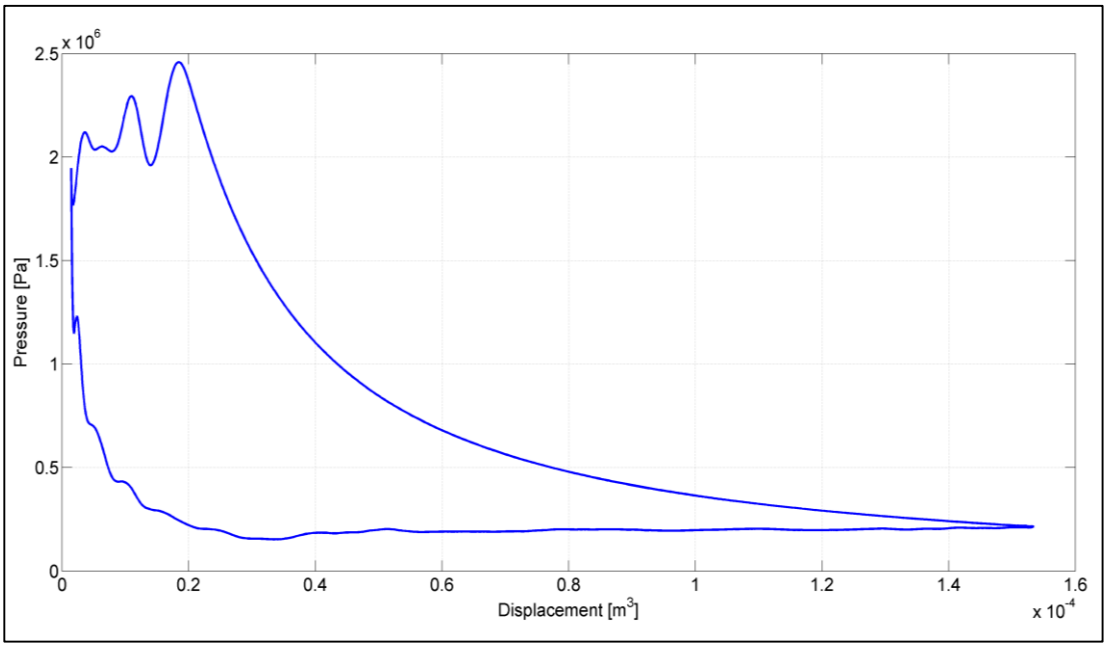

Figure 3.12 - Experimental pressure measurement, the curve represents the experimental indicating cycle.

The graph shows the classic shape of the real PV diagram of a reciprocating compressor provided with automatic valves.

During the suction phase the pressure inside the cylinder goes under the suction ambient pressure; the fluid-dynamic losses of the intake system and the automatic valve dynamics are the responsible of this effect; valves parameters like the mass, the springs stiffness, the rebound coefficient and the preload, have influence on the in-cylinder pressure of the suction phase. During the discharge phase the pressure inside the cylinder is higher than the mean pressure of the discharge ambient; the origins of this overpressure and those of the suction under pressure ones are the same. This phenomenon is much more evident than in the suction phase, above all because the mass flow rate at the discharge is higher than at the suction and, as a consequence, the fluid-dynamic losses increase.

The discussion above underlines the weight of the automatics valve parameters on the trends of the in-cylinder pressure. In order to perform an accurate simulation of the valve dynamics in the numerical model, it is carried out an experimental campaign aimed at the definition of the values of the valve mass and of the spring stiffness. In detail in this

case the compressor is provided with reed valves so there are no springs in the valve system but the valve system elasticity comes from the valve flexibility.

In Figure 3.13 is depicted the experimental apparatus set up for the measurement of the reed valves stiffness. The experimental chain is composed by:

- drilling machine;
- precision balance;
- mechanichal comparator;
- steel alloy precision tip.

The support plate for the reed valves is placed on the precision balance and it is suspended on two steel columns; the sensitive tip of the mechanical comparator is placed in correspondence of the reed valve (in the center of the hole for the flow passage) as Figure 3.14 illustrates. In this way the reed valve displacement can be read with high precision.

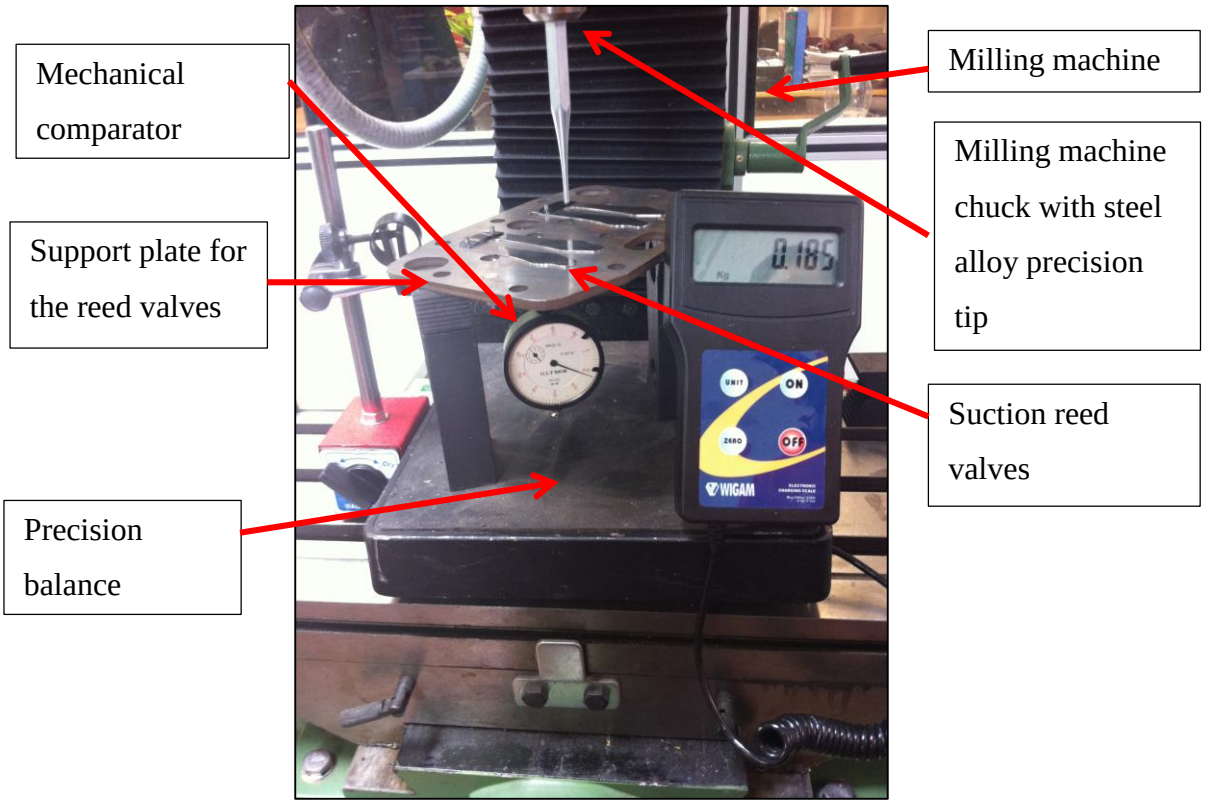

Figure 3.13 - Experimental setup for the measurement of the reed valve stiffness

The whole instrumentation described above is placed on the adjustable work table of the drilling machine. The depth adjustment system of the drilling machine is used to control the tip advance. Thus, the above described instruments allow the reed valve movement and, contemporary, the force employed to move the valve is measured with the digital balance.

Figure 3.14 - Detail of the mechanical comparator positioning, fit out in order to measure the reed valve displacement

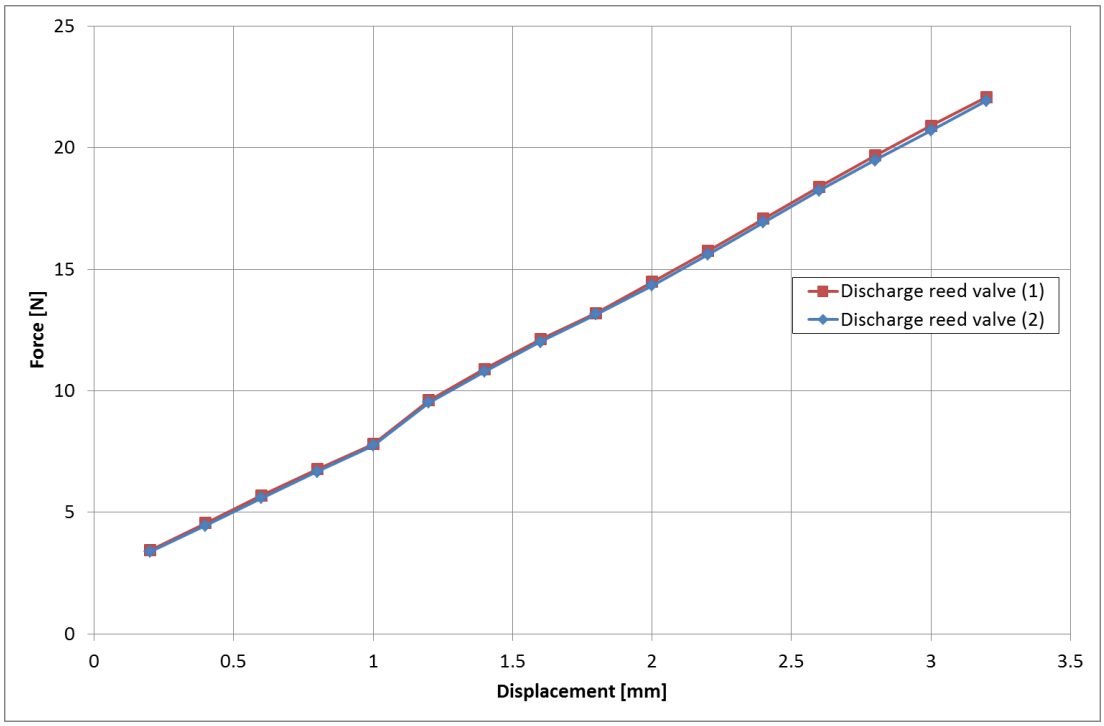

Figure 3.15 - Discharge reed valves stiffness diagram

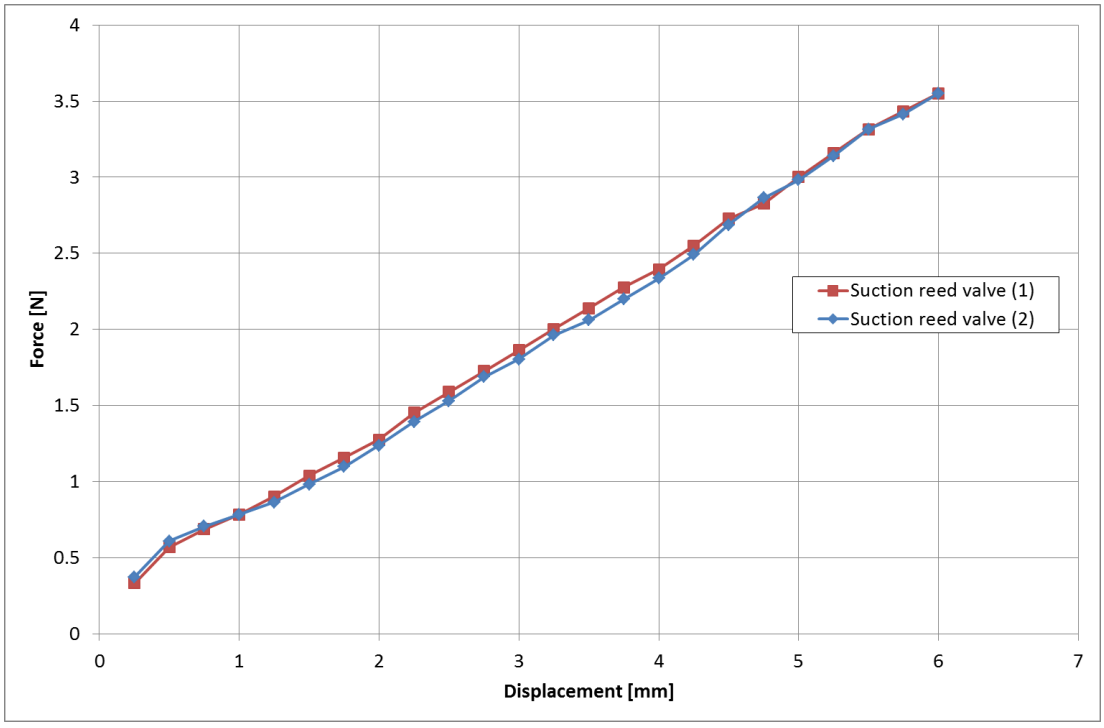

Figure 3.16 - Suction reed valves stiffness diagram

The graphs of Figure 3.15 and Figure 3.16 represent respectively the trends of the discharge and the suction valves stiffness, the indexes 1 and 2 refers to the first and the second valve (two valves for phase). The graphs show a linear trend of the valves stiffness as expected, only at the beginning of the suction valves curve there is a non-linearity; it is due to a little uncertainty of the valve movement (valve-plate conjunction). The mass of the entire reed valve is simple to measure but it is not simple to estimate the percentage of mass that is involved in the valve motion. This fact is due to the method adopted for the valve fixing on their support as shown in Figure 3.17. Especially for the discharge reed valve the definition of the real valve mass moving on the mass spring system is not simply to evaluate because of the presence of a limiter for the maximum lift which impedes the motion of about 2/3 of the valve, (Figure 3.18). In order to take into account this issue, in the numerical model a proper coefficient for the correction of the mass of the valves is considered.

Figure 3.17- On the left, the suction reed valves; on the right, the discharge reed valves

Figure 3.18 - Detail of the valve fixing: on the left, the discharge valve on the right, the suction valve

3.2.2 Numerical model calibration

The aim of the calibration of the 0D numerical model of a reciprocating compressor is that to realize a reliable simulation tool for the prediction of the thermodynamic cycle parameters. The calibration phase is necessary to characterize the uncertainty areas of the numerical model; precisely the calibration is focused on the valve dynamics and on the expansion and compression phases. For the calibration process, reference is made to the real in-cylinder pressure, measured during the experimental test on the compressor H503CS for cooling application (Figure 3.19). The test conditions are listed in the table below:

Gas	R404A
Suction pressure [bar]	2.2
Discharge pressure [bar]	19
Suction temperature [K]	294
Discharge temperature [K]	392
RPM	1440

Table - 3.2 Experimental conditions for the compressor testing

During the calibration phase the pressure of the inlet and the discharge ambient are considered as constant at their average value.

The first step is to define the matching of the compression and expansion curve. To reach this target the polytrophic coefficients ($\gamma=cp/cv$) of the compression and expansion process have been tuned; precisely for the compression phase an additive correction factor is introduced ($\gamma+\gamma_c$), vice versa, a reduction of the γ value is adopted for the expansion ($\gamma-\gamma_e$). These coefficients permit to consider mainly the phenomenon of the heat transfer typical of compression/expansion transformations and the phenomenon of the gas leakage between piston rings and cylinder.

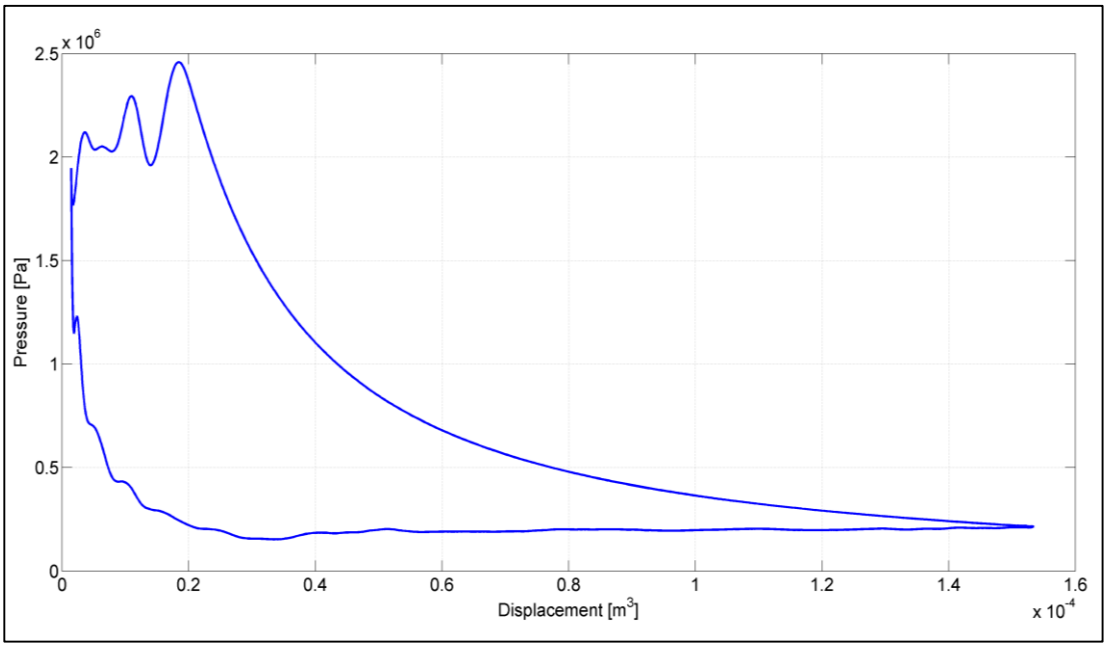

Figure 3.19 - Experimental PV Diagram of the H503CS compressor

The gas flow across the valves strongly influences the pressure trends inside the cylinder, during the suction and discharge phase; it is due to the automatic valve opening process. The valve dynamic is characterized by mechanical and by fluid -dynamic parameters. The mechanical ones are:

- the valve mass;
- the valve stiffness;
- the rebound coefficient;
- damping coefficient;
- the spring preload.

The above listed parameters strongly characterize the valve motion in terms of maximum lift, opening timing and oscillations; with reference to the considered valve typology no damping coefficient is taken into account. The valve stiffness is a known value (experimental test), while the valve mass is tuned using a proper coefficient in order to take into account the valve connection method as described in the preceding paragraph. For the rebound coefficient it is used a generic value typical of the impact between steel

bodies. In the this case no preload value is imposed because it is not present; however the valve model takes into account the case of spring preload. The fluid-dynamic parameters are:

- the flow coefficient;
- the drag coefficient.

The flow coefficient reduces the valve geometrical section to the real flow section directly influencing the mass flow rate. In first analysis the flow coefficient is considered constant and not in function of the Reynolds number or of the mass flow rate. To introduce the real valve flow coefficient a dedicated experimental campaign need to be performed, [28], [29]. The drag coefficient influences the driving force system acting on the valve surface and, as a consequence, the valve dynamics, its base value is the one typical of flat plate multiplied for a calibration factor (valve shape). The graph depicted in Figure 3.20 shows the comparison between the experimental and the calibrated numerical PV diagram. The comparison shows that the calibrated numerical model follows the real behavior of the pressure inside the cylinder, especially during the expansion, suction and compression phases. The zone in which the numerical model is less accurate is the discharge zone; the origin of this discrepancy probably is due to the following reasons:

- the valve dinamics, during the dischrge phase, have an influence on the in-cylinder pressure greater than the influence they have in the suction phase (fuid-dynamics parameter);
- pressure fluctuation of the discharge ambient (small effect).

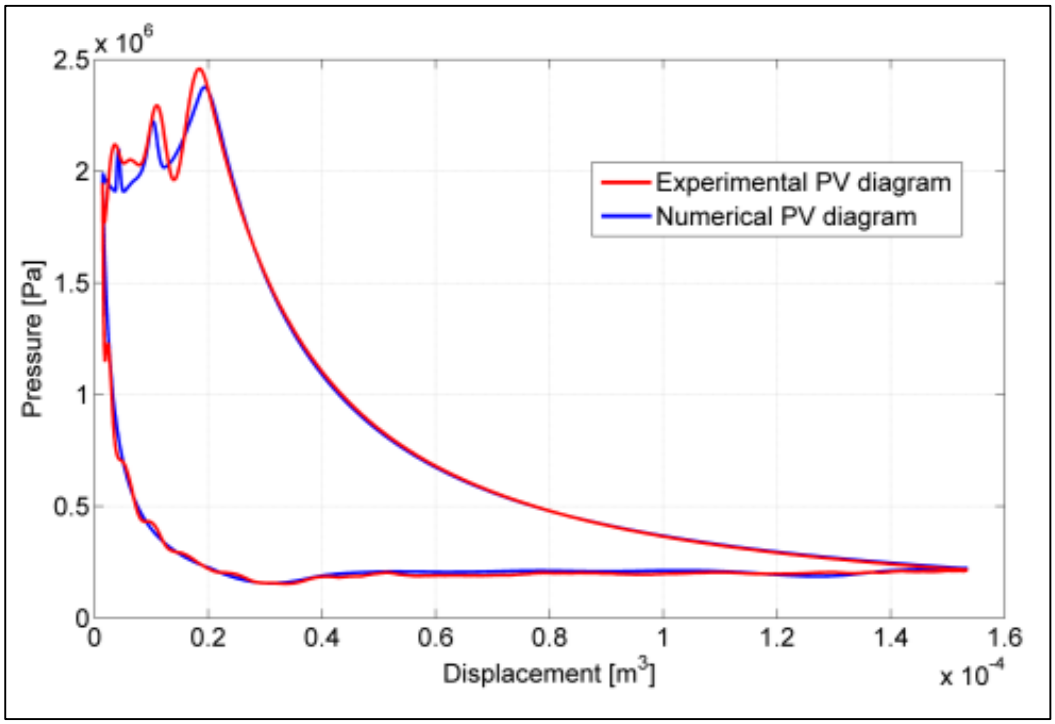

Figure 3.20 - Comparison between the experimental and the numerical cylinder pressures

In particular the mass flow rate (Figure 3.21) at the discharge is more pulsating than that at the suction, moreover the flow peaks reached are two or three times greater than the values reached during the suction phase. Therefore the approximation of constant flow coefficient results heavier for discharge valve than for suction valve. The same line of thinking can be adopted for the drag forces.

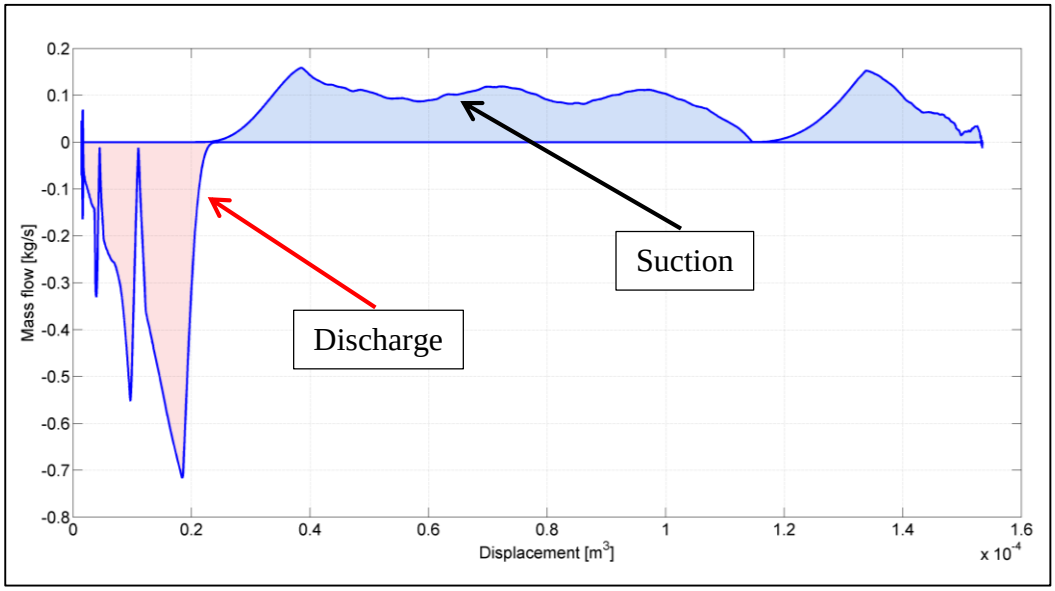

Figure 3.21 - Mass flow rate [kg/s], in blue the suction phase, in red the discharge phase.

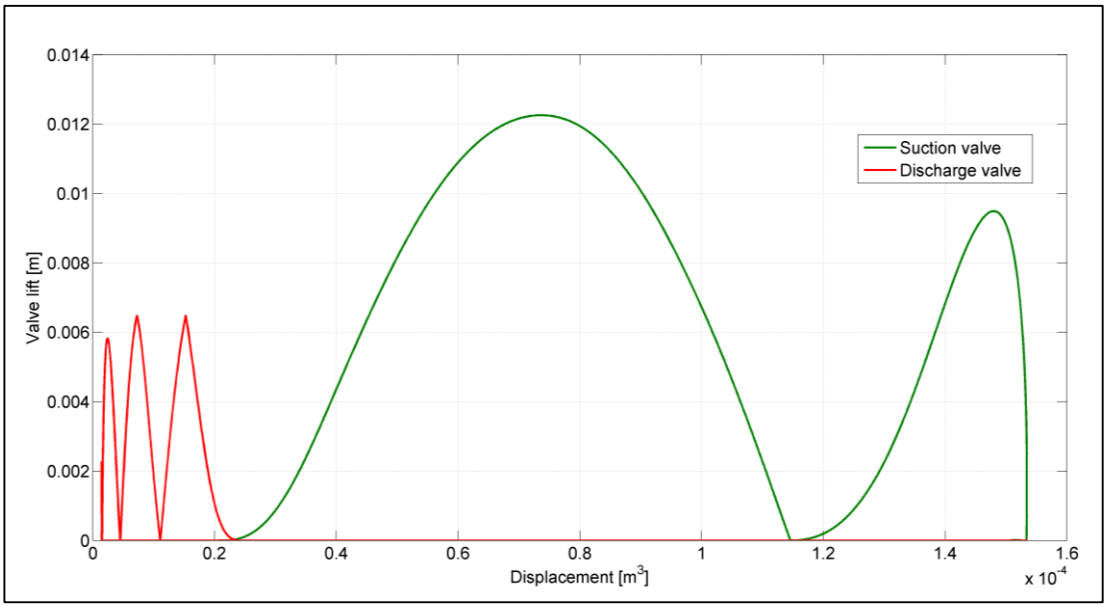

Figure 3.22 - Valve lift [m]

The valve lift diagram in Figure 3.22 shows the relationship between the PV diagram and the valve dynamics, It is clear the interaction between the valve dynamics, the mass flow rate, and the in-cylinder pressure; for example: looking at the discharge phase, it can be noticed the correspondence between the valve maximum lifts, the maximum mass flow rate peaks and the pressure peaks inside the cylinder.

The present paragraph wants to report the calibration of the numerical model, giving particular significance to the coherence of the numerical model: in fact it treats the relation between the two main numerical models, pressure calculation and valve dynamics, and describes their direct relationship.

3.2.3 Results

In present paragraph are depicted some investigations that can be carried out using the RE.CO.A code. In Figure 3.23 the analysis of the influence of the clearance volume on the PV diagram is shown. The blue line refers to the compressor in the base configuration, the red dash-dot line refers to the compressor with an halved clearance volume and the green dashed curve refers to the compressor with a double clearance volume. You can notice that the variation of the clearance volume causes a reduction or a growth of the residual gas trapped inside the cylinder at the TDP, as a direct

consequence the expansion phase behaves differently. There is a steeper expansion phase in case of smaller clearance volume vice versa in case of bigger clearance volume.

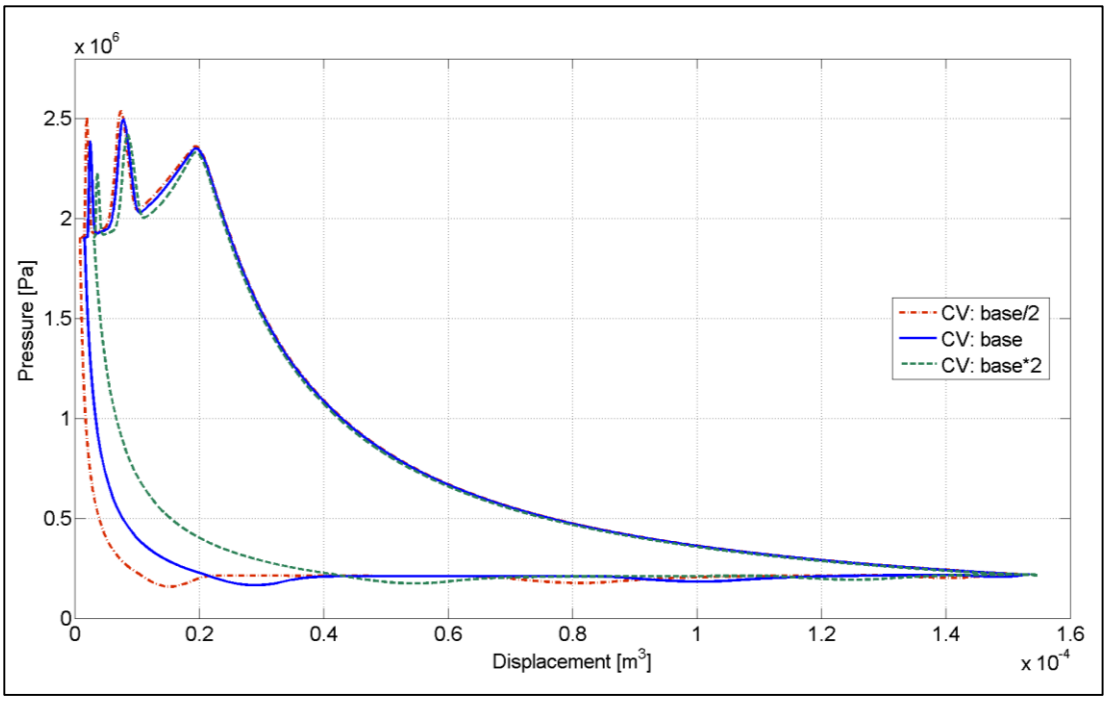

Figure 3.23 - Analysis of the influence of the clearance-volume variation on the PV diagram

In Figure 3.24 the influence of the compressor speed variation on the PV diagram is investigated. In blue is represented the PV diagram of the compressor in the base configuration: 1440 RPM; the red dashed curve is relative to a simulation in which the compressor speed is increased respect to the base configuration, (+30%); the dash-dot violet curve refers to a simulation in which the compressor speed is reduced respect to the base configuration (-30%). The graph shows a clear reduction of the overpressure during the discharge phase in case of low compressor speed. A reduction of the compressor speed causes a direct reduction of the instantaneous mass flow at the discharge (and suction) section and as a consequence there is a reduction of the fluid-dynamic losses across the valves. For this reason there is a global reduction of the discharge overpressure.

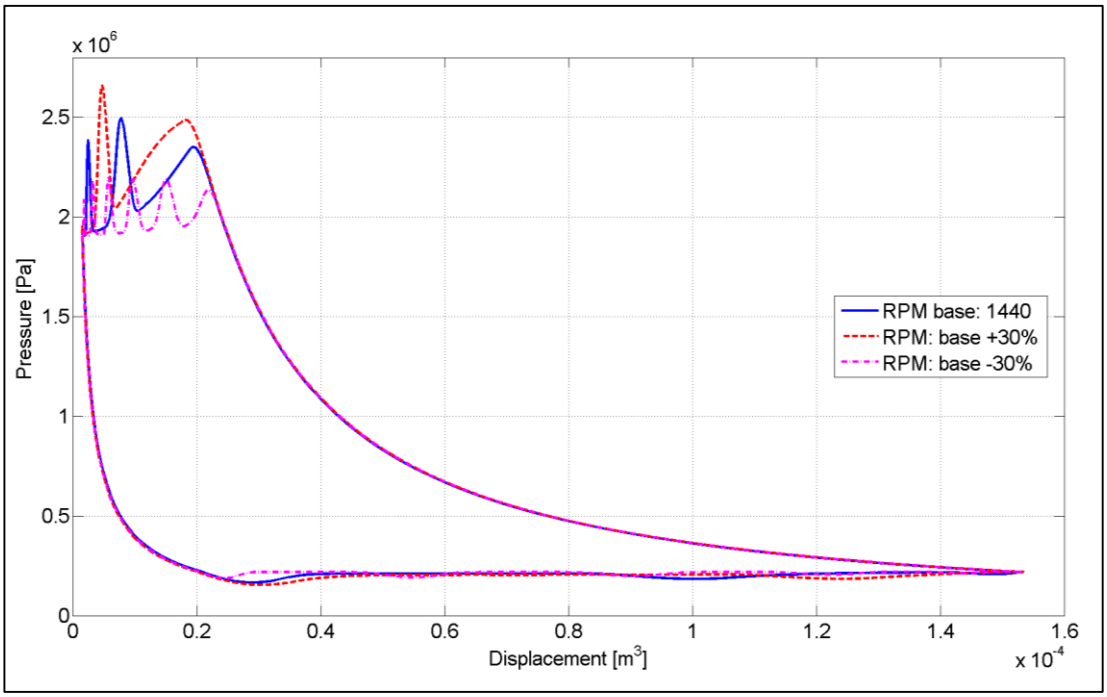

Figure 3.24 - Analysis of the influence of the compressor speed on the PV diagram

At the suction side this phenomenon is less evident because during the suction process the instantaneous mass flow rate is globally lower than during the discharge process (Figure 3.21) and the variation of the compressor speed don't cause appreciable differences on the in-cylinder pressure.

Following the influence of the discharge valves dynamics on the behavior of the reciprocating compressor is analysed. In Figure 3.25 there is depicted the effects that a variation of the discharge valve mass causes on the indicating cycle. An increase in the valve mass causes a growth of the valve inertia, as a consequence you can obtain: a delay in the discharge valve opening and a reduction of the valve natural frequency. In Figure 3.26 the detail of discharge phase is depicted; the blue line is the base configuration, the dashed green line refers to the configuration in which the mass of the discharge valves is double respect to the base configuration, the violet dashed curve is relative to the configuration in which the mass of the discharge valves is halved respect to the base configuration.

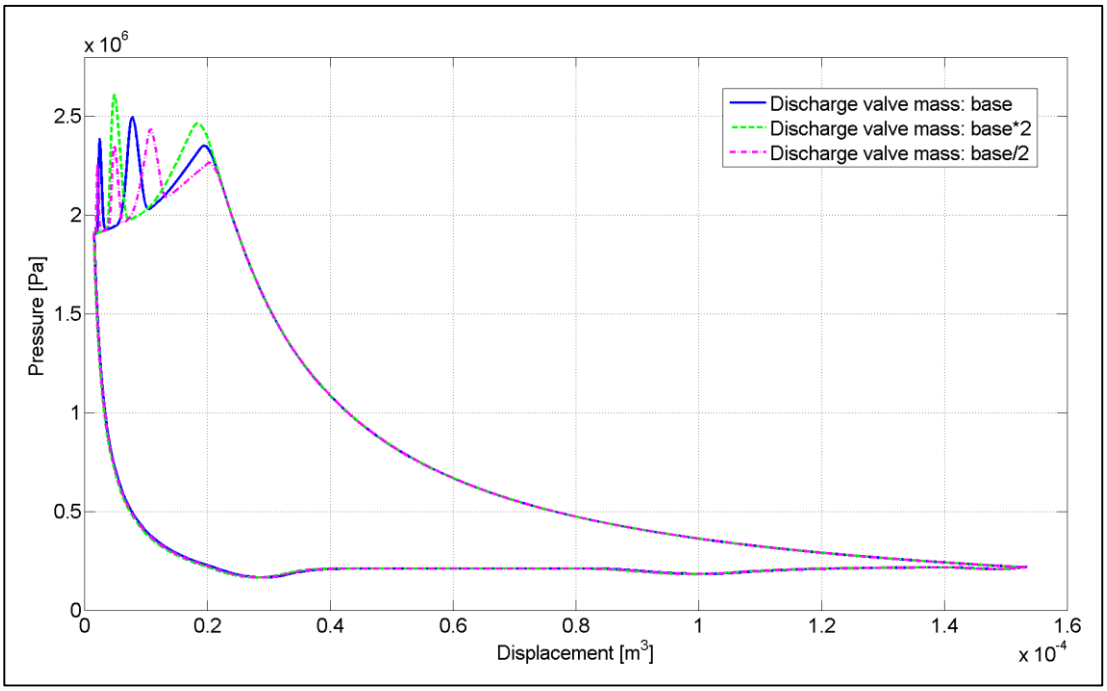

Figure 3.25 - Analysis of the influence of the reed valve mass on the PV diagram

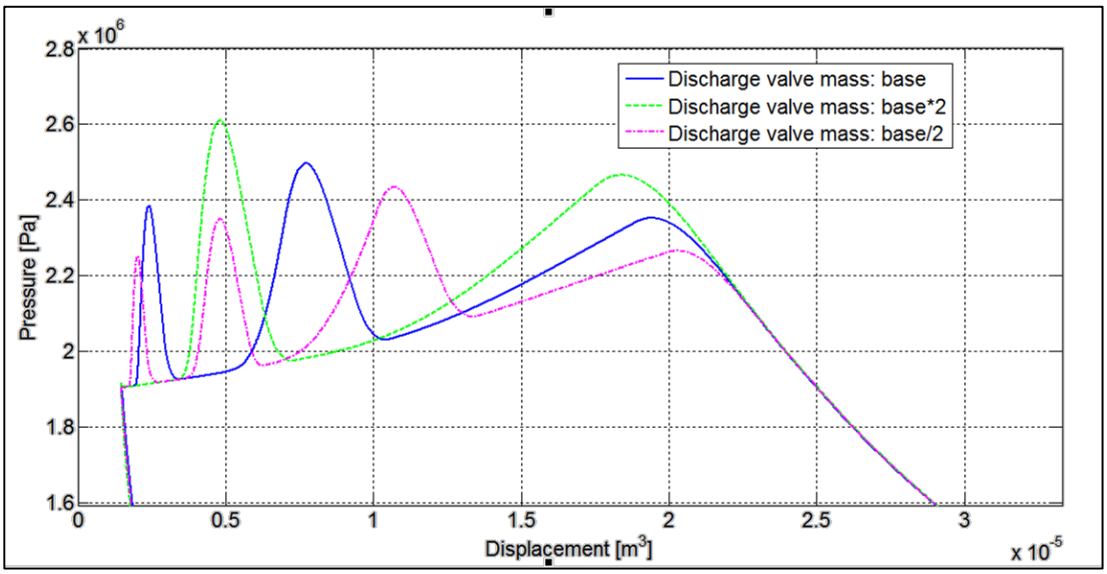

Figure 3.26 - Detail of the discharge section (valve mass)

The trends of the indicating cycles confirm what above mentioned. In fact for the configuration in which the valve mass is greater (green line), the first pressure peak is higher and postponed respect to the other configuration; moreover there are a less number of pressure peaks (2) which means a lower valve natural frequency (each in-cylinder pressure peak correspond to a valve closure, Figure 3.22)

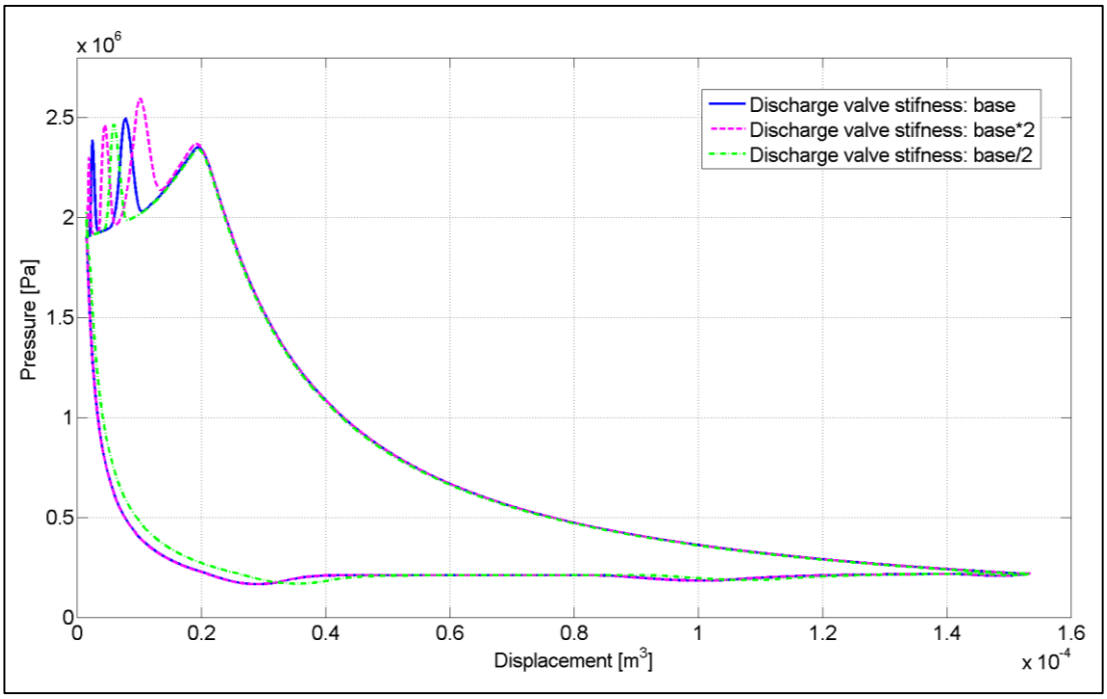

Figure 3.27 - Analysis of the influence of the reed valve stiffness on the PV diagram

In Figure 3.27 the effects of the stiffness of the discharge reed valve on the in-cylinder pressure is shown; in blue the curve relative to the base configuration, in green the curve relative to the configuration with the valve stiffness halved respect to the base configuration, in violet the curve relative to the configuration with the valve stiffness double respect to the base configuration. Even in this case is valid what above mentioned for the valve mass. The greater the valve stiffness the higher is the natural frequency of the valve (oscillation of the valve) and as a consequence there are more in-cylinder pressure peaks (valve closures).

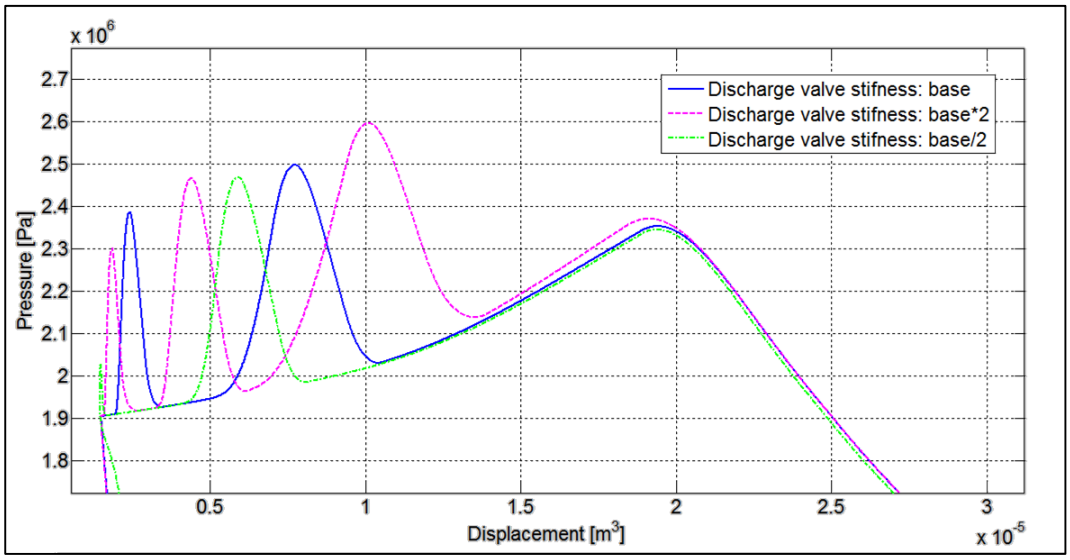

Figure 3.28 - Detail of the discharge section (valve stiffness)

The detail of Figure 3.28 illustrate the physical coherence of the RE.CO.A code. In the graph depicted in Figure 3.29 there is depicted the analysis of the compress functioning with different typologies of gasses: Air and R404A. This test wants to show again the flexibility and the potentiality of this numerical tool for the preliminary analysis of the compressor performance; it is clear its support during the design stage of the reciprocating compressor.

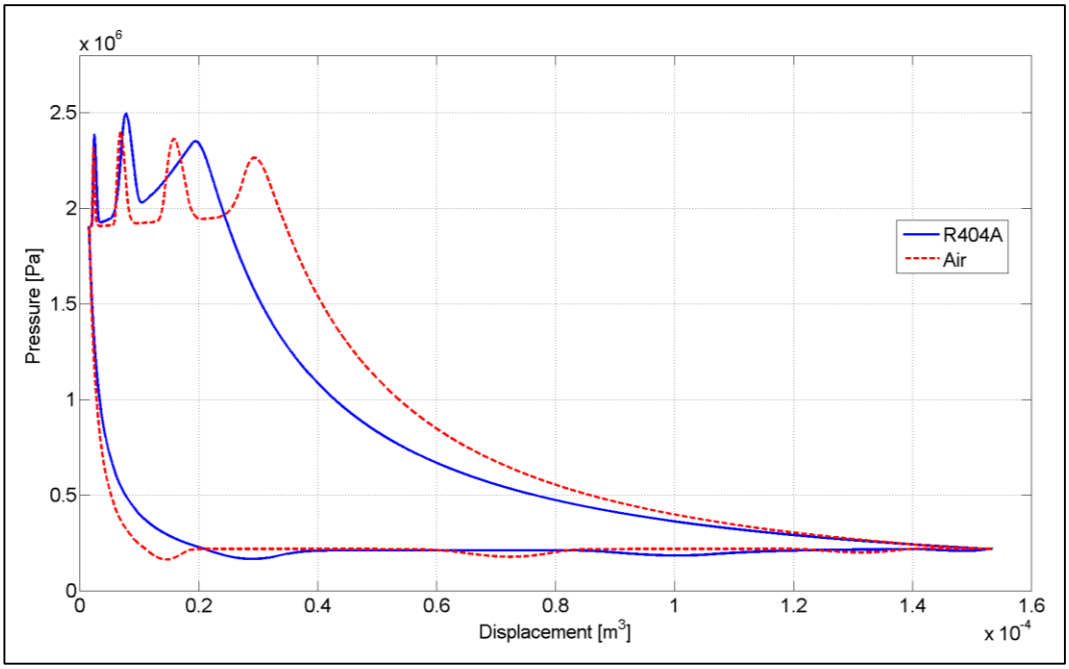

Figure 3.29 - Analysis of the functioning of the compressor provided with different gasses; in blue the indicating cycle with R404A and in red the indicating cycle with Air

3.3 Acoustic hybrid approach

The frequency domain modelling is simple and ideally suited for synthesis of acoustic elements like mufflers, acoustic filters for pipeline, discharge systems. This kind of treating acoustic issues is frequently adopted in automotive field for the analysis of the noise of the exhaust systems [30] or the analysis of the inlet waves in the intake system; however, it requires a prior knowledge of the source characteristics. The hybrid approaches developed essentially try to couple the acoustic description of the muffler piping system to the acoustic source. In this kind of approach, the mass flux at the exhaust valve is calculated by the method of characteristics and it is used as an input to the frequency domain analysis of the exhaust muffler. The simplest aspect of these hybrid approaches is that discussed by Jones et al. [31] who studied the possibility of using a nonlinear calculation to determine the instantaneous volume velocity at the source and, then, applying the linear acoustic description of the piping system in order to compute the volume velocity at the open end. This simple solution represents an obvious limitation, since the first nonlinear calculation cannot take into consideration the information related to the acoustic behaviour of the piping system. In this way no account is taken for the interaction between the source and the system. Davies et al. [32] coupled the frequency response of an open end to the flow calculation in the duct, making use of the inverse Fourier transform of the termination impedance and an acoustic filter placed downstream of the exhaust pipe. Later on they came up with a new hybrid approach in which pressure and velocity in the time domain are coupled with those in the frequency domain at the interface [33], [30]. Sathyanarayana et al. [7] apply a new hybrid approach for the prediction of the noise radiation from the engine exhaust systems; it couples the time domain analysis of the engine and the frequency domain analysis of the muffler, and has the advantages of both. The engine behaviour is modelled in the time domain in order to calculate the exhaust mass flux at the exhaust valve by means of the method of characteristics.

In the reciprocating compressor field main attention is paid to the pressure waves propagating in the discharge and suction pipelines. Oscillating pressure waves may lead to mechanical vibrations and failures: the pipelines acoustic response affects also the

machine performance. So it is fundamental to estimate the pressure wave dynamics in suction and discharge pipelines of the reciprocating compressors plants.

In this work a hybrid time-frequency domain approach is realized: the reciprocating compressor thermodynamic cycle is modelled in the time domain while the pressure wave propagation in the pipelines is modelled with the transfer matrix method in the frequency domain. An iterative method is at the basis of the approach and allows the mutual interaction between the source (compressor) and its boundary conditions (pipelines): using the FFT theory the matching between the time domain and the frequency domain is obtained.

The main structure of the system can be schematized as shown in Figure 3.30, at the center the primary source, the compressor, at the left and right ends there are the pipe line elements that represent the boundary conditions.

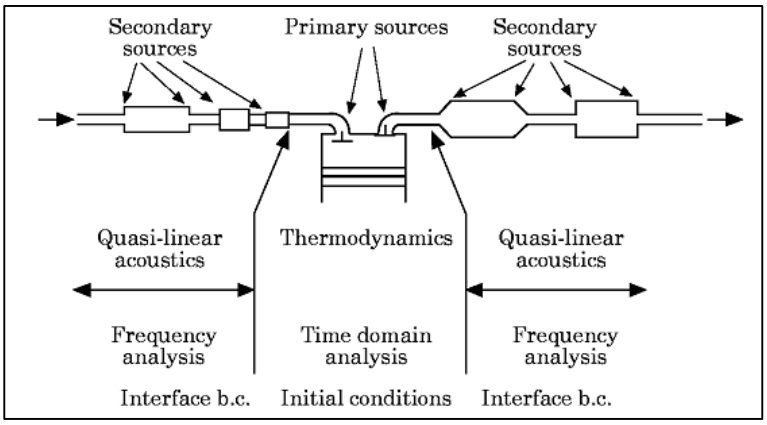

Figure 3.30 - Hybrid system scheme

3.3.1 Pipeline elements (frequency domain)

The elements composing the suction and discharge line of a compressor system usually are:

- ducts;
- simple volume, usually of cylindrical shape with one inlet and outlet or multiple terminations;

- orifices;
- complex volume, for example the interface between the reciprocating compressor chamber and the suction and discharge lines.

A way to treat simply their influence during the suction and discharge phases is to analyse their behaviour, making use of the transfer matrix method described in the paragraph 2.2. In order to clarify, the transfer matrixes of the elements used in the numerical model are shown below.

For the duct element the transfer matrix is the one shown in the equation 3.X:

$$\begin{bmatrix} \cos(k * L) & i * Y_0 * \sin(k * L) \\ i * \frac{1}{Y_0} * \sin(k * L) & \cos(k * L) \end{bmatrix} \qquad 3.X$$

Where k=2·pi·f/a is the wave number, Y0 = a/pi·D^2/4) is the characteristic impedance, L is the duct length, D is the duct diameter.

The discontinuity element represents a cross-section variation along the duct, at the interface there is the same pressure upstream and downstream and the same particle velocity as expressed by equation 3.XI.

$$\begin{bmatrix} 1 & 0 \\ 0 & 1 \end{bmatrix} \qquad 3.XI$$

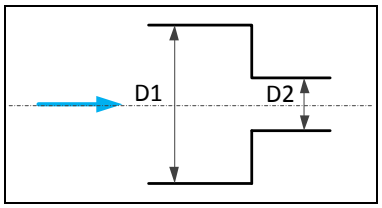

Figure 3.31 - Duct discontinuity

In case of lateral discontinuity, like a T duct with a closed end (Figure 3.32), the transfer matrix changes as shown in equation 3.XII.

$$\begin{bmatrix} 1 & Yd\cdot\left(i\cdot 0.85\cdot k\cdot\frac{D1}{2}\right) \\ \frac{1}{Z_{lat}} & 1 \end{bmatrix} \qquad 3.XII$$

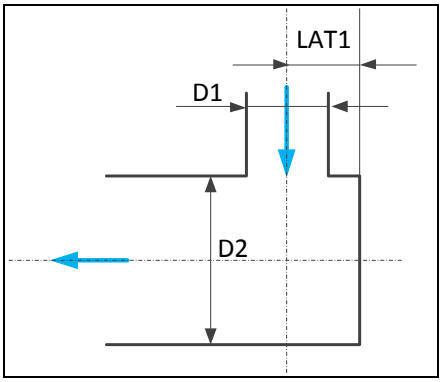

Figure 3.32 - Lateral discontinuity

Where $Yd = a/S_1$, $Yc = a/S_2$ and $Z_{lat} = -i\cdot Y_c/\tan(k\cdot L_{lat})$; S_1 and S_2 are the cross-sections of the lateral duct and of the main duct, L_{lat} is the distance between the closed end and the intersection between the lateral axis and main ducts axis. The plenum element is realized as a composition of duct and discontinuity elements. Below it is described the related transfer matrix which is the assembly of the ducts and the lateral discontinuity transfer matrixes.

$$[[Duct\ 1]\quad [Lat.Disc.1]\quad [Duct\ 2]\quad [Lat.Disc.2]\quad [Duct3]] \qquad 3.XIII$$

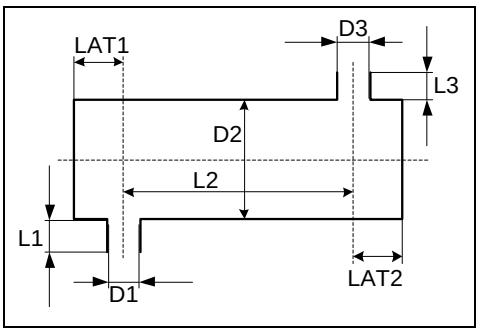

Figure 3.33 - Scheme of plenum with one inlet and one exit

In the acoustic theory, the driving force of the system it is represented by the pressure wave or by the mass flow. In the present work, the interaction between the compressor and the line is estimated at the interface of the suction and the exhaust valves

with the line. To estimate correctly the driving force for the line it is more appropriate to adopt the mass flow rate at the valve which is the same upstream and downstream of the valve, rather than the pressure; in fact the pressure is calculated inside the cylinder so that, to evaluate its values at the interface with the line, it is necessary to know the pressure drop at the valves.

3.3.2 Interaction between source and pipeline

As described in paragraph 3.1 the numerical model of the reciprocating compressor generates as outputs one by one the thermodynamic parameters of the machine and the mass flow rate at the suction and at the discharge valves with the related pressure trends. In order to treat the signals in the piping system, using the transfer matrix method, it is necessary to convert the signals from the time domain to the frequency domain. In Figure 3.34 it is depicted a typical trend of the mass flow rate at the discharge valve of a reciprocating compressor for refrigeration systems.

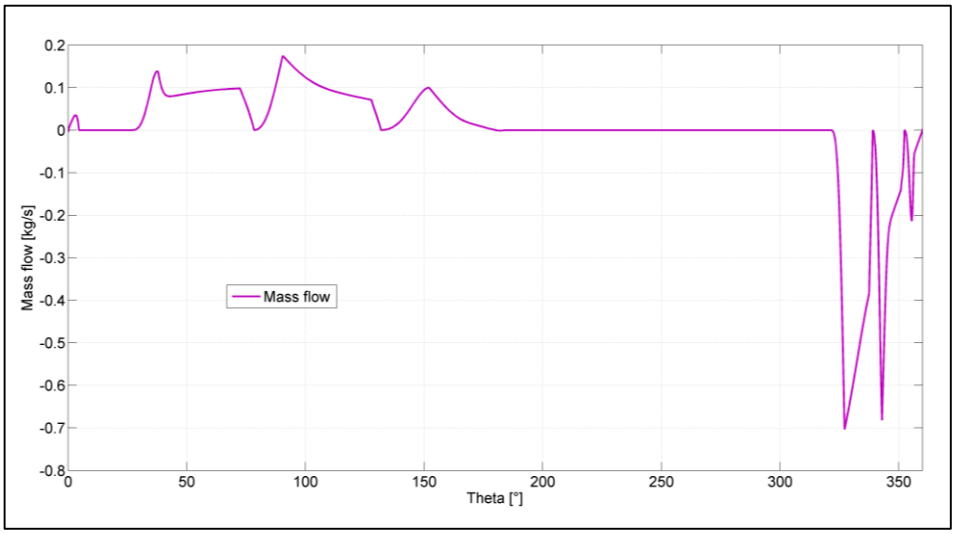

Figure 3.34 - Mass flow rate at the discharge valve

Once treated the signal in the frequency domain it should be reconverted in the time domain in order to generate the new boundary condition for the numerical model of the source; this procedure is shown in Figure 3.35.

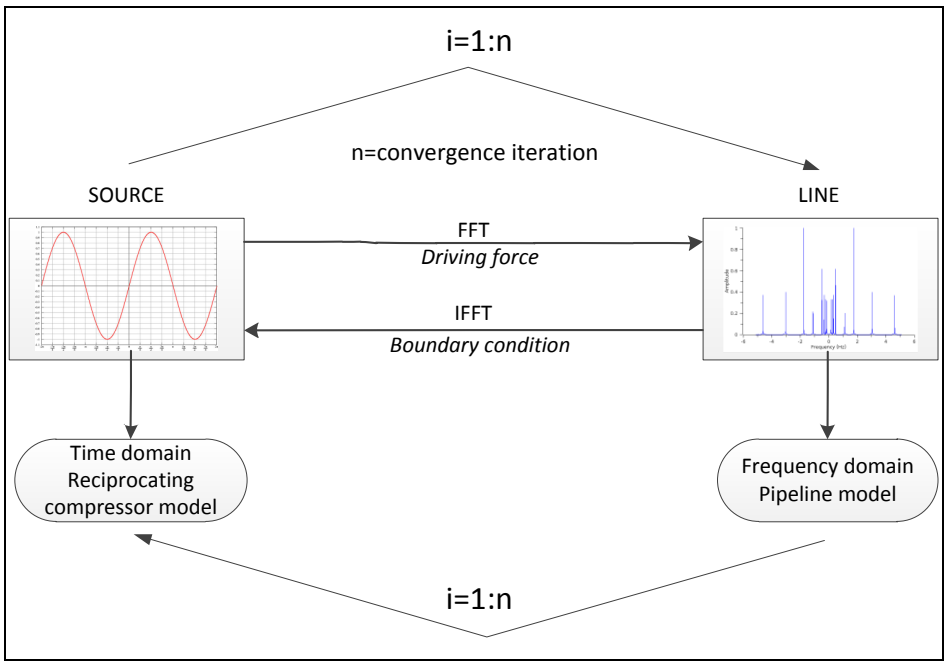

Figure 3.35 - Source / line interaction

3.3.3 FFT analysis

The mass flow rate at the suction and discharge valves is represented by a discontinuous signal of null value for about 2/3 of the thermodynamic cycle (closed valves) and by a pulsating trend when the valve opens.

In order to evaluate the reliability of the fast Fourier transform in case of such a signal, an analysis with known signals has been performed

The first case is represented by a continuous signal composed by two sinusoidal functions:

$$f(x) = A \cdot \cos(2 \cdot \pi \cdot f \cdot x + phi) + g(x) \qquad 3.XIV$$

$$g(x) = \frac{A}{4} \cdot \cos\left(2 \cdot \pi \cdot 10 \cdot f \cdot x + \left(\frac{phi}{2}\right)\right) \qquad 3.XV$$

Where:

- f = 10 is the signal frequency;
- phi = 30 is the signal phase;
- A = 5 is the signal amplitude.

In Figure 3.36 is depicted the FFT (fast Fourier transform) analysis of the *f(x)* function, it is possible to observe that the FFT tool allows to obtain the right amplitude and phase values in the frequency domain.

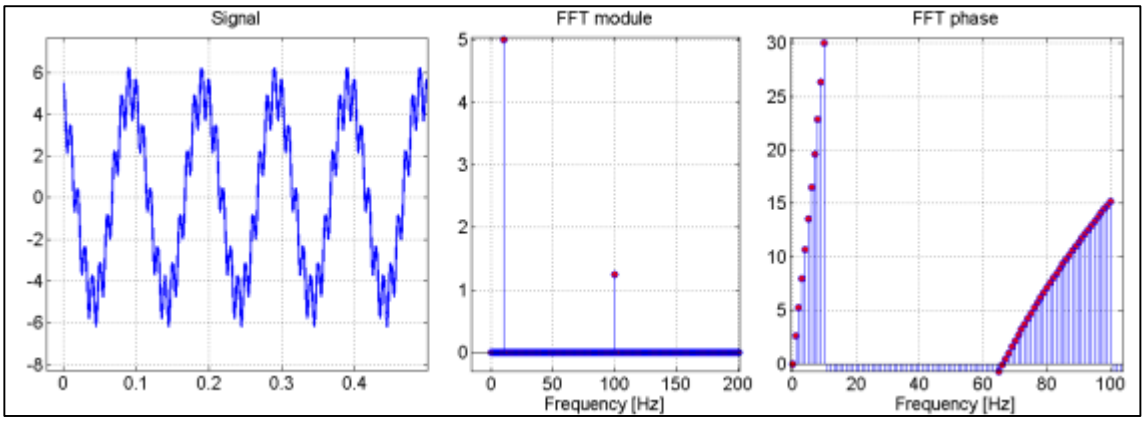

Figure 3.36 - FFT analysis of a composed signal

Now the signal is reconstruct in the time domain using the IFFT (standing for inverse fast Fourier transform) tool starting from the frequency data; Figure 3.37 shows the comparison between the original signal and the reconstructed one. The comparison demonstrates the reliability of the numerical model to reconstruct the signal in the time domain, starting from a signal in the time domain and passing through the frequency domain.

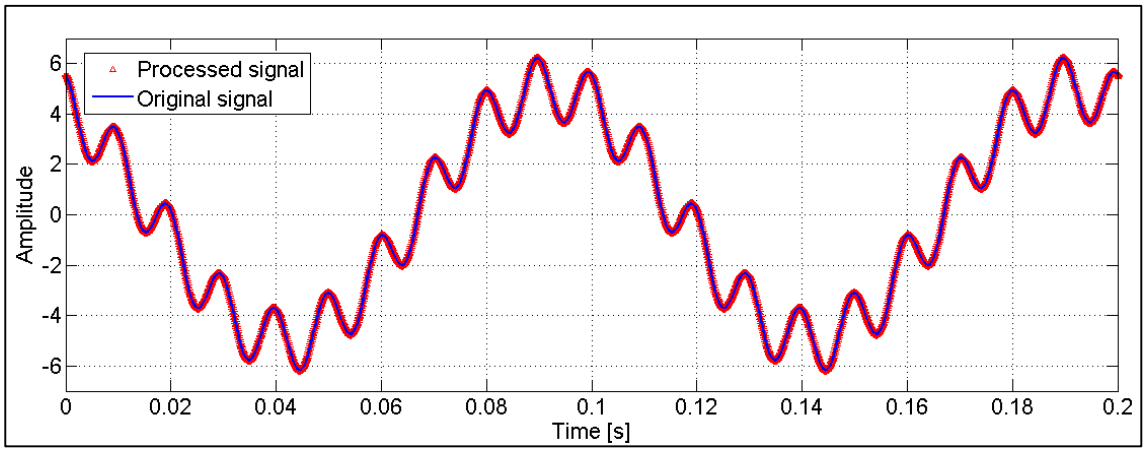

Figure 3.37 - Comparison between the original signal and the processed signal

As shown in Figure 3.34, the mass flow rate signal is not continuous and it is clear the importance of analysing how to treat a signal like that. The second object analysed is a signal composed by null values, sinusoidal signal and again null values, this is a first simplification of the real mass flow rate signal. In this way it is possible to estimate a signal with anomalous frequency content. The comparison between the original signal and the processed signal is shown in Figure 3.38: the processing of the signal allows the right reconstruction from time domain to frequency domain and again to time domain.

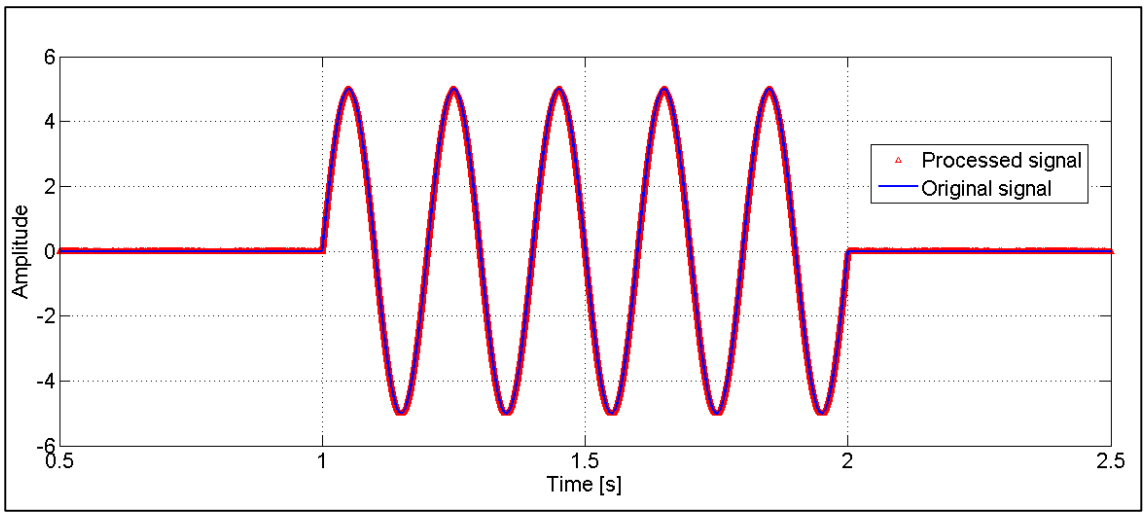

Figure 3.38 - Analysis of a null - sinusoidal - null signal

The same analysis is done for a signal with the average value different than 0.

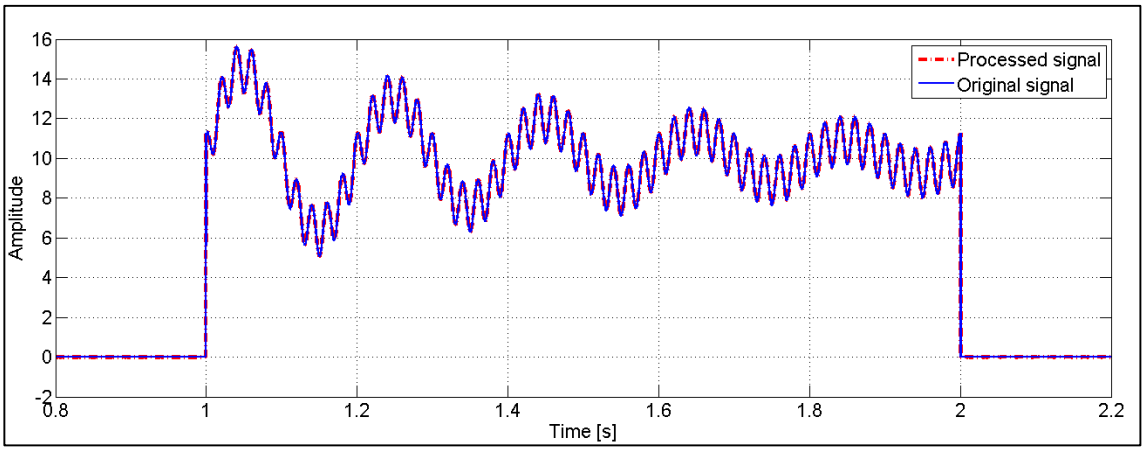

Figure 3.39 - Analysis of a null - sinusoidal - null signal with mean value different from 0

In Figure 3.39 is depicted the trend of a discontinuous sinusoidal decaying signal and the related processed signal; it is evident that the methodology adopted is suitable even for complex discontinuous signals like this. Finally, to be thorough, the analysis of the real mass flow signal of a reciprocating compressor is taken into account.

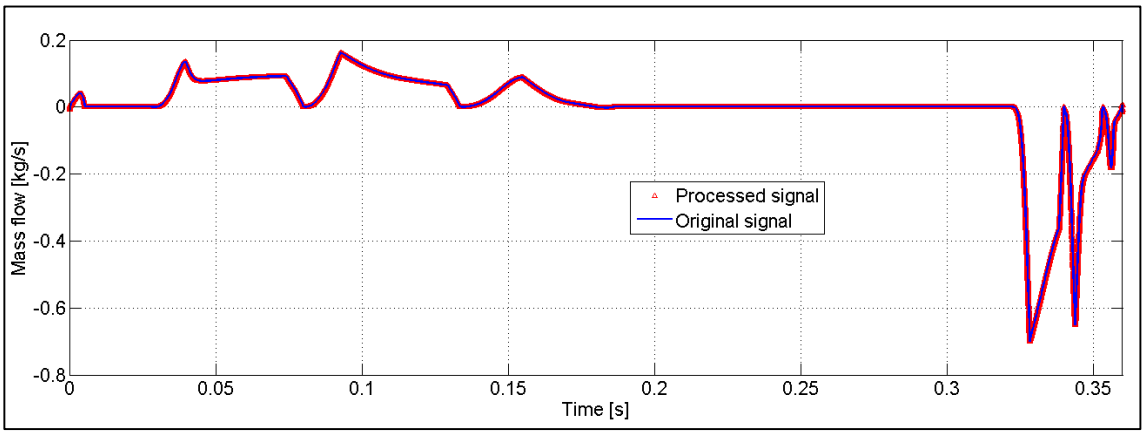

Figure 3.40 - Real mass flow rate original signal vs reconstructed signal

This case shows that a real variable signal with random frequency content can be converted in the frequency domain using the numerical FFT tool and then, using the IFFT tool, it is possible to bring it back in the time domain again; in fact the signals depicted in Figure 3.40 correspond one another. The above treatise about FFT and IFFT is taken on in order to be sure that the use of a real signal passage from the time domain to the frequency domain -and vice versa- doesn't cause a lack of information and, as a consequence, a wrong signal reconstruction.

3.3.4 Base example: Wave propagation in a duct

The base of the hybrid model is represented by the interaction between the time domain of the source and the frequency domain of the line, so it is clear the importance to validate the interaction between the two domains. The idea is to realize a model, able to simulate simple configurations, in which the source is represented by a sinusoidal signal and the line is composed by simple elements. The configuration analysed is a simple straight duct with open ends; the duct at one end is connected to the source and at the other end it discharges in an open ambient: the scheme is shown in

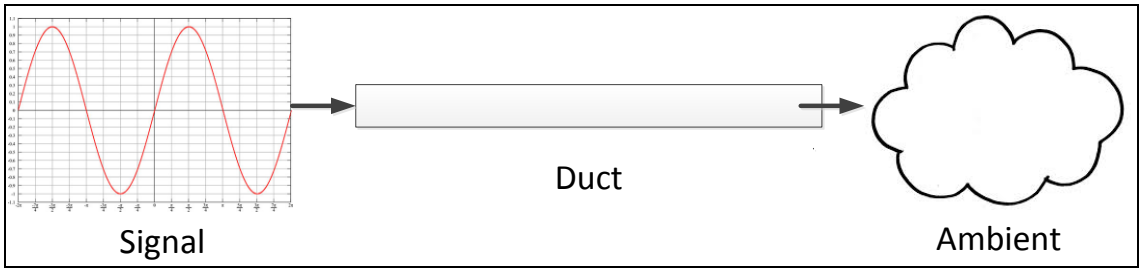

Figure ***3.41***.

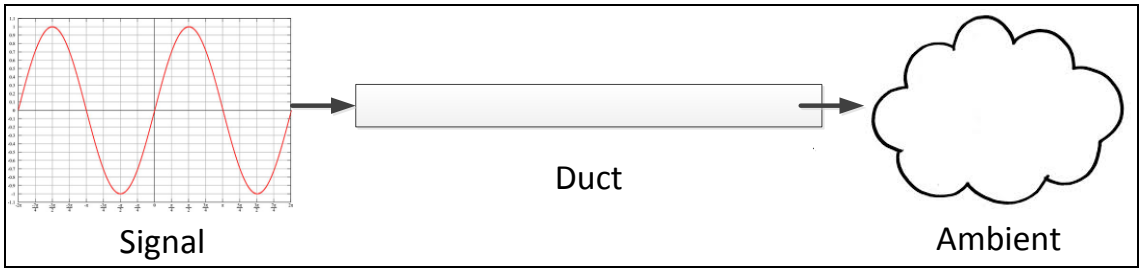

Figure 3.41 Scheme Signal-Duct-Ambient

The signal is represented by a sinusoid defined in the time domain, the duct and the ambient are described using the transfer matrix method. When the signal reaches to the open end of the duct, it reflects and goes back.

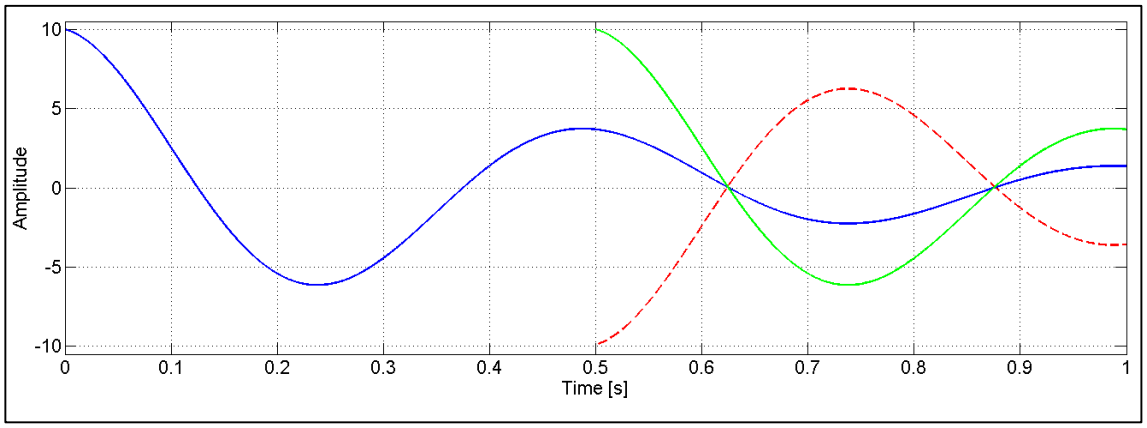

Figure 3.42 - Open end duct simulation

In the picture above, the blue curve represents the input signal that is a sinusoidal decaying signal described by the following equation:

$$f(t) = \mathrm{A} \cdot \cos(2\pi \cdot f \cdot \mathrm{t} + \mathrm{phi}) \cdot e^{2t} \qquad \textbf{3.XVI}$$

The signal is comparable to the wave propagation into a duct; the wave propagates at sound velocity in air (medium). To understand if the phenomenon is well modelled it is taken into account the case of a duct of length *a/2* [m], where *a* is the length covered by a wave travelling for a second at the sound speed (medium is air at STP conditions). In this way, performing a simulation that lasts for a second, the wave propagating into the duct after half second reaches the open end and then it goes back, up to the starting point. Looking at the graph of Figure 3.42: the blue curve is obtained monitoring the wave amplitude with a virtual sensor at inlet duct, the green and the red dashed curves are obtained monitoring the signal at open end. So, after 0.5 s, the input signal reaches the end of the duct (green curve); at this point the reflected wave (red dashed curve) appears and starts its propagation back in the duct with the opposite amplitude. The graph of Figure 3.42 illustrates the correct ideal behaviour of a wave propagating in a duct with open end, this process includes the passages from time domain to frequency domain and vice versa, and, moreover , the treating of the duct and of the discharge ambient with the transfer matrix theory. Now the reliability of the adopted methodology is proved.

4 Hybrid model

In the previous chapter the calibration and the validation of the reciprocating compressor numerical model is described; also the acoustic approach adopted for the modelling of the line elements is described and a rigorous numerical process for the validation is shown. On the basis of the above considerations in the present chapter are shown the results of the hybrid approach application; in particular some examples of compressor-line systems are tested.

4.1 Configuration 1

In Figure 4.1 is depicted the scheme of a reciprocating compressor provided with two plenums respectively on the suction and discharge line.

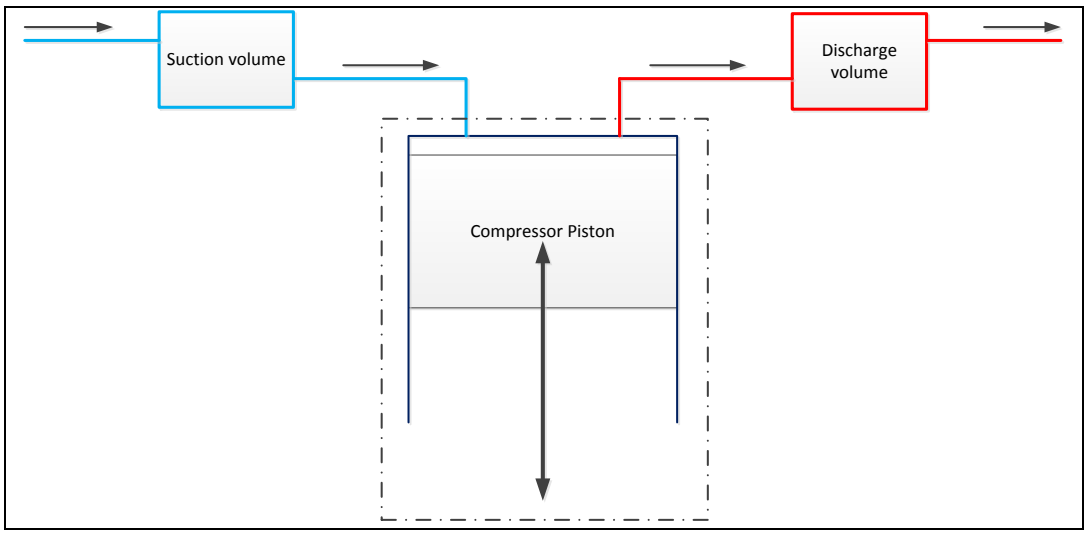

Figure 4.1 - Scheme of the compressor provided with the plenum on the suction and the discharge line

The plenum applied is schematized in Figure 4.2; the plenum is characterized by an inlet and an outlet duct, the ducts are not coaxial each other and they are joined orthogonally to the central body (cylindrical shape). For the suction plenum the inlet duct is directly connected to the constant pressure suction ambient while the outlet duct is connected to the compressor head, vice versa for the discharge plenum. In order to verify the reliability of the hybrid approach, some plenum geometries are tested.

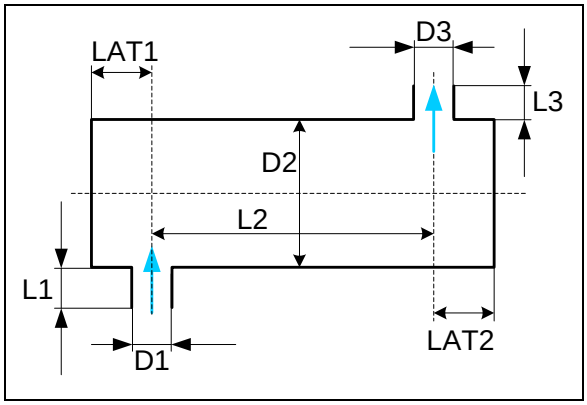

Figure 4.2 - Plenum scheme

The geometry values of the plenum for the first test are shown in the table below, the same geometry values are adopted for suction-discharge line.

Plenum Geometry values [m]			
L1	0.08	***D2***	0.55
D1	0.05	***LAT2***	0.15
LAT1	0.15	***L3***	0.08
L2	0.5	***D3***	0.05

Table - 4.1 Plenum geometry values

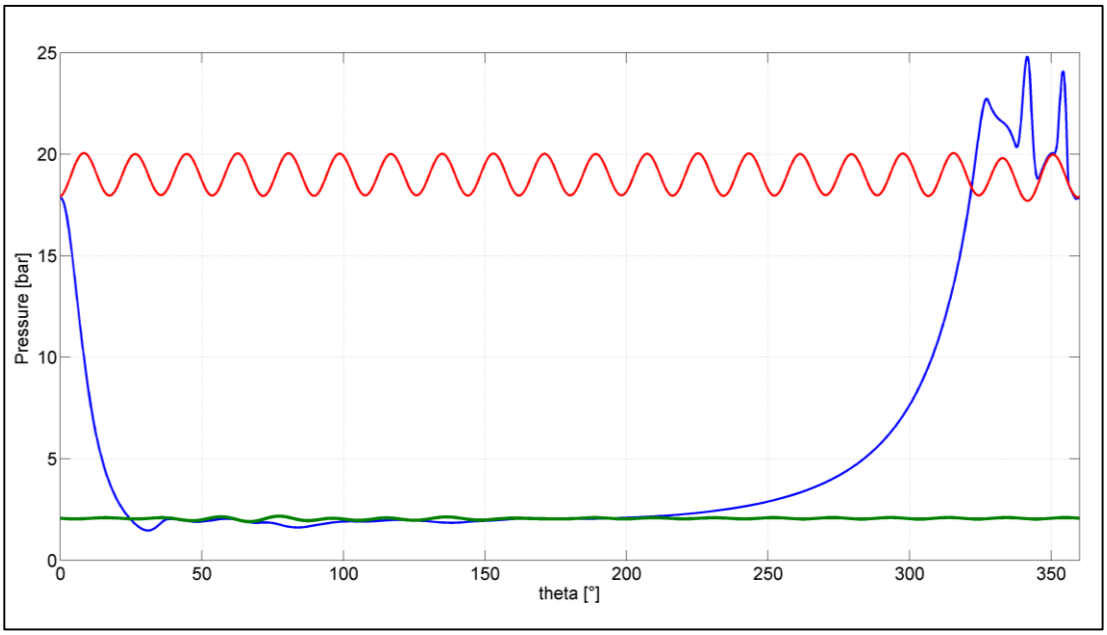

Figure 4.3 - PV diagram, blue in-cylinder pressure, red discharge pressure, green suction pressure. Plenum cylindrical body diameter D2=0.55m

The graph of Figure 4.3 shows the results of the first simulation, in blue the indicating cycle, in red the discharge pressure and in green the suction pressure; precisely the suction and discharge pressures are the reflected pressure computed at the interface between the compressor and the plenum. In this case the reflected pressure oscillation is appreciable especially for the discharge phase. The pressure transmitted downstream the plenum are depicted in Figure 4.5 and Figure 4.6 respectively for the suction area and for the discharge area.

A first comparison is done changing the plenum cylindrical body diameter, D2 dimension. Changing the D2 value, vary the discontinuity ratio between the inlet duct and the cylindrical body (both for the inlet and the outlet duct). Moreover the greater the plenum the less is the transmitted pressure oscillation but there is a greater reflected wave component at the interface between the plenum and the compressor. In Figure 4.4 is shown the PV diagram of the compressor provided with the suction and the discharge plenum with the cylindrical body diameter (D2=0.2 m) reduced respect to the previous case. This variation reduces the ratio between the inlet (outlet) duct and the cylindrical body. Observing Figure 4.4 can be noticed that the discharge pressure fluctuation reflected toward the compressor are strongly reduced respect to the previous configuration, this fact confirms that reducing the plenum volume the reflection effect is

reduced (the plenum takes the behavior of a simple duct); on the contrary the transmitted wave oscillation grows, it is possible to see the direct comparison between the two cases in Figure 4.5 and Figure 4.6 for the suction and the discharge plenum.

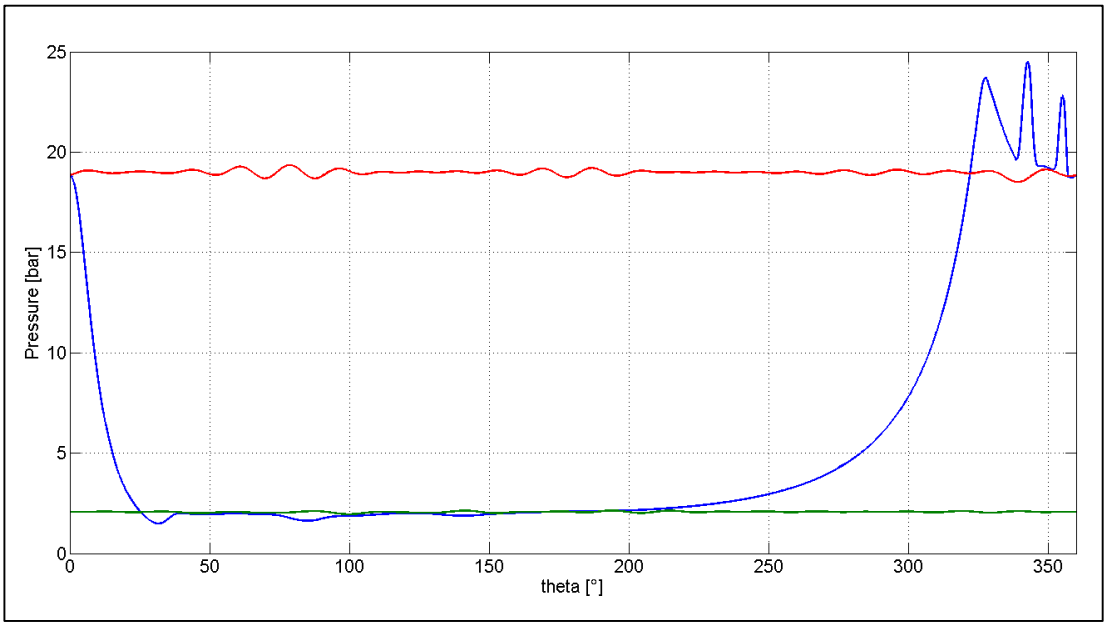

Figure 4.4 - PV diagram, blue in-cylinder pressure, red discharge pressure, green suction pressure. Plenum cylindrical body diameter D2=0.2m

Precisely in the graph of Figure 4.5 is depicted the pressure transmitted from the plenum to the suction line. The green line is relative to the plenum with the cylindrical body of diameter 0.2m while the blue line is the relative to the plenum with the cylindrical body of 0.5m. The comparison highlights a reduction in the pressure amplitude oscillations for the compressor provided with the bigger plenum as expected from the acoustic theoretical analysis.

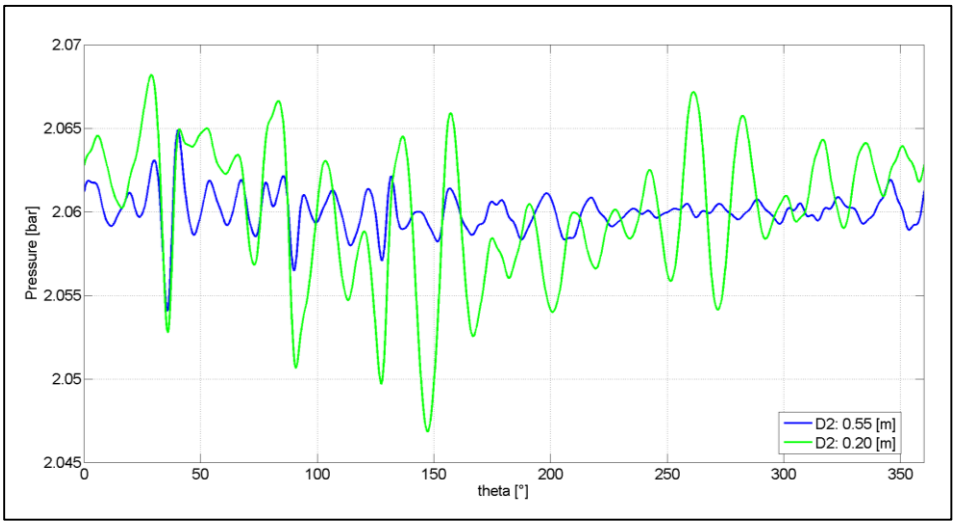

Figure 4.5 - Suction: transmitted pressure downstream the plenum. Plenum cylindrical body dimension: blue D2=0.55 m, green D2= 0.2 m

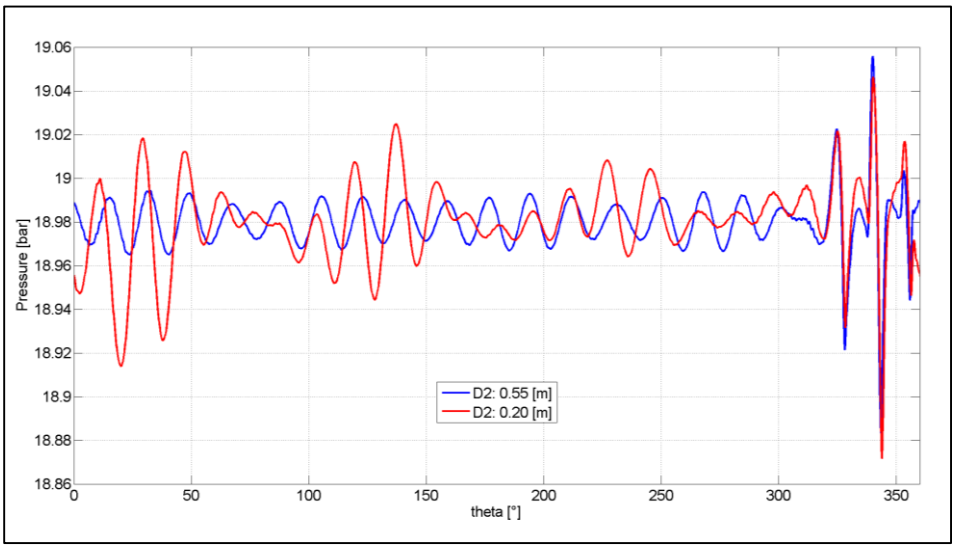

Figure 4.6 - Discharge: transmitted pressure downstream the plenum. Plenum cylindrical body dimension: blue D2=0.55 m, red D2= 0.2 m

The same treating can be considered for the discharge line, Figure 4.6; in this case the reduction of the pressure fluctuations is relatively more limited than in the suction case. Up to now it is described the pressure wave propagation along the suction and the discharge lines, now the influence on the PV diagram is shown. In Figure 4.7 is depicted the comparison of the in-cylinder pressure applying, to the same compressor, two different typology of plenum; in each case on the suction and discharge line it is modelled the same plenum. The blue line of the graph below refers to the compressor provided with the plenum of diameter D2 equal to 0.55m, the red line refers to the compressor provided

with the plenum of diameter D2 equal to 0.20m. Observing Figure 4.7 can be noticed that the plenum volume variation influences the PV diagram trend; the more evident variations of the in cylinder pressure arise during the discharge phase. This fact is a direct consequence of the different pressure fluctuation at the discharge interface (compressor-plenum) in the two considered configurations. In fact observing Figure 4.3 the discharge pressure fluctuation is consistent (red line) while in Figure 4.4 it is much more flat. These pressure fluctuations influence directly the valve dynamics and as consequence the pressure inside the cylinder. During the suction phase this phenomenon is almost imperceptible because of in both cases the suction pressure is the same and it is quite flat.

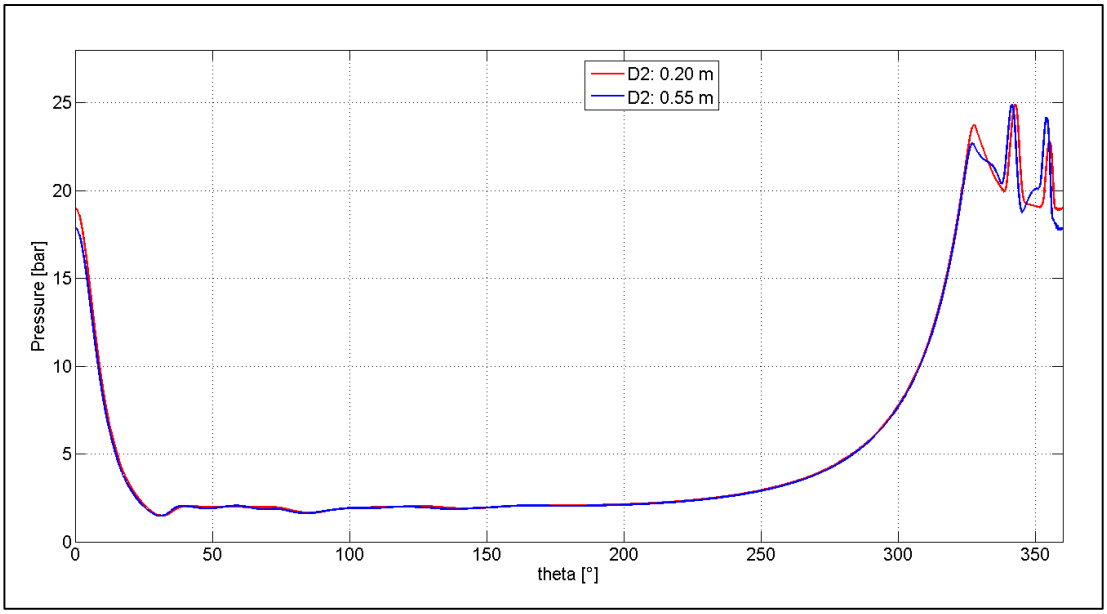

Figure 4.7 - Comparison between the PV diagrams, in blue plenum with the greater volume, in red the plenum with the smaller volume

The above treating highlights the capability of the hybrid approach to numerically estimate the reciprocal interaction between the machine and the line; the model appreciates the dimension variations of the line elements both in terms of pressure wave propagation and in terms of compressor-line interaction.

4.2 Configuration 2

The second configuration tested is relative to a reciprocating compressor provided with two cylinders. The flow sucked from the suction valves of both cylinders comes from the same suction chamber, even for the discharge side is simulated the same configuration, where the flow crossing the discharge valves of both the cylinders converge to the same discharge chamber. The scheme of this configuration is depicted in Figure 4.8.

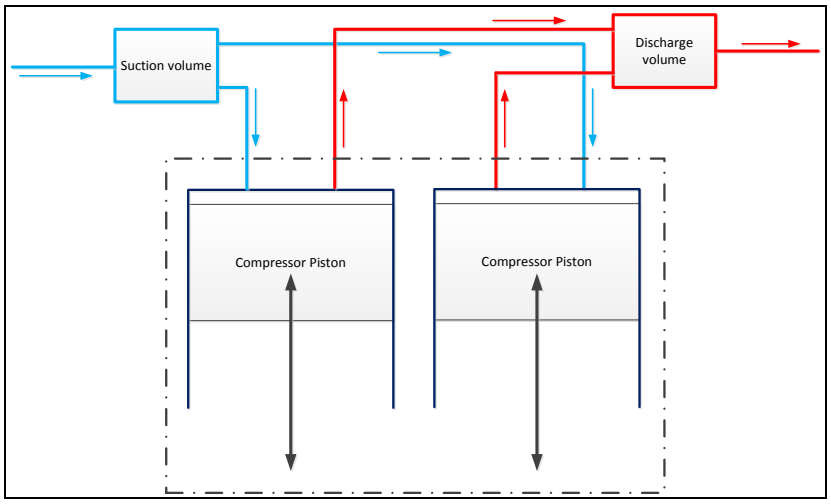

Figure 4.8 - Bi-cylindrical compressor scheme

The chamber is approached to a plenum composed by a central cylindrical body with two inlets and an outlet, in Figure 4.9 the scheme of the plenum is depicted.

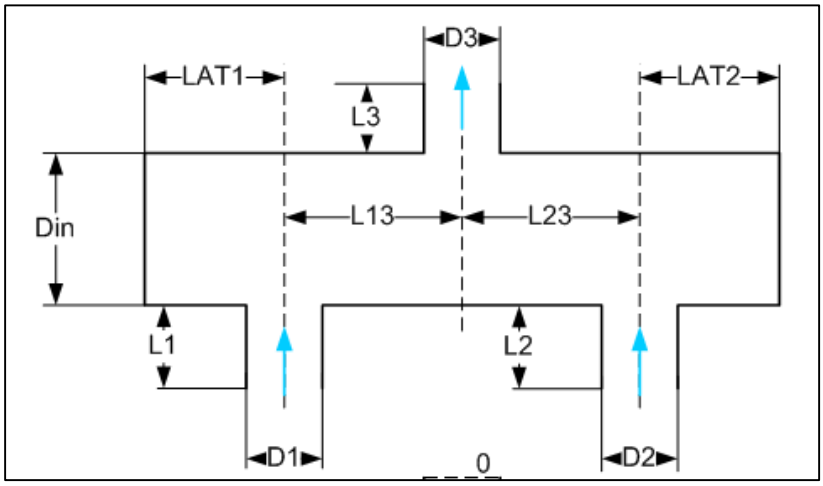

Figure 4.9 - Plenum scheme, 2 inlet - 1 outlet

In order to simulate the behavior of the reciprocating compressor provided with two cylinders the hybrid model has been structured in the way describe in the scheme below.

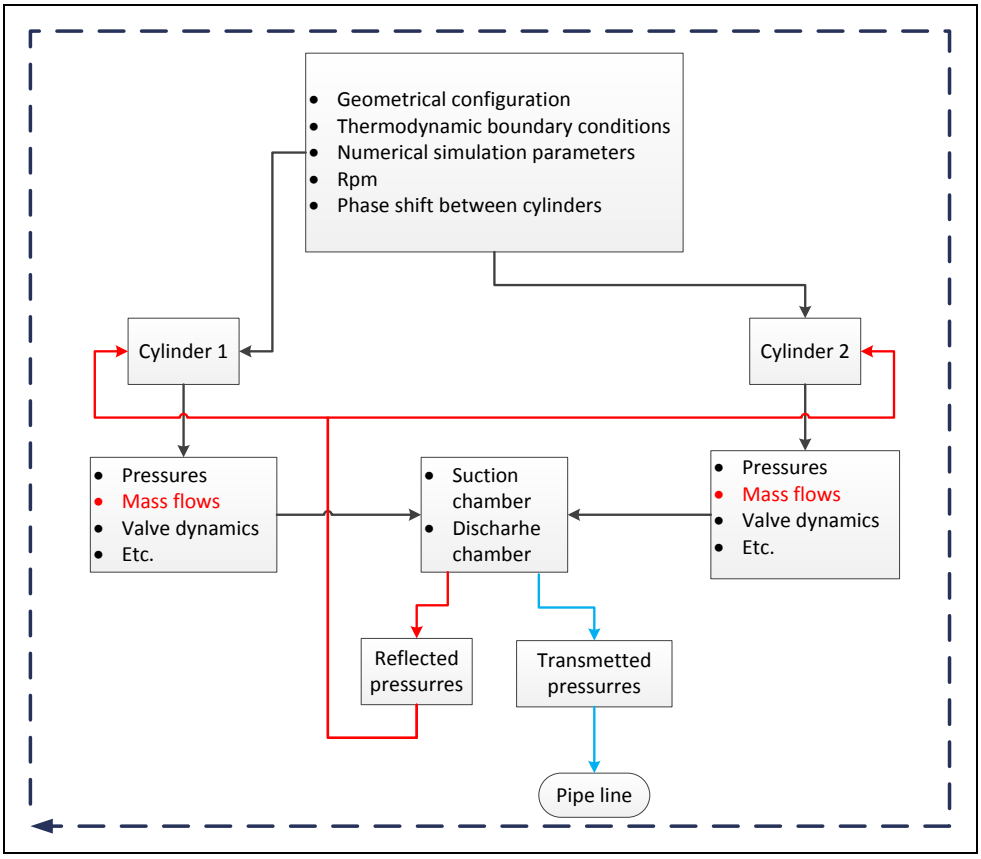

Figure 4.10 - Flow diagram of the bi-cylindrical configuration

The main parameters like: geometrical configuration, valve mechanical parameters, thermodynamic boundary conditions, rpm, shift between cylinder and so on, are imposed in the first main block of the model. Then two compressor simulations, relative to the cylinder 1 and to the cylinder 2, start in parallel. The thermodynamics parameters computed during the cylinder simulation go to the suction and discharge chambers models. Now the reflected and transmitted pressures estimated during the simulation of the chamber are directed respectively to cylinder and to the pipe line.

The results of the simulation of the bi-cylindrical configuration are exposed in Figure 4.11. The graph shows the P-theta diagram of the cylinder 1 (continuous line) and of the cylinder 2 (dashed lines), contemporary are depicted the suction and the discharge pressure fluctuations for both the cylinders. The phase shift between the two cylinders is 180°.

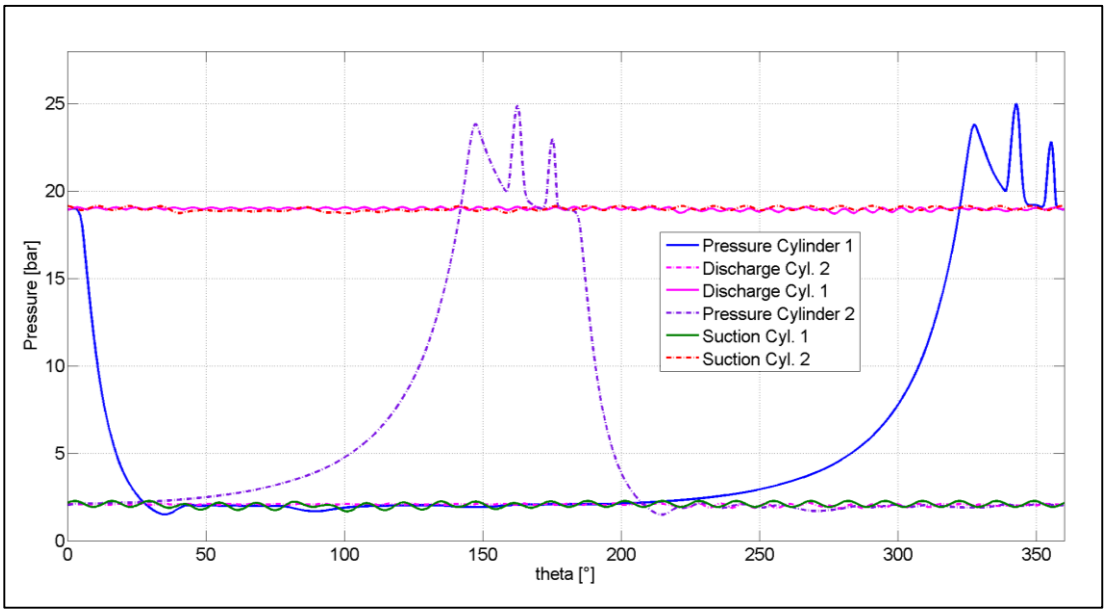

Figure 4.11 - P-theta diagram of the bi-cylindrical compressor, the phase shift between the cylinders is 180°; cylinder 1 continuous lines, cylinder 2 dashed lines

The configuration of the suction and the discharge plenum is the same and the geometrical values are depicted in Table - 4.2. The subscripts 1 are relative to the inlet 1, the subscripts 2 are relative to the inlet 2 and the subscripts 3 are relative to the outlet 3. For example looking at the suction chamber, the suction side of the cylinder 1 is connected to the inlet 1, the suction side of cylinder 2 to the inlet 2 and both the cylinders suck from the duct 3. The same treating is adopted for the discharge.

Plenum Geometry values [m]					
L1	0.13	***D2***	0.055	***L13***	0.25
D1	0.055	***LAT2***	0.050	***L23***	0.25
LAT1	0.055	***L3***	0.3	***Din***	0.55
L2	0.09	***D3***	0.10		

Table - 4.2 Plenum geometry values -Two inlets and one outlet configuration

From the graph of Figure 4.11 it arises that for the configuration tested the two cylinders behave in the same way, in fact the in-cylinder pressure are almost identical, moreover the pressure fluctuations reflected from the plenum to the compressor are limited both at the discharge side and the suction side. Precisely the pressure fluctuations are limited in amplitude and are at a relative high frequency respect to the main frequency

of the driving forces (mass flow). The same consideration is valid for the pressure fluctuations transmitted to the pipeline: in Figure 4.13 and Figure 4.14 are depicted the pressures transmitted upstream the suction plenum and downstream the discharge plenum.

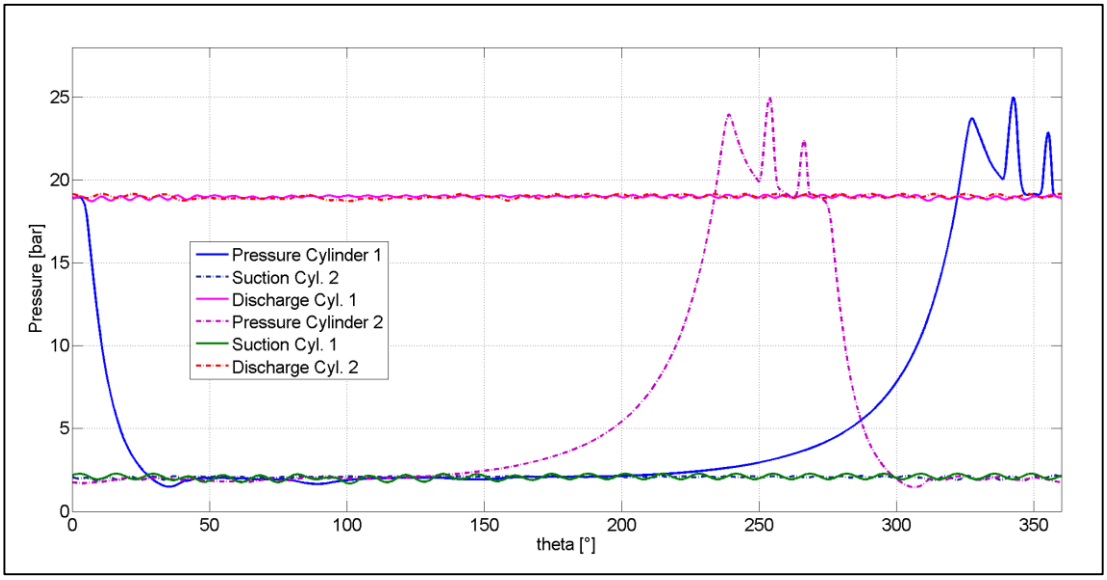

Figure 4.12 - P-Theta diagram of the bi-cylindrical compressor, the phase shift between the cylinders is 90°; cylinder 1 continuous lines, cylinder 2 dashed lines

Maintaining the same configuration for the plenums, the hybrid model is tested varying the phase shift between the cranks of the two cylinders from 180° to 90°. The in-cylinder pressures are depicted in Figure 4.12; from the simulation arises that no evident variations occur, in term of reflected or transmitted pressure waves respect to the previous configuration. In confirmation of what written above there are the graphs of Figure 4.13 and Figure 4.14 where there are depicted the comparisons between the transmitted pressures in case of phase shift between the cranks of the two cylinders of 90° and 180°. It is evident that no consistent variations are appreciable from the comparison of the two configurations.

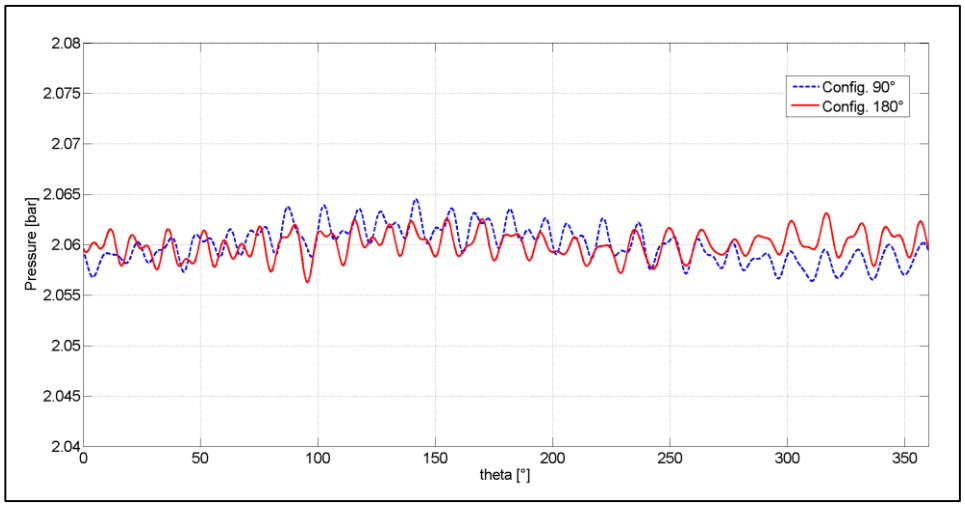

Figure 4.13 - Comparison between the pressure fluctuations upstream the suction plenum; the blue line is relative to the compressor with a phase shift between the cranks of the two cylinders of 90°, the red is relative to a phase shift between the cranks of the two cylinders of 180°.

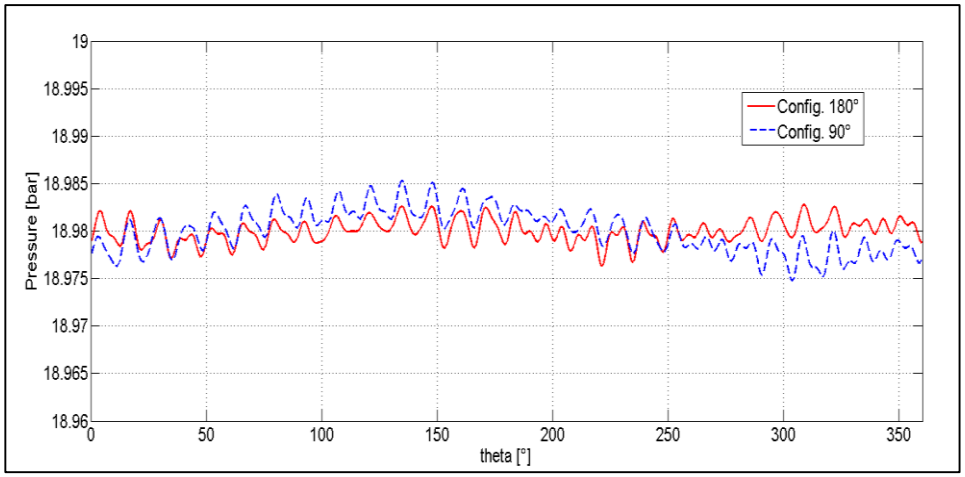

Figure 4.14 - Comparison between the pressure fluctuations downstream the discharge plenum; the blue line is relative to the compressor with a phase shift between the cranks of the two cylinders of 90°, the red is relative to a phase shift between the cranks of the two cylinders of 180°.

The simulations show that no appreciable variations in terms of pressure fluctuation are caused by the variation of the reciprocal position of the cranks of the two cylinders. The above treating is an example of investigation about the thermodynamic behaviour of the reciprocating compressors. In order to exemplify the capability of the hybrid approach another test case is reported below. In this second simulation the bi-cylindrical compressor is tested with a phase shift between the cranks of 180° and a reduction of the dimension of the cylindrical body of the suction and discharge plenum, passing from a value of ***Din*** equal to 0.50m to a dimension of 0.15m.

This consistent reduction in the plenum dimension is applied in order to change appreciably the behaviour of the suction and the discharge chambers. Precisely, this modify makes the plenum acoustic behaviour similar to that of a simple duct; so it is expected a reduction of the pressure reflected to the compressor and an increase of the pressure transmitted to the pipeline. It is important to underline that in all the simulation at the duct 3 of the plenum it is applied an anechoic end.

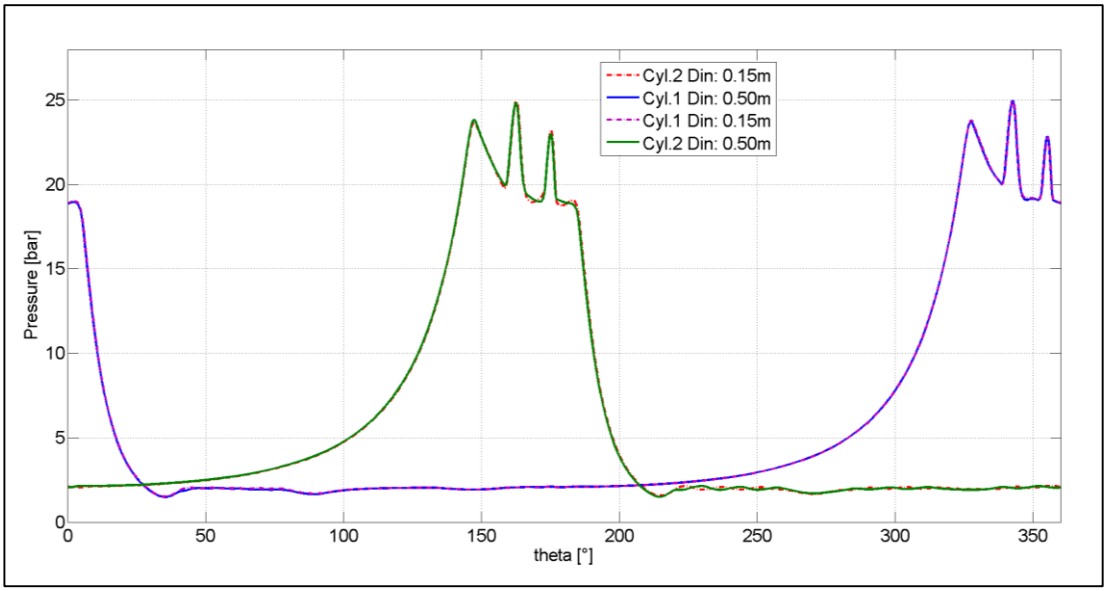

Figure 4.15 - Comparison of the in-cylinder pressure trends varying the plenum Din dimension

In Figure 4.15 there is depicted the comparison between the indicating cycles varying the ***Din*** dimension of the plenums from 0.55m to 0.15m; the pressure of the cylinder 1 and cylinder 2 in both the configurations of the plenum are identical. Its due to the fact that the pressure reflected from the suction and discharge plenum to the cylinder are almost the same and quiet flat and as consequence not influences the pressure trends inside the cylinder. More significant are the pressure fluctuations downstream the discharge volume and upstream the suction volume: observing the graph of Figure 4.16 and Figure 4.17, it is possible to appreciate the variation, in terms of pressure fluctuation, caused by the use of plenums with different dimension of the central cylindrical body. In particular there is an appreciable increase of the transmitted pressure to the pipeline as a consequence of the ***Din*** dimension reduction, both at the suction side and at the discharge side. The results show that the hybrid model in the present configuration returns a response that is coherent with the expected behaviour of the compressor-pipeline system.

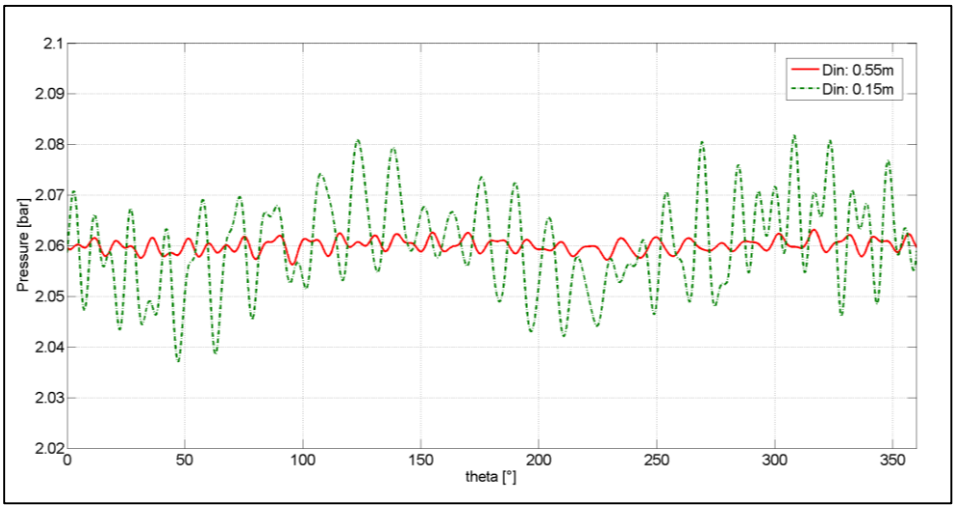

Figure 4.16 - Pressure fluctuation at the suction side, comparison between plenum of different Din dimension

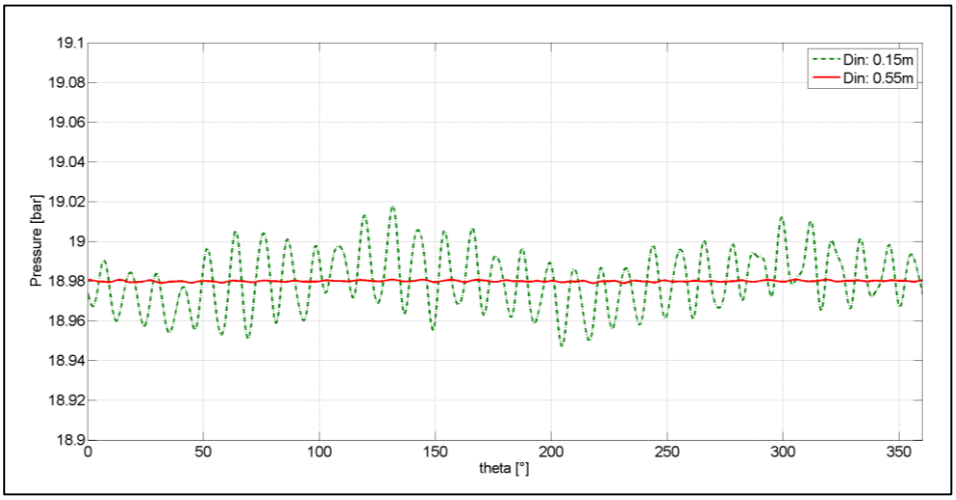

Figure 4.17 - Pressure fluctuation at the discharge side, comparison between plenum of different Din dimension

The cases studied in the previous configurations are the ideal simplifications of the coupling between the compressor and the pipeline, the aim of this activity is to show the potentiality of the hybrid model for the simulation of the coupling between the compressor and the line.

4.3 Configuration 3

One of the aims of the hybrid approach is to be a versatile and quick tool for the preliminary estimation both of the compressor performance and of the compressor-pipeline interactions in terms of pressure wave propagation. Usually, in the real applications the mass flow processed by the compressor passes across areas of complex geometry. An example is represented by the chambers for the pulsation control located on the compressor head and placed upstream the suction valves and downstream the discharge valves. These chambers are volumes of complex geometry which have the objective to reduce the pressure fluctuation caused by the pulsating flow generated from the functioning of the reciprocating machine; the complexity of the chamber geometry is usually caused by layout reasons.

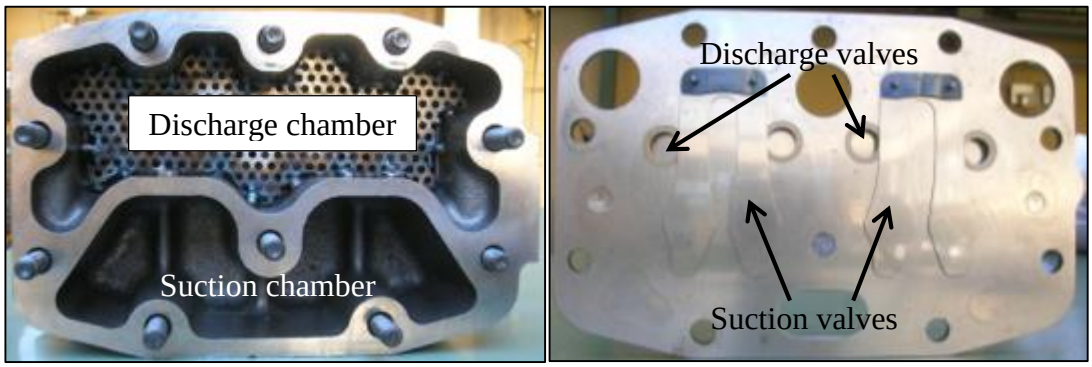

Figure 4.18 - Suction and discharge chambers of a compressor for refrigeration applications

An example is represented in Figure 4.18 where it is shown the discharge and the suction chambers of a compressor for cooling system. It is clear that in this case the acoustic theory for one-dimensional plane wave can't be adopted because of the strong three dimensionality of the problem. So the acoustic behavior of such a volume must be treated using a 3D analysis (paragraph 2.2.1).

In the present activity it is evaluated the possibility to treat elements with complex 3D geometry inside the hybrid approach. This possibility would allow the hybrid approach to overcome the limitation of the mono-dimensional codes that is the treating of elements with 3D features.

To introduce the 3D elements into the hybrid approach it is necessary a preliminary characterization of the elements with an acoustic fem tool which allows to estimate the coefficients (transmission and reflection coefficients) of the elements and to create the relative transfer matrix. So the acoustic transfer matrix isn't obtained from the 1D acoustic theory of the plane wave but its coefficients are calculated thanks to the use of a 3D acoustic solver (paragraph 2.2.1). Once defined the transfer matrix of the elements it is possible to introduce it inside the hybrid model and to perform the simulation.

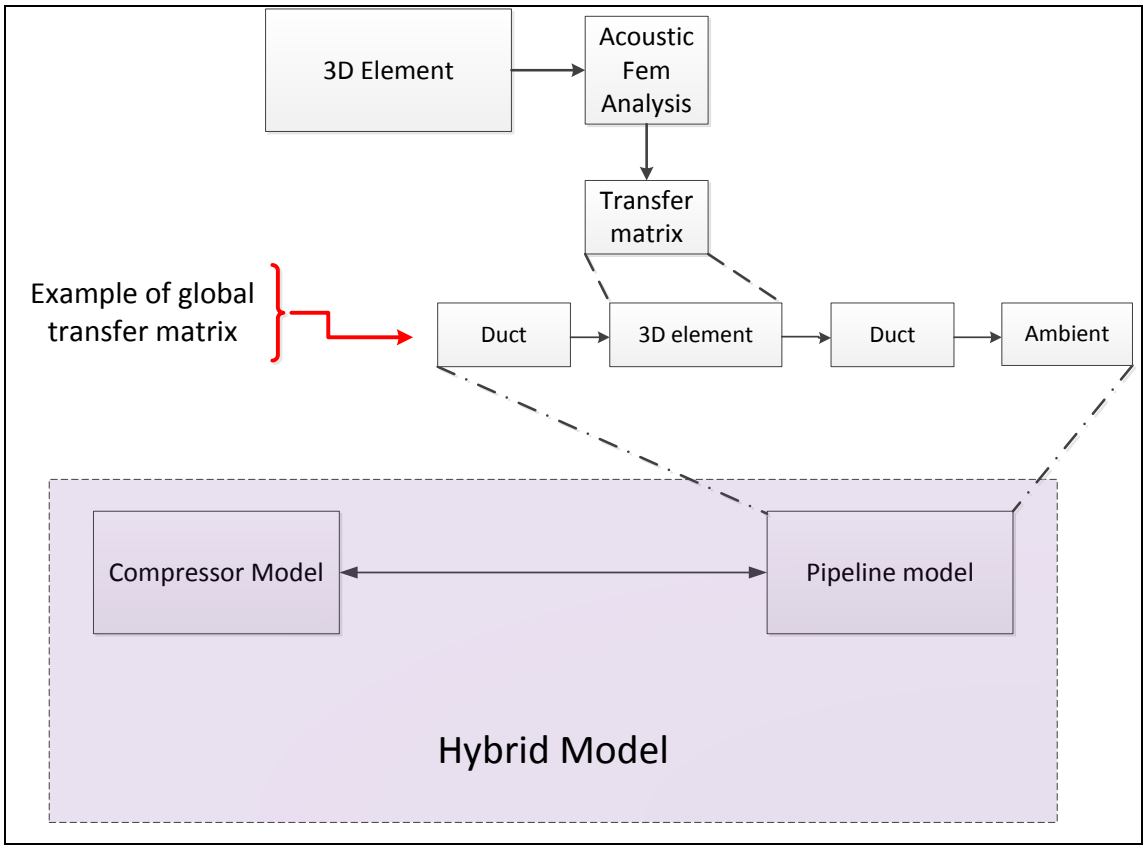

Figure 4.19 - Scheme of the hybrid approach with the introduction of the modelling of a 3D element

The scheme of Figure 4.19 summarizes the preceding treating about the introduction of 3D elements inside the hybrid model; once defined the transfer matrix of the 3D element, it can be assembled in the global transfer matrix of the pipeline which, in turn, is then coupled with the compressor model.

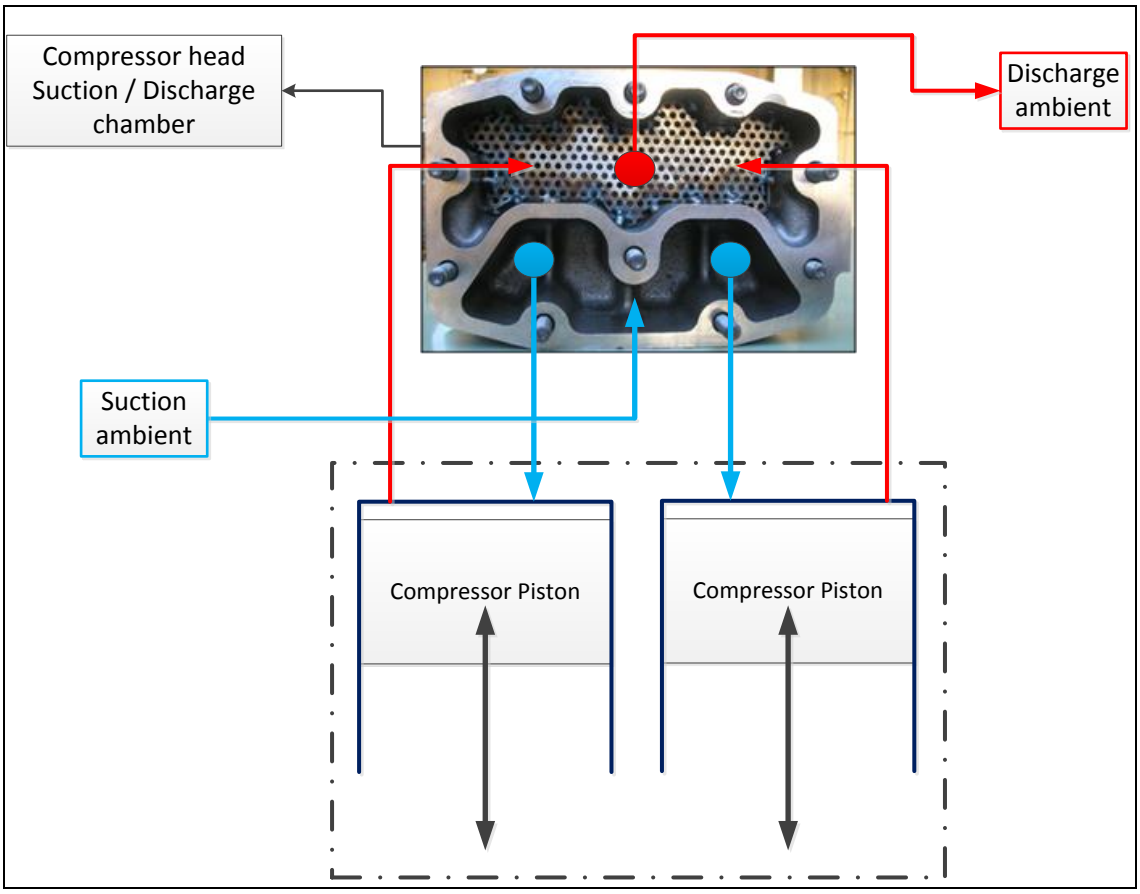

Figure 4.20 - Bi-cylindrical compressor scheme

In Figure 4.20 it is depicted the scheme of the third configuration tested during the present activity: the twin cylinders compressor is coupled with the 3D model of the compressor head which is composed of two chambers, the suction chamber and the discharge chamber. So the flow sucked by the compressor passes from the ambient to the suction chamber and then into the compressor; conversely for the discharge, first the compressed gas passes from the compressor to the discharge chamber and then to the discharge ambient. The approach adopted for the modelling of this configuration is the same adopted for the configuration 2, its schematization is depicted in Figure 4.10. In the present configuration the suction and discharge volume are substituted by the real suction and discharge chambers. So in this configuration the hybrid model is composed of:

- the numerical model of the reciprocating compressor, twin cylinder configuration;
- the model of the line elements, which is constituted of the transfer matrix of the compressor head (in which are conteined the suction and the discharge chambers).

The cylinder head on one hand communicates with the compressor through the valves, on the other communicates with an anechoic termination. The anechoic end it is adopted in order to focus the analysis only on the interaction between the reciprocating compressor and the suction and the discharge chambers, excluding the effects due to the other pipeline elements.

The aim of this test is to evaluate if the hybrid approach is effectively able to manage 3D elements treated with the transfer matrix method.

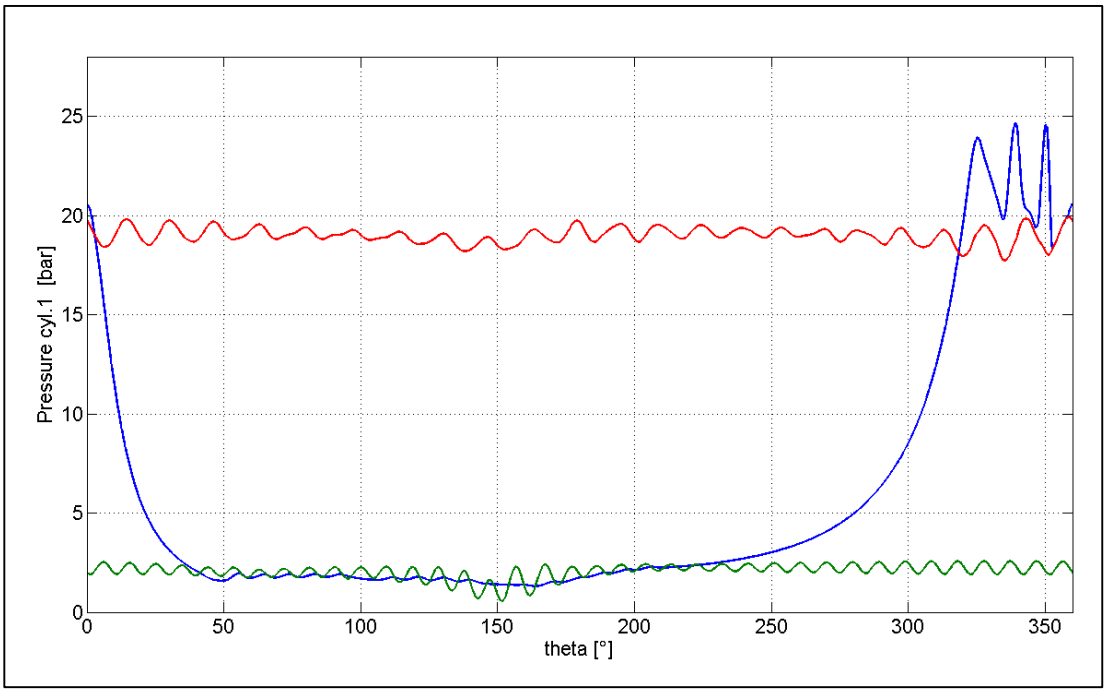

Figure 4.21 - Cylinder 1, blue line in cylinder pressure, red line discharge pressure, green line suction pressure

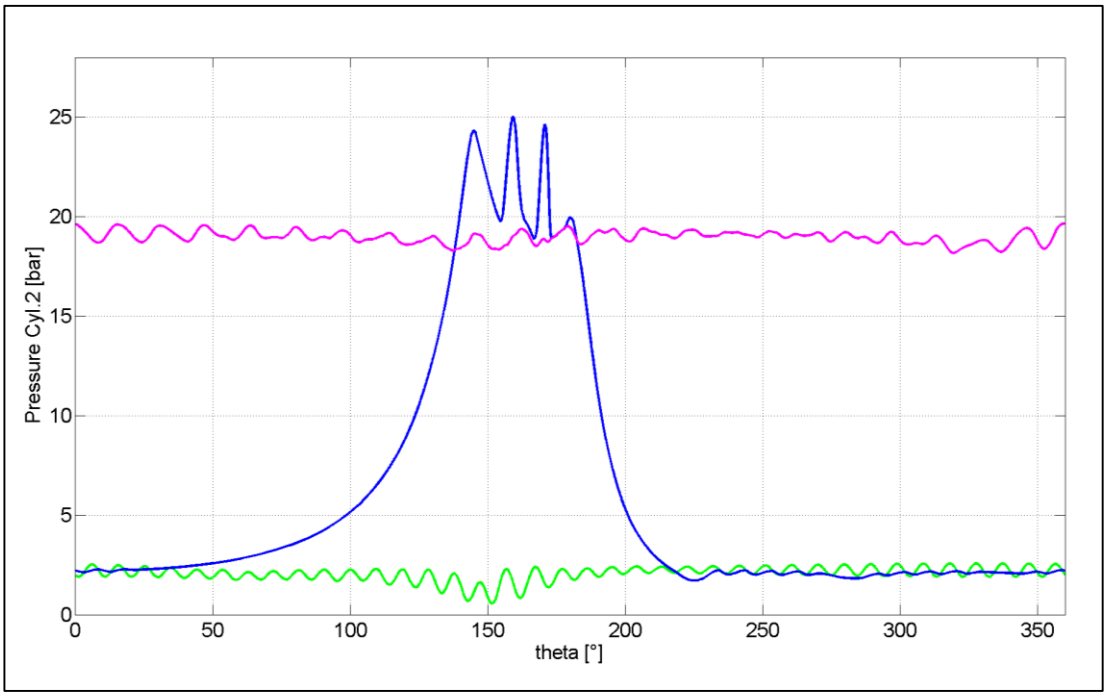

Figure 4.22 - Cylinder 2, blue line in cylinder pressure, violet line discharge pressure, green line suction pressure

The graphs of Figure 4.21 and Figure 4.22 are the pressures trends respectively of the cylinder 1 and of the cylinder 2 obtained from the simulation of the third configuration. In blue are depicted the in-cylinder pressures while the red and the green lines represent respectively the pressure at the suction and at the discharge valves. These graphs are the demonstration of the potentiality of the hybrid approach in treating the pipeline elements having complex 3D geometry. The results show that the hybrid model returns a plausible behaviour of the reciprocating compressor in terms of indicating pressure and of pressure oscillations at the suction and at the discharge valves. This is the first step for the evaluation of the interaction between the reciprocating compressor and the pipeline using 3D elements. The hybrid approach described in the present activity feels the effects of some simplifications:

- no mass flow across the pipelines;
- pipelines elements with infinitely rigid walls.

So the wave propagation is calculated without taking into account the mass flow across the elements, as a consequence the pressure waves don't undergo the dumping

effects. Moreover, during the gas flow, the pressure losses are not considered. The approximation of infinitely rigid wall is equal to not consider the interaction between the structure and the fluid and as a consequence the effects the structure has on the wave propagation. The elimination of these simplifications allows the hybrid model to be more accurate in the simulation of the whole compressor system; in this way a greater reliability and a better predictability can be obtained in the estimation of the real phenomena concerned to this topic.

5 Conclusion

The PhD project presented in this work focuses on the development of an advanced numerical methodology for the estimation of the reciprocating compressor performances and of the interaction between the reciprocating compressor and its piping system. The numerical model realized has the aim to be a tool in support of the first stage of the design of the reciprocating compressors.

This activity, born from the collaboration between the University of Florence and some industries working in the field of oil & gas and in the field of the refrigeration systems, has been carried out in order to get a quick numerical model able to simulate the global behaviour of the machine.

A so devised hybrid model simulates not only the thermodynamic performances of the reciprocating compressor but also the pressure waves propagation along the piping system connected to the machine; moreover the methodology spent to face this object gives the chance to study the reciprocal interaction, between the compressor and the pipeline, in terms of pressure fluctuations.

From the analysis of the state of the art about the argument and taking into account the necessities of the industrial partners, this work of research deals with an hybrid model in which the compressor and the piping system are modelled using two different approaches:

- A 0D quasi-stationay modelling defined in the time domain is adopted for the thermodynamic cycle of the reciprocating compressor;

- A model defined in the frequency domain based on the one-dimensional acoustic theory of the plane waves is realised for the wave propagation along the piping system.

The pressure fluctuations, calculated at the suction and at the discharge sections of the compressor, represent the input signals for the pipeline model, vice versa, the acoustic response of the pipeline model represents the boundary condition for the compressor model.

5.1 Numerical models

The numerical code for the simulation of the thermodynamic cycle of the reciprocating compressor is developed in MATLAB® environment. The code name is RE.CO.A, which means: reciprocating compressor analysis. It is a quasi-stationary modelling through which, step by step, it is calculated the compressor piston displacement inside the cylinder starting from the TDP. Each cycle the displacement evolves from 0° to 360° of the crank angle and the angular step can be set $\leq 1°$. At each step all the thermodynamic quantities characteristic of the fluid processed by the compressor are calculated; some examples of them are: the in-cylinder pressure, the gas temperature and density, the Cp and Cv parameters and so on. The calculation is based on the first law of thermodynamic. The model can deal with the libraries for calculating the real gas properties, in order to compute analytically the desired gas variable in function of pressure and temperature. The inlet and outlet of the gas across the compressor is regulated by the automatics valves; precisely it is developed a dedicated sub-model for the calculation of the valve motion. The valve system is physically schematized as a mass-spring-dumper system where the driving forces are represented by the pressure difference upstream and downstream of the valve.

The simulation of the piping system is based on the one-dimensional acoustic theory of the plane wave; the modelling is defined in the frequency domain. Precisely

every simple element of the pipeline (such as ducts, volumes, orifices, T junctions and so on) it is modelled separately obtaining its own acoustic response one by one. Therefore, imposing a pressure profile, defined in the frequency domain (amplitude and phase) at one end, each element returns its specific acoustic response at the opposite end. In this way it is possible to concatenate the simple elements and to simulate a complex piping system.

This activity of research aims to estimate the influence of the reciprocating compressor on the piping system in terms of pressure fluctuations. The adopted methodology imposes straight to the piping system the pressure fluctuations generated by the reciprocating compressor. To get this goal it is used an hybrid approach in which the RE.CO.A model and the model of the piping system are coupled and work together. The RE.CO.A code represents the source of the hybrid model and the piping model represents the boundary conditions for the source. Precisely at each cycle the RE.CO.A code produces the mass flow profile at the suction and at the discharge side of the compressor: these mass flow profiles are the driving force of the pipeline system. The response of the pipeline, in terms of pressure fluctuation, represents, in turn, the new boundary condition for the RE.CO.A model; the hybrid model iterates up to reach the point of convergence. Since the modelling of the reciprocating compressor and the piping system are defined respectively in the time domain and in the frequency domain, the passage of the information between the two models is possible thanks to the use of the FFT and IFFT numerical tools. The above-mentioned approach allows the investigation of the influence of the compressor on the pipeline and vice versa.

The work has also taken into account the introduction, inside the hybrid model, of elements characterized by a strong 3D geometry. This topic has been faced in order to overcome the typical limitation of the one-dimensional code in the treating of the element with 3D geometry. The idea is that to get the transfer matrix of the 3D element, using a FEM acoustic solver, and to introduce it inside the modelling of the pipeline system.

5.2 Analyses

The challenge is to test and demonstrate the potentialities of the numerical model for prediction of the compressor performance. The RE.CO.A model in evidence has been calibrated on the basis of the indicating cycles, obtained during the experimental tests on a reciprocating compressor for refrigeration applications. Once the model has been calibrated, some analyses has been carried out in order to evaluate the reliability of the model. The estimation of the typical parameters characteristic of the reciprocating compressor (such as in-cylinder pressure and temperature, mass flow rate across the valves, suction and discharge valves displacement etc.) has been carefully made. The model turns out to be useful in the simulation of various geometrical configurations of the compressor, in order to investigate its behaviour during the design stage of the machine. The chance to evaluate the valves motion varying the valve geometry, the valve parameters like the valve mass, the spring stiffness and the dumping coefficient is a further possibility of likewise significance offered by the numerical model.

In the chapter 4 the results of the hybrid model are described. The aim is to give effective answers to the question about the possibility to adopt this kind of modelling in the field of the numerical simulation of the reciprocating compressors. Some configurations of the whole compressor-pipeline system are tested and supported with test results. It has been estimated how the pulsating flow, generated by the reciprocating compressor, propagates along simple piping system configuration and also how the pipeline response, in turn, influences the in-cylinder pressure of the compressor. Then the success of the introduction of pipeline elements whit complex 3D geometry inside the hybrid model has been tested too; in detail, the test has as object to couple a twin-cylinder compressor with 3D model of the suction and the discharge chambers. The results obtained in terms of pressure fluctuations return a physically coherent behaviour of the compressor-pipeline system.

The hybrid model, realized in this work, is the first stage of development of the numerical code for the simulation of the interaction between the reciprocating compressor and its piping system. Till now this kind of methodology has been investigated and evaluated in reference to its feasibility and potentiality. Further developments concern the

hybrid model both for the RE.CO.A model and for the numerical modelling of the pipeline. Since the indicating cycle of the compressor is strongly influenced by the amount of gas processed during the suction and the discharge phases, it is clear the importance of a good characterization of the valve dynamics. In order to get this aim, further developments regard the experimental measurement of the valve flow coefficient: this characterization must be performed varying the mass flow rate. Of great interest is the experimental investigation of valve motion by measuring the valves displacement just during the functioning of the compressor. In this way it can be estimated the real rebound coefficient of the valve and the possible presence of damping phenomena. An experimental validation of the model is necessary to the 3D acoustic analysis of the compressor head in order to attest the response. To develop the numerical model of the piping system an important aspect to be denoted is the presence of the mean flow. In the light of that the estimation of the flow friction phenomena and the damping factor of the wave propagation can be desumed. The proposed improvements are directed towards the growth of the hybrid model in order to make it a predictive numerical tool, able to help the design stage of the reciprocating compressor.

6 Bibliography

[1] R. Aigner, “Internal flow and valve dynamics in a reciprocating compressor,” Vienna, 2007.

[2] E. Winandy, C. Saavedra and J. Lebrun, “Simplified modelling of an open-type reciprocating compressor,” *International journal of thermal sciences,* vol. 41, p. 183–192, 2002.

[3] M. Elhaja, “Numerical simulation and experimental study of a two-stage reciprocating compressor for condition monitoring,” *Mechanical Systems and Signal Processing,* vol. 22, p. 374–389, 2008.

[4] Marybeth G. Nored, *Compressor station piping noise: noise mechanisms and prediction methods,* Gas Machinery Research Council Southwest Research Institute, 2011.

[5] D. Deffenbaugh, *Advanced Reciprocating Compression Technology (ARCT),* Pittsburgh, 2005.

[6] P. Davies, “Predictive acoustic modelling applied to the control of intake/exhaust noise of internal combustion engines,” *Journal of Sound and Vibration,* vol. 202, no. 2, pp. 249-274, 1997.

[7] Y. Sathyanarayana and M. Munjal, “A hybrid approach for aeroacoustic analysis,” *Applied Acoustics,* vol. 60, pp. 425-450, 2000.

[8] A. Kwang-Hyup, "Performance Prediction of Reciprocating Compressor," in *International Compressor Engineering*, 2002.

[9] Nuovo Pignone, "Cylinder valve training".

[10] Nuovo Pignone, *Calcolo delle pulsazioni di pressione,* Pisa, National museum of degli strumenti per il calcolo 1965.

[11] D. M. Deffenbaugh, "ARCT," Pittsburg, US, 2005.

[12] M. Munjal, Acoustics of ducts and mufflers, New York: Wiley Interscience, 1987.

[13] L. J. Eriksson, "Noise control in internal combustion engine," *D.E.Baxa,* Chapter 5, 1982.

[14] A. C. Fagerlund, "Sound transmission through a cylindrical pipe wall," *ASME,* 1980.

[15] A. Selamet, V. Easwaran, J. M. Novak and R. A. Kach, "Wave attenuation in catalytic converters: Reactive versus," *Acoustical Society of America,* 1998.

[16] A. Almasi, "Pulsation Suppression Device Design for Reciprocating Compressor," *World Academy of Science, Engineering and Technology,* pp. 321-329, 2009.

[17] J. Wachel, "Vibrations in reciprocating machinery and piping system," in *23th Turbomachinery Symposium,* San Antonio Texas, 1994.

[18] M. Costagliola, "Theory of spring loaded valves for reciprocating compressors," *The Journal of Applied Mechanics,* 1950.

[19] Munson, "Fundamentals of fluid mechanics," Wiley student edition, 2000.

[20] J. Heywood, Internal combustion engines fundamentals, McGraw Hil, 1998.

[21] F. Balduzzi, "Development of a CFD approach for the performance prediction of reciprocating compressors," Firenze, Biblioteca di ingegneria, 2013.

[22] W. H. Hsieh, "Experimental Investigation of Heat Transfer in a High-Pressure Reciprocating Gas Compressor," *Experimental thermal and fluid science,* vol. 13, pp. 44-54, 1996.

[23] E. Giacomelli, "Simulation of cylinder valves for reciprocating compressor," in *ASME Conference on Engineering Systems Design and Analysis*, Torino, 2006.

[24] X. Lin, *Simulation of valve dynamics in a large reciprocating compressor*, Beijing University of Aeronautics & Astronautics, 1986.

[25] B. D. Storey, "Numerical methods for ordinary differential equation".

[26] Matlab, "www.mathworks.com," [Online].

[27] M. A. Real, "Using PV Diagram Synchronized With the Valve Functioning to Increase the Efficiency on the Reciprocating Hermetic Compressors," in *International Compressor Engineering*, Purdue, 2010.

[28] W. S. Fu, "A concise method for determining a valve flow coefficient of a valve under compressible gas flow," *Experimental Thermal and Fluid Science*, vol. 18, no. 4, pp. 307-313, 1998.

[29] A. Grace, "Experimental parametric equation for the prediction of valve coefficient for choke valve trims," *International journal of pressure vessels and piping*, vol. 88, pp. 109-118, 2011.

[30] P. Davies and M. Harrison, "Predictive acoustic modelling applied to the control of intake/exhaust noise of internal combustion engines," *Journal of Sound and Vibration*, vol. 202, pp. 249-274, 1997.

[31] A. Jones, W. Moorhem and . R. Voland, "Is a full nonlinear method necessary for the prediction of radiated engine exhaust noise," *Noise Control Engineering Journal*, vol. 26, pp. 74-80, 1986.

[32] M. Harrison and P. Davies, "Rapid predictions of vehicle intake/exhaust radiated noise," in *Institute of Mechanical Engineers*, 1994.

[33] P. Davies, "Aeroacoustic and time varying systems," *Journal of Sound and Vibration*, 1995.